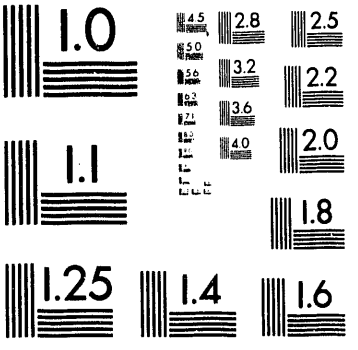
1.0
4.5
2.8
2.5
5.0
3.2
2.2
5.6
3.6
2.0
4.0
1.1
1.8
1.25
1.4
1.6

1 of 1

PNL-8745
UC-902

STATISTICAL EVALUATION OF CORE SAMPLES FROM HANFORD TANK B110

P. G. Heasler
C. M. Anderson
D. B. Baird
R. J. Serne
P. D. Whitney

August 1993

Prepared for
the U.S. Department of Energy
under Contract DE-AC06-76RLO 1830

Pacific Northwest Laboratory
Richland, Washington 99352

MASTER

DISTRIBUTION OF THIS DOCUMENT IS UNLIMITED

Executive Summary

This report presents an analysis of the core samples extracted from tank B110. The sampling campaign was quite extensive and resulted in a total of 9,179 chemical analyses on B110 waste. Approximately 70 different chemical constituents were measured in the laboratory, as well as physical and rheological properties. Many different types of replicate measurements were taken so that laboratory, sampling and spatial variability could be quantified. The sampling of tank B110 was part of an in-depth pilot study to determine the adequacy of current chemical analysis and sampling procedures. The major objectives of the analysis included:

- estimation of the average concentration of the measured analytes in the tank,
- estimation of the laboratory, sampling, and spatial variability within the tank, and
- evaluation of the sampling methodology.

The B110 data presents the most detailed picture of waste tank contents to date and allows one to compare measured results with historical predictions. Table 1 presents an important example of such a comparison. In this table, predictions from a computer program called TRAC are compared with estimates obtained from core sampling. The TRAC computer program uses historical records to make its predictions, so this table provides an elementary comparison between historical information and measured reality.

Table 1: Comparison of TRAC Radionuclide Estimates with Measured Results in B110

Radio-nuclide.	TRAC Estimate	Core-Sample Est.	RSD
^{241}Am	0.356	0.072	34%
^{244}Cm	3.39-03	1.28-03	50%
^{137}Cs	20.30	14.90	4%
^{129}I	1.69-04	3.61-05	38%
^{237}Np	1.02-05	1.12-04	25%
^{238}Pu	3.52-03	3.21-03	25%
^{90}Sr	21.7	108	41%
^{99}Tc	0.102	0.017	14%

Units are μCi/g

As one can see from the table, some estimates are fairly close, and all are within an order of magnitude. From the relative standard deviations (RSD) presented, one can see that there are significant differences between TRAC and the estimates produced from core sampling.

The statistical analysis also produced estimates for spatial, sampling, and measurement variability. It is not possible to produce a simple ordering of these three types of variability; The ordering depends on the constituent under consideration. However, sampling variability generally was largest, indicating that current core sampling methods have difficulties producing repeatable measurements.

Spatial variability can be decomposed into vertical and horizontal components, and vertical variability was generally larger than horizontal variability. It is important to note that the amount of **vertical** spatial variability present in the data was strongly influenced by the incompleteness of the segment-level measurements. All core segments were not analyzed in the lab and the missing measurements make the tank appear more homogeneous in the vertical direction than it actually is. Very few measurements were made on the waste crust, which was chemically very different from the rest of the waste. If one discounts the variability caused by the waste crust, then the tank is fairly homogeneous in the vertical and horizontal directions.

It was also possible to determine how well the waste could be homogenized during the sampling process. This is a very important issue, because it determines whether the laboratory aliquots are representative samples from the cores. This analysis shows that the blender used to homogenize the waste produced

samples that were indeed homogeneous. In most cases, the homogenization variability was not significantly different from zero.

Another important issue investigated was the comparability of estimates produced by composite and segment-level sampling. Generally, there was no significant difference between the two types of sampling. In those cases where significant differences did exist, they were due to the incomplete nature of segment-level measurements.

Contents

Executive Summary . . . iii
1 Introduction . . . 1

2 Description of Data . . . 3

2.1 Chemical Analysis Methods and Reporting Units . . . 4
2.2 Descriptive Statistics and Plots of Raw Data . . . 6
2.3 Statistical Models . . . 9
2.3.1 Segment-Level ANOVA Model . . . 9
2.3.2 Composite Data ANOVA Model . . . 10

3 Estimates of Variance Components . . . 11

3.1 Segment-Level Results . . . 11
3.2 Composite Results . . . 15
3.3 Adequacy of Homogenization Procedure . . . 18
3.4 Comparison of Composite and Segment-Level Results . . . 18
3.4.1 Riser RSD . . . 18
3.4.2 Homogenization RSD . . . 19
3.4.3 Replication RSD . . . 19
3.4.4 Laboratory Measurement RSD . . . 19

4 Concentration Estimates . . . 20

4.1 Average Concentration Estimates . . . 20
4.2 Vertical and Horizontal Concentration Estimates . . . 20
4.3 Comparison of Composite and Segment-Level Estimates . . . 23

5 Analysis of Holding Time Effects . . . 25

5.1 Statistical Model . . . 25
5.2 Results . . . 27

6 Conclusions . . . 31

6.1 Adequacy of Sample Homogenization (Mixing) . . . 31
6.2 Spatial Variability . . . 31
6.3 Comparison of Segment and Composite Sampling . . . 31
6.4 Holding Time Results . . . 31

7 References . . . 32

Appendix A - B110 Data Set Format . . . 33
Appendix B - Box Plots of the Raw Data . . . 35
Appendix C - Results of REML ANOVA Fits . . . 48
Appendix D - Plots of Constituents by Riser and Segment . . . 59
Appendix E - Comparison of Segment and Composite Measurements . . . 69

List of Figures

1 Positions of Cores and Risers in Tank B110 3
2 RSD Distributions for Variance Components Calculated from the Segment-Level Data 13
3 RSD Distributions for Variance Components Calculated from Composite Data 16
4 Segment-Adjusted Data Versus Time 28
5 Segment-Adjusted Data Versus Time (cont) 29
6 Segment-Adjusted Data Versus Time (cont) 30
7 Box Plots of Segment Level Radionuclides 39
8 Box Plots of Composite Level Radionuclides 40
9 Box Plots of Segment Level Cations 41
10 Box Plots of Composite Level Cations 42
11 Box Plots of Segment Level Cations 43
12 Box Plots of Composite Level Cations 44
13 Box Plots of Segment Level Anions 45
14 Box Plots of Composite Level Anions 46
15 Box Plots of Composite Level Isotopic Mass Ratios 47

List of Tables

1 Comparison of TRAC Radionuclide Estimates with Measured Results in B110 iii
2 Summary of Concentration Estimates for Tank B110 2
3 Analytic Techniques and Analytes Measured 5
4 Preferred Measurement Method for Tank B110 Constituents 7
5 Overview of Measurements Taken in B110 8
6 Detection Limit Summary 8
7 Summary of Segment-Level Outlier Values 12
8 Level of Significance for Segment-Level Variance Components 14
9 Composite Values Omitted from Analyses as Suspect 15
10 Level of Significance for Composite Variance Components 17
11 Average Concentrations of Radionuclides, Isotopic Ratios, and Below Detection Limit Constituents 21
12 Average Concentrations of Anions and Cations 22
13 Numbers of Significant Differences between Segment and Composite Estimates 23
14 Raw Holding Time Data (ppm) 26
15 Summary of ANOVA Fits 27
16 Description of B110 Data Base Fields 33
17 Explanation of Analysis Method Codes 34
18 Excerpt from B110 Data Base 34
19 Segment Level Radionuclides 35
20 Composite Level Radionuclides 35
21 Segment Level Cations 36
22 Composite Level Cations 37
23 Segment Level Anions 38
24 Composite Level Anions 38
25 Composite Level Isotopic Mass Ratios 38
26 Segment Data: Relative Standard Deviations for Cations (ppm) 49
27 Segment Data: Relative Standard Deviations for Cations (ppm, Continued) 50
28 Segment Data: Relative Standard Deviations for Anions (ppm) 51
29 Segment Data: Relative Standard Deviations for Radionuclides (μCi/g) 52
30 Composite Data: Relative Standard Deviations for Cations (ppm) 54
31 Composite Data: Relative Standard Deviations for Cations (ppm, continued) 55
32 Composite Data: Relative Standard Deviations for Anions (ppm) 56
33 Composite Data: Relative Standard Deviations for Radionuclides (μCi/g) 57
34 Composite Data: Relative Standard Deviations for Isotopic Mass Ratios 58

1 Introduction

In 1990, seven core samples were obtained from the B110 single shell tank at Hanford. This report presents a statistical analysis of the extensive chemical measurements performed on these core samples. This tank sampling is part of the ongoing tank characterization efforts at Hanford, which is a multi-year effort to measure the waste in all tanks at the site. The sampling of the B110 tank, along with U110, was meant to furnish "pilot" data for the characterization effort. Consequently, more data was collected from these tanks than is planned for future tanks.

The primary objectives of the data gathering and analysis efforts being conducted under the auspices of tank characterization are outlined in [10]. This report states,

> The SST waste characterization project is responsible for sampling and analyzing the waste in Hanford Site's 149 SSTs to support regulatory, safety (waste reactivity) evaluation, performance assessment, waste retrieval and treatment technology development, supplemental environmental impact statement (EIS), and closure plan activities. The purpose of Phase I of the waste characterization project is to obtain information as quickly as possible on all 149 tanks to support the planning and development of the above activities. If this information is insufficient to support an activity, then additional waste characterization will be performed in Phase II with a revised QAPJP to meet any new objectives. The project addresses only characterization of the waste in the tanks and not the soils or the ancillary equipment associated with the tank system. ...These data permit the project to identify and evaluate additional characterization and waste treatment requirements. The project also will provide data to support regulatory and safety evaluations for storage and treatment of the waste.

The primary objective of this report is to present a summary of the data and estimate some important quantities, such as;

1. the average concentration of measured analytes in the tank
2. the sources of variation present in the data (spatial, sampling, mixing, measurement)
3. the adequacy of mixing used in sample preparation
4. the adequacy of composite samples
5. holding time effects.

The major statistical tool employed for this report is Analysis of Variance (ANOVA). The employed ANOVA models are variants of the ANOVA models described in references [10] and [5]. The objective is to utilize fairly simple, standard statistical procedures for the characterization reports. Other, more specialized statistical analysis will inevitably be applied to the data in follow-up reports. However, the procedures in this report establish a valuable reference point for more sophisticated analysis and can also be easily understood by the general scientific audience.

Table 2 presents a brief overview of the most important ANOVA result, an estimate of the average concentration for the measured constituents. The table presents estimates derived from the "composite" sampling scheme because it generally represented the most complete sampling within the tank. The ANOVA fits also produce information about the uncertainty of the estimate, expressed in the table as a "relative standard deviation" (the standard deviation of the estimate divided by the average concentration). The estimates are expressed in three units, depending on the constituent of interest: parts per million (ppm), micro-Curies per gram (μCi/g) and as a dimensionless ratio of concentrations (from mass spectrometry). The concentration data (ppm or μCi/g) are based on the **wet** weight of the composite core material.

Table 2: Summary of Concentration Estimates for Tank B110

Constituent	Mean Conc.	RSD*	Constituent	Mean Conc.	RSD
	(ppm)			(ppm)	
Ag	46.73	0.50	Al	1,133	0.15
B	49.43	0.13	Ba	14.14	0.04
Bi	18,520	0.07	Ca	810	0.07
Cd	5.29	0.13	Ce	37.14	0.28
Cl	1,234	0.07	Cr	810	0.03
Cu	42.52	0.28	Fe	18,060	0.04
F	1,895	0.07	K	312	0.05
La	31.81	0.30	Mg	179	0.04
Mn	66.78	0.11	Mo	13.54	0.40
NO_2	10,290	0.04	NO_3	187,100	0.08
Na	97,730	0.04	Nd	15.86	0.30
Ni	18.63	0.04	P	16,060	0.04
PO_4	25,250	0.04	Pb	528	0.23
Re	6.5	0.06	Ru	111	0.24
SO_4	11,530	0.06	Si	9,358	0.04
Sr	211	0.10	TIC	900	0.07
TOC	381	0.06	Te	19.26	0.22
Ti	8.41	0.16	U	208	0.09
V	2.79	0.18	Zn	80.51	0.08
Zr	6.25	0.12			
(Below Det)	(ppm)			(ppm)	
As	432.24	$< DL$	Be	0.11	$< DL$
Ce	77.07	$< DL$	Co	121.64	$< DL$
Dy	4.79	$< DL$	Li	4.93	$< DL$
Rh	74.79	$< DL$	Sb	156.29	$< DL$
Th	57.36	$< DL$	Tl	923.71	$< DL$
	(μCi/g)			(μCi/g)	
^{241}Am	0.07254	0.34	^{243,244}Cm	0.001279	0.50
^{60}Co	0.01527	0.45	^{137}Cs	14.9	0.04
^{152}Eu	0.06748	0.39	^{3}H	0.002167	0.35
^{129}I	3.6-05	0.38	^{237}Np	1.1-04	0.25
^{238}Pu	0.003212	0.25	^{90}Sr	108	0.41
^{99}Tc	0.01648	0.14	Total α	0.1555	0.10
Total β	183	0.37			
	(Mass Spec)			(Mass Spec)	
^{238}Pu/^{239}Pu	0.002729	0.78	^{240}Pu/^{239}Pu	0.03322	0.11
^{241}Pu/^{239}Pu	7.5-04	0.22	^{242}Pu/^{239}Pu	3.6-04	0.22
^{234}U/^{238}U	6.4-05	0.05	^{235}U/^{238}U	0.006757	0.003
^{236}U/^{238}U	1.1-04	0.02			

* RSD = Relative Standard Deviation (StDev/Mean)
< DL = Below Detection Limit

2 Description of Data

Seven cores were extracted through four riser-locations (see Figure 1) paired at opposite ends of the B110 tank[1]. A core from this tank consists of five 19-inch segments which were sequentially extracted by the coring machine. Two separate mixing procedures formed two different types of samples: segment-level and composite-level samples.

A **segment-level** sample was created by mixing (homogenizing in a milkshake-like blender) the contents of a segment, to produce a sample yielding information about vertical variations in the tank with a resolution limit of 19 inches. The **composite** sample was created by mixing portions of each segment-level sample from a core together. If the mixing step is efficient, the composite sample should provide the best data for determining average concentration in a core (or tank). For both the homogenized segment-level and composite-level samples, two replicates were analyzed to evaluate adequacy of mixing.

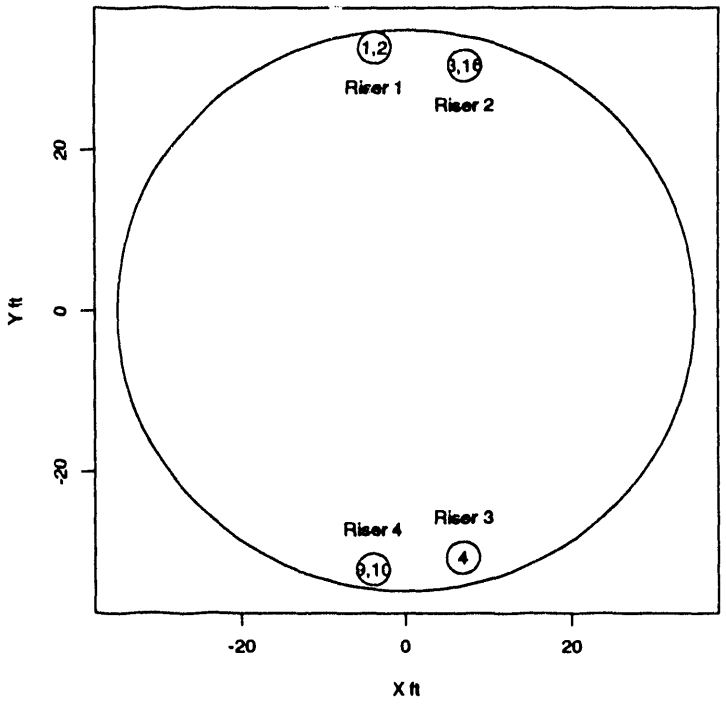

Figure 1: Positions of Cores and Risers in Tank B110

At the end of the segment-blending step, an aliquot of mixed solids was removed from the top of the container. The bulk of the contents of the milkshake container was poured onto a tray and a second aliquot was then taken from the bottom of the container. These two aliquots were submitted for ICP-fusion and GEA-fusion analyses to allow a determination of the adequacy of blending.

[1] Riser-location 2 consists of two risers adjacent to each other.

The remaining sample in the blender was poured onto the mixing tray, and the segement samples needed for the other chemical analyses described in Table 3 were obtained. The next step was to remove a sub-sample from each homogenized segment sample to produce a core composite sample. The core composite sample consists of a set percentage by weight of each homogenized segment sample, which is remixed in the "milkshake" blender. After blending this core composite sample, an aliquot was removed from the top of the container and most of the material poured onto a tray. A second composite sample was removed from the bottom of the blender. These two core composite samples were submitted for ICP-fusion and GEA-fusion analyses to evaluate the efficiency of mixing. Finally, the blended material in the tray was subsampled numerous times to create all the other core composite aliquots required to perform the analyses described in Table 3.

For the ICP-fusion and GEA-fusion analyses the above sampling and blending strategy often produced three data points for ostensibly the same sample. These three samples for either a segment or core composite are the "top", "bottom" and final random sample taken from the tray when all aliquots are dispensed for the various analyses. These three data points can be statistically evaluated to assess the adequacy of mixing.

A second check on mixing is to take the average concentrations of analytes from all segments of a given core and compare this value with the core composite value. These types of statistical evaluations and others are described further in this report.

Since the dominant interest for characterization is to measure average properties within a tank, the composite data will constitute the majority of data produced for future tanks. However, for B110, extensive segment-level data was produced, so that vertical variations in the tank could be analyzed and so that the composite measurements could be compared to the segment-level measurements.

2.1 Chemical Analysis Methods and Reporting Units

For each sample, the number of constituents chemically analyzed depended on the number of isotopes found in gamma energy analyses. Typically, about 50 to 70 constituents (including isotopic ratios) were measured on B110 core samples. The analytical methods employed on most cores are listed in Table 3, along with the specific analytes measured. Many of the analyses yielded results below the detection limit, so the measurements present on a specific core may not include all the analytes listed in the table (see Table 2 for the analytes that are consistently below their detection limits).

Inductively coupled plasma emission spectroscopy (ICP) was used to measure inorganic metals and selected anionic elements on samples prepared by three pretreatments. The first pretreatment technique was to fuse a small weight of solid sample in a large amount of KOH (potassium hydroxide). After dissolution of the fused material in hydrochloric acid (HCl), the sample was analyzed. This treatment resulted in a total dissolution of the original core solids but also led to a rather large dilution of trace constituents because of the large quantity of KOH and HCl used compared to original core material. The KOH fusion results yield the most realistic values for silicon (Si) and perhaps aluminum (Al), iron (Fe), phosphorus (P), bismuth (Bi) and other refractory oxides compared to results from other pretreatments. The ICP fusion method cannot be used to measure potassium (K) because of the use of KOH. Also, fusion pretreatment adds considerable contamination of metals such as nickel (Ni) and zirconium (Zr) which originates from the crucible used to heat the KOH/sample flux. The PNL analytical chemists reported values for Zr, but deleted all Ni results because of the crucible contamination.

The second pretreatment for ICP analyses was digestion of core solids in a mixture of concentrated nitric and hydrochloric acids. This pretreatment does not guarantee complete dissolution of all the core matrix, especially Si, but does generally dissolve a high percentage of the trace metals of interest. Because the ratio of core solids digested in the acid is much higher than the ratio for KOH fusion, the resultant solutions are more concentrated in trace metals and yield more useful data.

The final ICP sample pretreatment is a water leach with a known mass of tank solids in deionized water for a set time period (in this case several hours). Depending on the slurry pH, a water leach is expected to dissolve only the most soluble constituents such as alkali metals (Na, K, Li, Cs) and portions of the moderately soluble alkaline-earth metals (Ca, Mg, Sr, Ba) as well as anions (halogens, NO_2, NO_3 and SO_4). A comparison of the ICP water leach results with the ICP acid digestion and KOH fusion results identifies

Table 3: Analytic Techniques and Analytes Measured

Core Pretreatment Scheme Detector*	Clean Up	Analytes
KOH fusion/HCl dissolve		
ICP	NO	Ag, Al, As, B, Ba, Be, Ca, Cd, Ce, Co, Cr, Cu, Dy, Fe, La, Li, Mg, Mn, Mo, Na, Nd, P, Pb, Re, Rh, Ru, Sb, Se, Si, Sr, Te, Th, Ti, Tl, U, V, Zn, Zr, Bi
GEA	NO	^{60}Co, ^{134}Cs, ^{137}Cs, ^{154}Eu, ^{155}Eu, ^{144}Ce, ^{106}Ru, ^{153}Gd, ^{241}Am
GP	NO	Total Alpha, Total Beta
LF	NO	U
GP	YES	90Sr, 99Tc
GEA	YES	129I
AEA	YES	^{241}Am, $^{243,244}Cm$, ^{238}Pu, $^{239,240}Pu$, ^{237}Np
MS	YES	$^{234}U/^{238}U$, $^{235}U/^{238}U$, $^{236}U/^{238}U$, $^{238}Pu/^{239}Pu$, $^{240}Pu/^{239}Pu$, $^{241}Pu/^{239}Pu$, $^{242}Pu/^{239}Pu$
Mixed HNO_3/HCl acid dig.		
ICP	NO	Ag, Al, As, B, Ba, Be, Ca, Cd, Ce, Co, Cr, Cu, Dy, Fe, La, Li, Mg, Mn, Mo, Na, Nd, Ni, P, Pb, Re, Rh, Ru, Sb, Se, Si, Sr, Te, Th, Ti, Tl, U, V, Zn, Zr, Bi
HNO3 acid digestion		
AAGF	NO	As, Se, Sb, Tl, Pb
Core Material		
CVAA	YES	Hg (H_2SO_4 digestion)
UV-VIS	YES	CN
Water Leach		
ICP	NO	Ag, Al, As, B, Ba, Be, Ca, Cd, Ce, Co, Cr, Cu, Dy, Fe, La, Li, Mg, Mn, Mo, Na, Nd, Ni, P, Pb, Re, Rh, Ru, Sb, Se, Si, Sr, Te, Th, Ti, Tl, U, V, Zn, Zr, Bi
IC	NO	F, Cl, NO_2, NO_3, PO_4, SO_4
CA	NO	Total inorganic carbon, Total dissolved organic carbon
UV-VIS	NO	Cr(VI), NH_3
GEA	NO	^{134}Cs, ^{137}Co, ^{155}Eu, ^{154}Eu, ^{241}Am, ^{144}Ce, ^{60}Co, ^{106}Ru, ^{153}Gd
GP	NO	Total Alpha, Total Beta
LF	NO	U
GP	YES	^{90}Sr, ^{99}Tc
GEA	YES	^{129}I
LS	YES	^{3}H (distillation), ^{14}C
AEA	YES	^{241}Am, $^{243,244}Cm$, ^{238}Pu, $^{239,240}Pu$ and ^{237}Np

* See Appendix A for a description of detector codes

the percentages of a given analyte that are readily soluble in aqueous solutions similar to groundwaters, natural recharge waters, etc.

Two pretreatment schemes, KOH fusion and water leach, were also used to prepare samples for radionuclide analyses. Again the KOH fusion pretreatment is expected to dissolve all the material and yield useful results for the most concentrated and most insoluble radioisotopes. The water leach sample provides data on readily leachable radionuclides, such as ^{137}Cs, ^{99}Tc, and ^{3}H.

A few of the trace metals (As, Se, Sb, Tl and Pb) are not analyzed very well by ICP. A separate sample of core material was acid digested with nitric acid for subsequent analysis by graphite-furnace atomic absorption (GFAA). Further, an aliquot of core material was digested in sulfuric acid and then treated to release mercury (Hg) directly into a cold vapor atomic absorption system (CVAA). The water extract of core material was also used to measure hexavalent chromium [Cr(VI)] and ammonia by UV-VIS spectroscopy.

Radiochemical analyses for specific radionuclides such as ^{90}Sr, ^{99}Tc, ^{129}I were performed on both KOH fusion-treated and water-leached core material. A comparison of the fusion and water-leached results for specific radionuclides yields useful data on the relative mobility of the nuclides in natural aqueous solutions, such as groundwater. This information can be used to evaluate contaminant mobilities for water infiltration and subsequent leakage from tanks. Similar comparisons for U (measured by laser fluorescence) and trace metals (measured by ICP) can be used for risk assessment.

The data was originally condensed into 7 bound volumes, one for each core, after thorough review by analytical chemists. ICP instrumental readings below the 3σ value for background were designated as below detection limit. Values between 3σ and 10σ of background were noted as provisional, meaning that the chemists have less confidence in the quality of these data. Data values above the 10σ background value (the "quantitation" limit) are considered to be of high quality. All the IC and carbon analyzer data were well above the instrument detection limits. Therefore, these data should be considered of high quality. The percent uncertainty or error in counting are given for all radionuclide measurements for which values are reported in the bound data reports.

All data values reported in the bound core reports are based on the wet mass of solids used in each test. The percent moisture content of homogenized segments and core composites was often determined in duplicate on small samples subjected to scanning thermogravimetry up to temperatures of 150C. On other larger samples of homogenized segment and core composite samples, the percent moisture was determined by traditional oven-drying at 105C in an oven. The latter technique is preferred, but when no oven drying data are available, the scanning thermogravimetric data can be used to convert wet mass data to dry mass data for specific segments.

2.2 Descriptive Statistics and Plots of Raw Data

The complete electronic database consists of 9,179 measurements taken on 7 cores extracted from the B110 tank. A description of the format of this data set is given in Appendix A.

Figure 1 illustrates the locations of the cores extracted from the tank. The seven cores were extracted from four riser-locations located in pairs at opposite ends of the tank. The riser pairs were about 10 feet apart, while the risers at opposite ends of the tank were separated by 70 feet. "Replicate" cores were taken from Risers 1, 2 and 4 to evaluate sampling repeatability. Riser-location 2 actually consisted of two risers separated by about 3 feet. Since these two risers were so close together, they were grouped into one riser-location. In this report, we will refer to the four riser-locations as risers for the sake of simplicity.

To obtain the most useful information from the sampling campaign, cores should be taken on some sort of regular grid within the tanks. Closely spaced coring locations such as risers 1 and 2 can result in inefficient sampling. The pattern of riser locations has implications for the ANOVA analysis, also. The pattern in Figure 1 suggests that our analysis should provide for the possibility of both long and short-distance spatial variations. These two types of spatial variations are not necessarily equivalent and the pattern in Figure 1 will produce estimates for spatial variability that are mixtures of long and short-distance spatial variations.

All 9,179 measurements present in the B110 data set were not fitted to ANOVAs. Approximately 60% of the measurements were deleted for one of the following reasons:

Table 4: Preferred Measurement Method for Tank B110 Constituents

Constituent	Meas. Method	Constituent	Meas. Method	Constituent	Meas. Method
Ag	ICP:A	Al	ICP:A	^{241}Am	GEA:F
As	ICP:A	B	ICP:A	Ba	ICP:A
Be	ICP:A	Bi	ICP:F	^{14}C4	RAD:W
Ca	ICP:A	Cd	ICP:A	Ce	ICP:A
^{144}Ce	GEA:F	Cl	IC:	^{243,244}Cm	RAD:F
Co	ICP:A	^{60}Co	GEA:F	Cr	ICP:A
^{134}Cs	GEA:F	^{137}Cs	GEA:F	Cu	ICP:A
Dy	ICP:A	^{152}Eu	GEA:F	^{154}Eu	GEA:F
^{155}Eu	GEA:F	F	IC:	Fe	ICP:F
^{153}Gd	GEA:F	^{3}H	RAD:W	^{129}I	RAD:F
K	ICP:A	La	ICP:A	Li	ICP:A
Mg	ICP:A	Mn	ICP:A	Mo	ICP:A
NO_2	IC:	NO_3	IC:	Na	ICP:F
Nd	ICP:A	Ni	ICP:A	^{237}Np	RAD:F
P	ICP:F	PO_4	IC:	Pb	ICP:A
^{238}Pu	RAD:F	^{238}Pu/^{239}Pu	MASS:	^{239,240}Pu	RAD:F
^{240}Pu/^{239}Pu	MASS:	^{241}Pu/^{239}Pu	MASS:	^{242}Pu/^{239}Pu	MASS:
Re	ICP:A	Rh	ICP:A	Ru	ICP:A
^{106}Ru	GEA:F	SO4	IC:	Sb	ICP:A
Se	ICP:A	^{75}Se	GEA:F	Si	ICP:F
Sr	ICP:A	^{90}Sr	RAD:F	TIC	IC:
TOC	IC:	^{99}Tc	RAD:F	Te	ICP:A
Th	ICP:A	Ti	ICP:A	Tl	ICP:A
Total α	RAD:F	Total β	RAD:F	^{234}U/^{238}U	MASS:
^{235}U/^{238}U	MASS:	^{236}U/^{238}U	MASS:	U	RAD:F
V	ICP:A	Zn	ICP:A	Zr	ICP:A

(Measurement method codes are explained in Table 17, Appendix A)

- Measurements associated with certain constituents were too incomplete to allow estimates of average concentrations or the desired variance components.
- Too many of the measurements were below detection limit to allow a meaningful analysis.
- For each component, only data associated with the "best" chemical analysis method was utilized.

Table 4 specifies which measurement technique was used for each analyte. Since one of the objectives of the analysis is to measure the best average concentration for each constituent, the best analytical method was chosen to do this. Although other data is available, such as water extracts of metals and radionuclides, only the data expected to give the best value for total tank inventory is used.

Table 5 summarizes the measurements used within this report. The table lists the number of measurements associated with each sample method (Composite and Segment Level) and also shows how the measurements are spatially distributed in the tank. A cell in the table lists the number of measurements taken at a particular location in the tank. The number consists of various sorts of replicate measurements taken on up to 80 different constituents.

This table illustrates a very important point about the measurements: they are not *balanced*. In other words, the same set of measurements was not taken at every sampled location in the tank. Because the data is not balanced, it is not easy to compare the results obtained for different constituents. For example, the average concentration of one constituent may differ from another, simply because the first constituent was

Table 5: Overview of Measurements Taken in B110

Segment	Riser 1		Riser 2		Riser 3	Riser 4	
	Core 1	Core 2	Core 3	Core 7	Core 4	Core 5	Core 6
1	0[1]	47	0	0	0	12	0
	0[2]	12	0	0	0	3	0
2	148	107	0	0	130	0	0
	52	54	0	0	49	0	0
3	126	126	126	54	131	117	158
	52	52	52	18	50	50	60
4	126	108	0	0	131	0	0
	52	54	0	0	50	0	0
5	126	127	106	54	149	129	157
	52	53	53	18	50	53	60
comp	212	136	270	140	174	155	156
	68	56	62	61	69	61	60
	Total Measurements = 3,740						

[1] Number of measurements taken
[2] Number of constituents measured

sampled at different locations than the second. ANOVA procedures can mitigate the effects of unbalanced data, but cannot solve all problems. When too much data is missing, it is not possible to obtain unbiased estimates of average concentration or correct confidence bounds.

From Table 5, one can see the problems associated with unbalanced (or missing) data are more severe for the segment-level data. In fact, there is no data for several of the core-segments listed in the table. A particular problem exists with segment 1, the segment closest to the surface of the waste. For all except one core, the sampler had problems recovering the first segment. Consequently, information concerning the waste "crust" originates from only one location in the tank. Since information concerning the first layer in the tank was so sparse, all segment 1 data was analyzed separately from the main body of data.

Table 6 lists the number of measurements for each type of analysis that were above and below the detection limit. Under some conditions, the proportion of nondetections is substantial. If the detection limit of the analytical procedure is low, so that a measurement below the detection limit could be considered insignificant, the problem might be ignored. However, in many cases, the detection limit is not insignificant.

Table 6: Detection Limit Summary

Analysis Method	Composite		Segment	
	Above DL	Below DL	Above DL	Below DL
GEA:F	82	0	114	0
IC:	112	0	416	0
ICP:A	314	148	666	522
ICP:F	211	83	384	134
MASS:	42	0	0	0
RAD:F	228	0	259	0
RAD:W	25	0*	0	0*
total	1014	231	1839	656

*Many nondetects on preliminary water leach analyses caused test to be dropped

In fact, the detection limit is not even fixed; the detection limit for a particular constituent may vary by an order of magnitude or more. These complicating factors mean that values below the detection limit must be carefully dealt with.

For these analyses, we have eliminated constituents that are mostly (i.e., more than 85% of the time) below the detection limit. For all other constituents, the actual measurement is used instead of the detection limit. Fortunately, for the majority of constituents, the proportion of non-detects is low and non-detections aren't a significant problem. The detection limits exhibited in B110 should be typical for a bismuth phosphate waste tank. Other tanks contain predominately REDOX or PUREX waste and should exhibit an entirely different detection limit pattern.

Appendix B presents detailed plots of the raw data summarized in Table 5, as well as tables of summary statistics. The constituents in the data set are divided into 4 categories: metals, anions, radionuclides, and isotope ratios. The variability illustrated by the box-plots is a complicated mixture of sampling, measurement, and spatial variability. The plots in Appendix B provide the best overview of the data-set. A few important conclusions that these simple plots suggest are as follows:

1. "Outliers" occur in the data. Occasionally, one of the box-plots will have a tail that stretches over many orders of magnitude.

2. The anion measurements exhibit the lowest variability.

3. The composite and segment level box-plots generally match up, although there are a few constituents (such as ^{241}Am, ^{90}Sr, and Ag) that do not. Compare the segment and composite plots in Appendix E.

2.3 Statistical Models

Both segment-level and composite sampling produces data that can be most reasonably described as a random effects nested design (See [10] and [7]). In these models, each observation contains many different types of variability (measurement, mixing, sampling, and spatial) which are to be estimated. In order to successfully estimate these different sources of variability, the measurements must be taken according to a specific sampling design. For most constituents, the existing data allows acceptable estimation of the desired variance components.

The core-composite ANOVA model is a simplified version of the core-segment-level model. Compositing simply eliminates a term in the segment-level model. We have utilized several variants of the two basic models presented below to test certain assumptions about our analysis methods and quantify uncertainties from various sources. We generally believe that the presented model provides an adequate description of the B110 data.

2.3.1 Segment-Level ANOVA Model

The measurement of a particular constituent, which we identify as Y_{ijkmp}, can be described by the ANOVA model:

$$Y_{ijkmp} = \mu + Riser_i + Seg_{ij} + Rep_{ijk} + Hom_{ijkm} + Error_{ijkmp} \tag{1}$$

where μ represents the average concentration of the constituent in a tank and the other five terms in the model represent variations from the average. The first additional term, $Riser_i$, represents **horizontal spatial variability** in the tank due to the riser location chosen for the coring. The waste under each riser is divided into 19-inch segments that will be sampled. In the case of the B110 tank, the waste consists of 5 segments, with the top segment numbered one. The term Seg_{ij} represents the deviations of segment j from the riser average and therefore describes the **segment (or vertical) variability** in the tank.

Three of the four sampled risers in B110 were cored twice, resulting in replicate segment measurements. The term Rep_{ijk} represents the variability displayed by these replicate measurements. The term Hom_{ijkm} represents the **homogenization or mixing variability** present in the homogenized segments. Finally, the term $Error_{ijkmp}$ represents **laboratory measurement error.**

The index assigned to an individual observation, Y_{ijkm} therefore describes all the sources of variability it was exposed to. Specifically, the components of the index identify the following:

i: the riser ($i = 1, 2, 3, 4$) that the measurement originates from

j: the segment within the riser ($j = 1, 2, 3, 4, 5$) that the measurement originates from

k: the replicate segment sample ($k = 1, 2$) taken from riser i and segment location j

m: the sample taken from the homogenized segment ($m = 1, 2, 3$) to determine the adequacy of mixing. The first sample was taken off the top of the mixed segment, the second off the bottom, and the third, (which was rarely taken) came from a randomly chosen location.

p: The aliquot (replicate) from the sample that was sent through the laboratory to determine laboratory error. Typically, two aliquots were submitted on each sample ($p = 1, 2$), although for a few select samples 4 aliquots were submitted.

There is a variance associated with each of the terms in this model, and they are denoted by σ^2_{Riser}, σ^2_{Seg}, σ^2_{Rep}, σ^2_{Hom}, and σ^2_{Error}. These variances summarize the adequacy of sampling and measurement procedures. The smaller the variances, the more accurately tank concentration μ can be determined.

2.3.2 Composite Data ANOVA Model

The segment-level samples taken from a core are blended together to form a composite sample. For this tank, 4 complete segments were recovered, so a composite was formed by mixing together 8 samples (2 samples from each segment). Mixing the segment material together basically eliminates one term in Formula 1. The segment term Seg_{ij} is eliminated to produce a description of the data with the form

$$Y'_{ijmp} = \mu' + Riser'_i + Rep'_{ij} + Hom'_{ijm} + Error'_{ijmp} \tag{2}$$

What is the relationship between the composite and segment level models? If nothing unusual is happening during the compositing, one would expect that both models would provide the same estimate of what is in any core. In mathematical terms, this means

$$\mu' + Riser'_i = \mu + Riser \tag{3}$$

Now, it is possible for the composite and segment-level data to yield different estimates. For example, if the segments are quite different chemically, compositing may produce chemical reactions that will alter the concentration of a constituent. It may also be difficult to blend together segments that are quite different physically. However, for the type of waste obtained from B110, one would not expect such problems because the waste is fairly homogeneous.

The composite samples should, in fact, exhibit less variability than the segment samples, because they have gone through an additional stage of blending. On this basis, one would expect the composite data to provide better average concentration estimates than the segment level data – and to require less laboratory analysis. Composite sampling is generally the most efficient way to estimate average concentration. In fact, the most efficient sampling scheme for estimating average tank concentration would utilize a composite sample formed from all cores from the tank. However, since our objective is not only to estimate the average, but also to quantify vertical variability within the tank, segment samples were required.

3 Estimates of Variance Components

The variance components presented in this section were obtained by fitting the segment-level model in Section 2.3.1,

$$Y_{ijkmp} = \mu + Riser_i + Seg_{ij} + Rep_{ijk} + Hom_{ijkm} + Error_{ijkmp} \tag{4}$$

and the composite model in Section 2.3.2,

$$Y'_{ijmp} = \mu' + Riser'_i + Rep'_{ij} + Hom'_{ijm} + Error'_{ijmp} \tag{5}$$

to the analytical data from Tank B110. The statistical computing package used to fit the models is the variance component procedure, "varcomp," described in Reference [9]. The restricted maximum likelihood (REML) method was used to estimate the variances as explained in Reference [2].

The data set for these analyses consisted of a measured value and an associated detection limit for every constituent; the measured value was present even if the value was below the detection limit. If a constituent had 85% or more of its measured values reported as less than detection, then a model was not fit for that constituent. This resulted in no model fits for Arsenic (As), Beryllium (Be), Cerium (Ce), Cobalt (Co), Dysprosium (Dy), Lithium (Li), Rhodium (Rh), Antimony (Sb), Thorium (Th), and Thallium (Tl). For all other constituents, the measured value was used as the actual value whether or not the value was less than detection.

It should be noted that the detection limit for certain constituents is reported as 0 in the database; A zero here means that the detection limit was not recorded in the database because all measured values for that constituent were above the detection limit. The number of less-than values and the total number of observations reported for each constituent is presented in the variance component tables of Appendix C.

The results of fitting Models (4) and (5) to the segment-level and composite data are summarized in Appendix C. In this Appendix, relative standard deviations (RSD) quantify the variance components for the model terms. A RSD is the ratio of a standard deviation to the mean. It is a unitless measurement of variability and allows comparisons of variability across constituents whose magnitudes might differ widely. The RSD is computed by dividing the square root of the variance component by the estimated mean concentration μ.

Each constituent was fit to the appropriate models independently of the other constituents, so these fits do not model any multivariate relationships that may be present in the data. The subsections that follow contain summaries of the segment-level and composite RSD results.

3.1 Segment-Level Results

Complete results for the ANOVA fits to segment level data are reported in Appendix 6.4. The tables in this appendix contain the RSDs associated with each variance component, as well as the associated degrees of freedom. The degrees of freedom indicates how many "independent" observations are available to estimate each variance component. One would like to have 5 to 10 degrees of freedom for each variance component.

As one can see from the results presented in Appendix 6.4, not all terms in the ANOVA could be estimated for each constituent. For example, the homogenization term is only present on a subset of the constituents listed in the tables. The data is simply not complete enough to allow all variance components to be measured on each constituent.

Incomplete data also affects some of the variance components that can be estimated. Perhaps the most severe problem of this nature has to do with the term Seg_{ij}, which describes vertical variations. We know that the waste tank has a crust, and material from this crust is present in segment 1 and segment 2 extractions. (Segment 1 is entirely composed of this crust, while segment 2 contains varying amounts of the crust). From the very limited segment 1 data available, we know that the crust is much different than the rest of the waste (See Tables 11 and 12). Unfortunately, for most constituents, no segment-1 measurements were available, and very few segment-2 measurements; so the segment-level data contains almost no information concerning this crust. Therefore, for most constituents, the RSD associated with vertical variability is only describing the vertical variability in a portion of the tank.

Table 7: Summary of Segment-Level Outlier Values

	Riser	Core	Seg	Sample	Aliquot	Value	Detection Limit	Units
Bi	riser01	core01	seg02	samp1	al-2	23863	0	ppm
Cl	riser03	core04	seg02	samp1	al-1	1630	0	ppm
^{60}Co	riser02	core16	seg03	samp1	al-2	1.244000	0	μCi/g
Cr	riser03	core04	seg02	samp1	al-1	640	7	ppm
^{137}Cs	riser01	core01	seg02	samp1	al-2	37.92	0	μCi/g
Fe	riser01	core01	seg02	samp1	al-2	23754	54	ppm
NO_3	riser03	core04	seg04	samp2	al-2	142000	0	ppm
Na	riser01	core01	seg02	samp1	al-2	106543	354	ppm
Ni	riser02	core03	seg05	samp1	al-2	86	6	ppm
P	riser01	core01	seg02	samp1	al-2	17535	3993	ppm
^{238}Pu	riser04	core10	seg03	samp1	al-2	0.01234234	0	μCi/g
SO_4	riser03	core04	seg05	samp2	al-2	15000	0	ppm
Si	riser01	core01	seg02	samp1	al-2	11281	328	ppm
TIC	riser03	core04	seg02	samp3	al-1	2430	0	ppm
Total β	riser01	core01	seg02	samp1	al-2	1054.054054	0	μCi/g
Zr	riser01	core02	seg05	samp1	al-1	31	3	ppm

When the segment-2 measurements did occur, they were usually taken at only one riser location (riser-1, see Table 5), so it was not possible for the ANOVA procedure to always determine whether a variance in the second segment was due to horizontal or vertical effects. A similar problem occurs between the Seg_{ij} and Rep_{ijk} terms. Incomplete data can make it difficult for the ANOVA procedures to distinguish between segment and replicate coring variability. A good example of this is the segment 2 measurements for Al. Two segment 2 core replicates were taken from riser 1 and they resulted in an estimate of 2061 ppm for the first replicate and 190 ppm for the second, a huge difference. The ANOVA model would classify this as replicate variability, but it is probably due to crust material that was present in the first replicate but not the second.

Suspect values were identified in the segment-level data by looking at replicate values within a segment-core combination. If one value was much larger (or smaller) than the rest of the values, then it was regarded as suspect and was not included in the analysis. If there were only two values within the segment-core combination, then the value was compared with the values for other segments within that core. If the value was much larger (or smaller) than the other values within the core then it was regarded as suspect and was not included in the analysis. A summary of the values omitted from analysis is presented in Table 7. Note that 7 out of the 16 suspect values are from Core 1, Segment 2, Sample 1, Aliquot 2. This may be an indication of a problem with that particular sample. In general, outliers seem to occur at a rate of 1 in 125 measurements. This statistic provides an important description of laboratory reliability.

Figure 2 presents box-plot summaries of all the variance components presented in Appendix C.1. Each box-plot displays the following information about the RSD values. The line inside the box represents the median RSD, and the box itself contains 50% of the RSD values. The "whiskers" on the boxes identify the maximum and minimum RSD values. One would like to see a clear ordering of the different RSD values in Figure 2 but such a simple pattern does not exist. From the length of the whiskers on the box-plots, one can see that RSDs are occasionally very large. It is important to note that these summarize the RSDs *after* the outliers were removed.

Table 8 gives results from a significance test conducted on the variance components. This test determines whether or not the variance component is significantly different from zero. Significance is measured by a P-value which represents the chance that a RSD as large as the one obtained could occur when the RSD is actually zero. Significance tests were only conducted on constituents with a "complete" set of data; that is, for which all variance components in model 4 could be estimated. The tests that are significant at the 10%

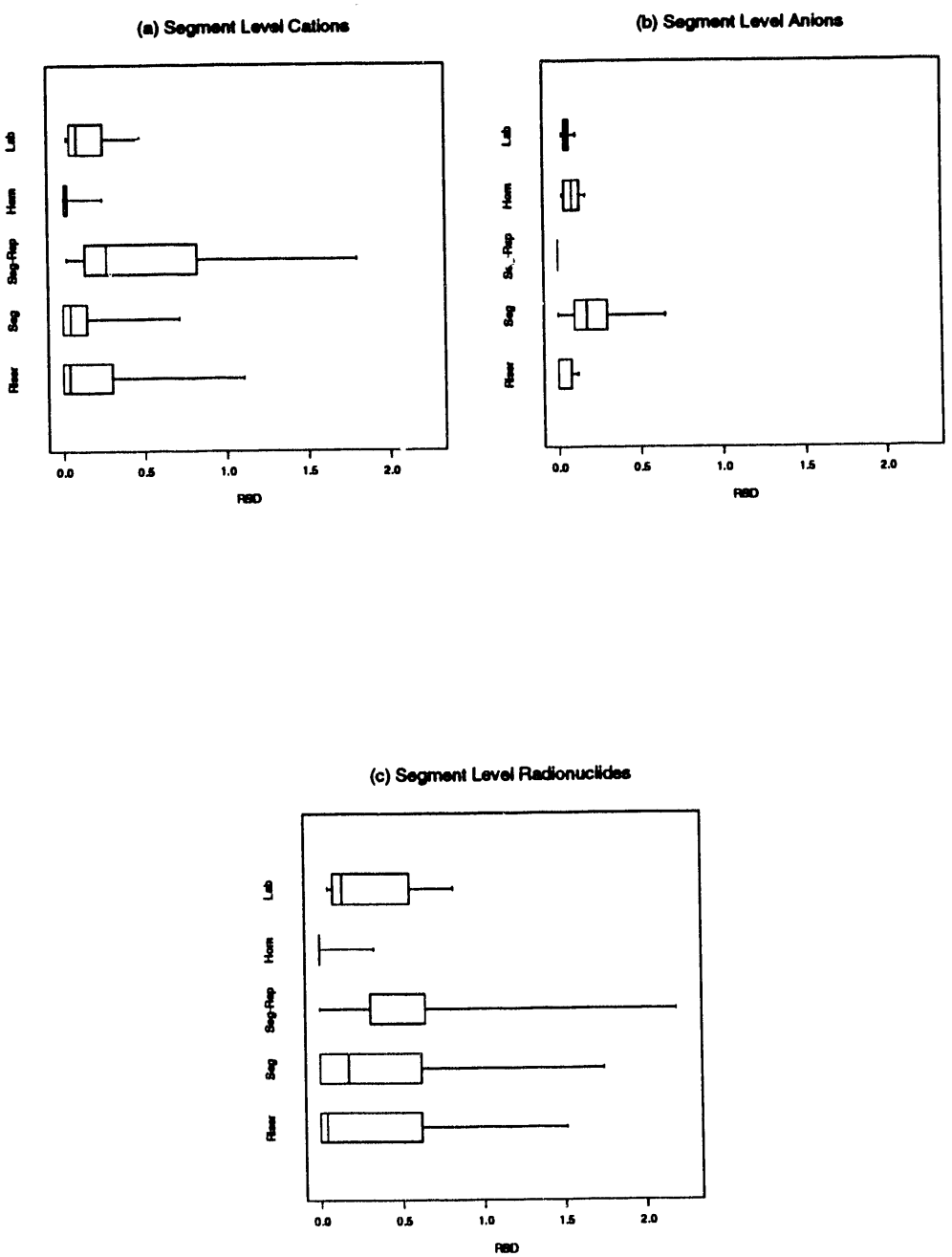

Figure 2: RSD Distributions for Variance Components Calculated from the Segment-Level Data

Table 8: Level of Significance for Segment-Level Variance Components

Constituent	Variance Component P-Values			
	Riser	Segment	Seg-rep	Homog.
		Cations		
Bi	0.11	0.60	*0.00	0.14
Fe	0.66	0.17	*0.001	0.85
Na	1.00	0.09*	0.28	0.18
P	0.94	0.20	*0.07	0.20
Si	*0.02	0.24	*0.07	0.84
U	1.00	*0.001	*0.00	1.00
		Anions		
Cl	*0.06	1.00	1.00	*0.00
F	1.00	*0.07	1	*0.00
NO_2	1.00	*0.00	1.00	*0.00
NO_3	1.00	*0.001	1.00	0.20
PO_4	0.99	*0.01	1.00	0.65
SO_4	1.00	0.21	1.00	*0.00
TIC	1.00	*0.00	1.00	*0.00
TOC	0.92	0.12	1.00	*0.001
		Radionuclide		
^{60}Co	0.56	0.12	0.80	0.73
^{137}Cs	1.00	*0.002	1.00	*0.01
Total α	1.00	0.90	*0.00	0.94
Total β	1.00	1.00	*0.00	1.00

* Significant at 10% level

level are marked with an asterisk.

One can extract several important conclusions about the segment-level RSDs from the tables and plots presented in this section:

1. Overall variability for the anions appears to be smaller than for the other constituent groupings.

2. Cobalt 60 (^{60}Co) appears to behave differently than the other radionuclides. In Figure 2(c), the maximum RSD for laboratory, homogenization, segment, and riser are all from ^{60}Co. See Table 29 for the specific RSD values.

3. The homogenization RSD is generally small. For the cations (Table 26, Appendix C), there were only six constituents that had enough data to estimate the RSD for homogenization. Among those six the homogenization RSDs are always the smallest among the model terms. For the radionuclides (Table 29), the homogenization RSD is almost always estimated to be 0 and is always the lowest among model terms. However, for the anions (Table 28), the homogenization RSD is almost always slightly higher than the laboratory RSD.

   From the significance tests reported in Table 8, most of the homogenization RSDs are not significantly different from zero, except for the anions. The majority of the anion homogenization RSDs are significantly different from zero, but they are comparable in magnitude to laboratory measurement error. Even though anion RSDs are significantly different from zero, they are not considered to be large.

4. The segment-replicate term describes how repeatable core-sampling is. The segment-replicate RSDs are the largest component of variation (see Figure 2) except for anions. This indicates that the present core sampling procedure is not producing a repeatable description of what's in the tank; at least not at segment-level resolution.

Table 9: Composite Values Omitted from Analyses as Suspect

	Riser	Core	Sample	Aliquot	Value	Detection Limit	Units
^{60}Co	riser02	core16	samp2	al-2	0.32	0	μCi/g
Cr	riser03	core04	samp1	al-2	1925	1	ppm
^{137}Cs	riser01	core01	samp3	al-2	3.65	0	μCi/g
^{137}Cs	riser01	core01	samp5	al-2	3.65	0	μCi/g
Fe	riser01	core01	samp1	al-1	28417	30	ppm
K	riser03	core04	samp1	al-2	1146	66	ppm
Mg	riser04	core10	samp1	al-2	251	0.17	ppm
Mn	riser03	core04	samp1	al-2	195	0.19	ppm
Mo	riser03	core04	samp1	al-2	37	2	ppm
Ni	riser03	core04	samp1	al-2	610	3	ppm
^{237}Np	riser01	core01	samp2	al-1	0.00049	0	μCi/g
Total β	riser03	core04	samp2	al-2	382	0	μCi/g
V	riser03	core04	samp1	al-2	8	1	ppm

5. Spatial variability is described by the two terms, riser and segment RSDs. The riser RSD measures horizontal variability, while the segment RSD measures vertical. The Riser RSD is generally not significantly different from zero (See Table 8); Only one out of 18 riser RSDs is significant, so horizontal variability does not appear to be the major source of spatial variability. (Of course this result might have been different if we had sampled from a different set of riser locations)

   On the other hand, many constituents do display a vertical variability. For the anions, vertical variability seems to be the largest form of variability. In many cases, the vertical variability seems to be associated with the crust at the top of the tank. One would expect vertical variability to have been the largest source of variability if a consistent set of segment 1 and 2 measurements had been included in the data set. For most constituents, the estimated RSDs presented in Appendix C.1 only describe the vertical variations below the crust.

6. The laboratory RSD appears to be reasonably small for the anions. However, in general, there are no distinct patterns in the laboratory error in relation to the other model terms; i.e., it is not always the smallest or always the largest, etc.

3.2 Composite Results

The relative standard deviations for the composite data are reported in Appendix 6.4 in a format similar to that described in the last section. The composite data is generally more complete than the segment level data. Consequently, interpretation of the ANOVA results associated with this data is easier.

This data was also subjected to an outlier analysis. We found the same types of extreme values in the composite data as we did in the segment-level data. Suspect values were identified in the composite data by looking at replicate values within a core. If one value was much larger (or smaller) than the rest of the values within the core, then it was regarded as suspect and was not included in the analysis. If there were only two values in the core, then both values were kept in the analysis. A summary of the values omitted from analysis is presented in Table 9.

Figure 3 summarizes the results presented in Appendix C.2 in box-plot format. Each box-plot displays the following information about the RSD values: The line inside the box represents the median RSD, and the box itself contains 50% of the RSD values. The "whiskers" on the box identifies the maximum and minimum RSD values. The composite data RSDs tend to be smaller than their segment-level counterparts (compare Figure 3 to Figure 2).

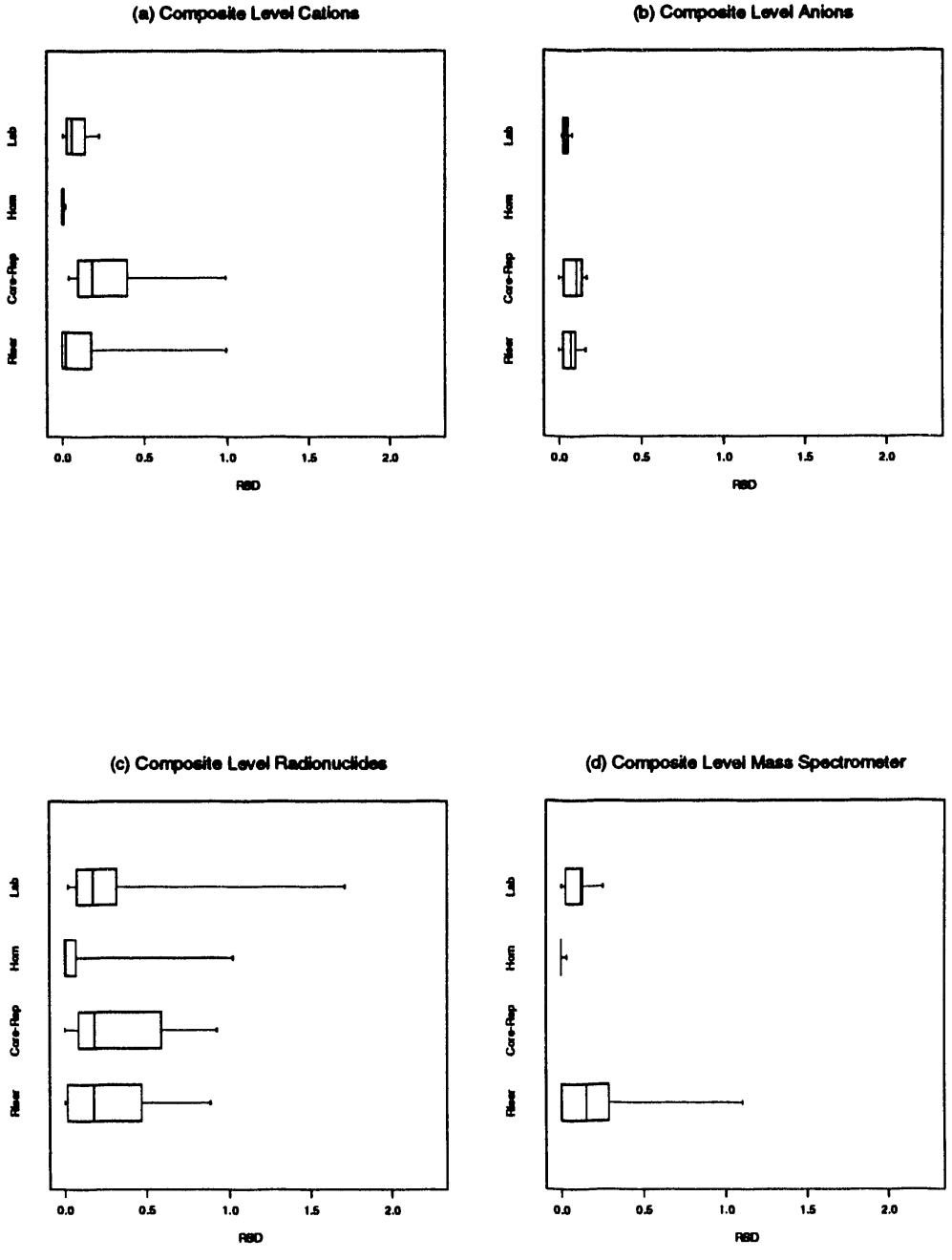

Figure 3: RSD Distributions for Variance Components Calculated from Composite Data

Table 10: Level of Significance for Composite Variance Components

Constituent	Variance Component P-Values Riser	Core	Homog.
		Cations	
Bi	0.154	*0.049	0.691
Fe	0.703	*0.004	1.000
Na	0.576	0.240	0.912
P	1.000	*0.004	1.000
Si	0.269	0.124	0.956
U	0.815	*0.000	0.367
		Radionuclide	
^{241}Am	*0.066	*0.009	1.000
^{243,244}Cm	1.000	0.249	1.000
^{60}Co	1.000	1.000	0.953
^{137}Cs	0.255	*0.021	0.103
^{129}I	1.000	*0.003	1.000
^{237}Np	0.491	1.000	*0.061
^{238}Pu	1.000	*0.028	0.146
^{90}Sr	*0.028	0.553	1.000
^{99}Tc	0.525	0.407	0.262
Total α	1.000	*0.000	1.000
Total β	0.832	*0.000	1.000

* Significant at 10% level

Table 10 presents significance tests for all constituents for which a complete model could be fit. For the composite data, the results of the significance tests are much clearer than for the segment level data. The homogenization RSDs are the least significant source of variability (1 out of 17), the Riser RSDs are also not very significant (2 out of 17), but the replicate RSDs are frequently significant (10 out of 17), indicating that replicate variability is the most significant term. This corresponds with the results presented in the box-plots, of Figure 3.

Some general observations about the composite results are:

1. The overall variability for radionuclides appears to be larger than for the other constituent groupings.

2. Cobalt 60 (^{60}Co) appears to behave differently than the other radionuclides. In Figure 3(c), the maximum RSD for laboratory and homogenization is from ^{60}Co. See Table 33 in Appendix C.2 for the specific RSD values.

3. The homogenization RSD was only estimable for the radionuclide and metal constituents. When estimable, the homogenization RSD was generally the smallest of the RSDs and showed the smallest variability across constituents.

4. The laboratory RSD was estimable for each grouping of constituents (cations, anions, radionuclides, and mass spectrometer). If the homogenization RSDs are ignored and the laboratory RSD for ^{60}Co is ignored, then the laboratory RSD was generally the smallest of the RSDs and showed the smallest variability across constituents. In general, the laboratory RSDs were extremely small for the anion constituents and were largest for the radionuclides. One could conclude that the laboratory introduces more measurement error into the data for radionuclide constituents than for the other constituents. However, as noted above, the laboratory RSD for radionuclides is still the smallest contributor (ignoring the homogeneity term) to the overall variability.

5. The RSD for core replicates was not estimable for the mass spectrometer data. For the other constituent groupings, the RSDs for core varied widely. The core component should represent both the variability due to the coring process and the laboratory's ability to make a core composite out of the individual segments that make up a core. The maximum number of degrees of freedom available for estimating the core RSD was 3. This fact alone could be the greatest cause of the wide variability in the core RSDs. With all this in mind, it can be observed that the core RSDs for the anions were smaller than for the other constituent groupings, and had smaller variability.

6. The riser spatial variability was not generally different from 0, indicating that horizontal spatial variability is the least important source of variability in this data. However, this conclusion must be tempered with the observation that the riser locations used for this sampling would not be expected to produce a great deal of horizontal variability.

3.3 Adequacy of Homogenization Procedure

One important objective for this set of measurements was to determine the adequacy of the homogenization procedure used in sample preparation. As mentioned in Section 2, the contents of each segment were put into a blender to produce a "homogeneous" waste sample. When the composite sample is formed from the segments, this sample is also homogenized. If the homogenization works correctly, all within-segment and within-core variability should be eliminated from the sampling process, which should result in more accurate composite estimates.

To determine whether or not the homogenization procedure worked well, replicate samples were taken from the top and bottom of the blended result and sent through the lab for analysis. The results allowed us to compute a homogenization RSD, which measures the variability in the blended sample. We would like these RSDs to be as small as possible.

Figures 2 and 3 provide a graphical summary of the homogenization RSDs, while Tables 8 and 10 provide the results of a formal significance test on these terms. As one can see from the tables, very few of the homogenization RSDs are significant, except for the anion RSDs. Even though the anion RSDs are significant, they are not large. The average anion homogenization RSD is in fact 9%, a relatively modest value.

Therefore, it is reasonable to conclude that the homogenization procedure is adequate: Homogenization produces a variability that is typically less than the other sources of variability in the data.

3.4 Comparison of Composite and Segment-Level Results

Before comparing the composite and segment-level results, it is useful to identify some of the patterns that would be expected from such a comparison. First, one would expect the RSDs for riser to remain constant; i.e., there is no reason to believe that making a composite sample should change the riser to riser variability. Also, the RSDs for homogenization should be smaller for the composite results. This is because the composite samples are mixed twice, once to homogenize the segments and then again to form the composite sample. The segment-level samples are mixed only once, to homogenize the segment. Another expectation is that laboratory RSDs should remain constant between composite and segment-level results.

3.4.1 Riser RSD

For the comparison of riser RSDs between segment-level and composite data, first consider Figure 2 and Figure 3. The box plots for riser RSDs can be said to be generally the same for segment-level and composite data within each constituent grouping. One must remember that the maximum number of degrees of freedom for risers is 3 for each estimate, so there is a considerable amount of uncertainty associated with these estimates. A constituent by constituent comparison using the tables in Appendix 6.4 and 6.4 reveals that no consistent pattern exists among cation and radionuclide constituents as to how close the two estimates are and/or which is bigger. For the anions, the segment-level RSDs are smaller than the composite RSDs for all but two constituents (Cl and TOC). With these results, there is not enough evidence to contradict our original assumption that the riser RSDs remain constant between the segment-level and composite data.

3.4.2 Homogenization RSD

The homogenization RSDs for segment-level and composite data can also be compared by observing Figure 2 and Figure 3. The box plots indicate that the homogenization RSDs are approximately equal for the cations. No comparison is possible for the anions. For radionuclides, the composite RSDs seem to be larger for the composite data than for the segment-level data which is the opposite of what was expected. A constituent by constituent comparison using the tables in Appendix 6.4 and 6.4 reveals that for 4 out of 6 cation constituents, the composite RSD is smaller than the segment-level RSD. For the radionuclides, 7 out of 11 composite RSDs were smaller than the segment-level RSDs. These numbers indicate that the majority of the composite homogenization RSDs are smaller than their corresponding segment-level RSDs.

3.4.3 Replication RSD

A direct comparison of the replicate RSDs in the composite and segment-level data should not be made, because the two replicates measure agreement on a different spatial resolution. If the replicate variability is small in the composite model, this means that core averages agree between replicates. For the segment-level model, a small replicate variability forces the replicates to agree on a segment level. Since core sampling can be expected to displace layers of waste, one might find that repeatability is poor on the segment-level but acceptable on the composite (core) level.

Comparison of the replication RSD in the composite data and the segment-level data through box plots (see Figure 2 and Figure 3) reveals that the segment-replicate RSDs are larger than the composite RSDs for the cation constituents, smaller for the anion constituents, and approximately the same for the radionuclide constituents. A constituent by constituent comparison from the tables in Appendix 6.4 and 6.4 shows that the segment-replicate RSDs are larger than the composite RSDs for 23 out of 30 possible cation comparisons. For the anions, the segment-replicate RSDs are always less than the core RSDs. For the radionuclides, there are only 4 possible comparisons. For 3 of those 4, the segment-replicate RSDs are larger than the composite RSDs (the exception is ^{137}Cs).

3.4.4 Laboratory Measurement RSD

The laboratory RSDs (see Figure 2 and Figure 3) appear to meet expectations (that they will be similar between segment-level and composite) for the cation and anion constituents. For radionuclides, the segment-level RSDs appear to be larger than the composite RSDs. A constituent by constituent comparison from the tables in Appendix 6.4 and 6.4 reveals that for cations, the absolute difference between segment-level and composite RSDs is less than 0.1 for 22 out of 30 possible comparisons. For absolute differences greater than 0.1, the laboratory RSD was always greater for the segment-level data. For the anions, the absolute difference in RSDs between segment-level and composite is always less than 0.1, but the RSD is always larger in the segment-level data. For radionuclides, there do not appear to be any strong patterns between the segment-level and composite RSDs, but 8 out of 12 were larger for the segment-level data. One could conclude that the laboratory RSDs are approximately equal for the segment-level and composite data, but there does seem to be a slight trend for increased laboratory RSDs in the segment-level data.

4 Concentration Estimates

This section presents ANOVA concentration estimates produced by the fits described in Section 3. Because of the nature of the data, several different types of concentration estimates can be computed, each with a different "resolution." For example, one can calculate the average concentration of a constituent within the entire tank, or the concentration at a particular riser, or at a particular vertical (segment) location within the riser. Standard deviations and confidence bounds can be calculated from the ANOVA fits for each of these different types of concentrations.

For both the segment-level and composite data models, the average concentration is represented by the model term μ, while the riser concentration is represented by the term

$$\mu + Riser_i \ . \tag{6}$$

The segment-level data can also produce a vertical profile for the tank. The model terms that describe a vertical profile are

$$\mu + \frac{1}{n_i}\sum_i (Riser_i + Seg_{ij}) \tag{7}$$

where n_i is the number of risers with an estimate for Seg_{ij}. Standard deviations and confidence bounds for these terms can be calculated using the formulas presented in Reference [4].

4.1 Average Concentration Estimates

A summary of the average inventory estimates is included in Tables 11 and 12. These tables list average concentration estimates calculated from both the composite and segment-level data. The associated relative standard deviations are also listed in the tables. Relative standard deviations range from a low of a few percent to almost 100%.

In most circumstances, there is reasonable agreement between the composite and segment-level averages. However, for 4 constituents, significant differences exist; these are marked by an asterisk. In the case of these 4 significant differences (i.e., Al, Am-241, Np-237, and Sr-90), incomplete segment-level data is the cause. Not enough segments-level measurements were taken to produce a correct description of vertical variability in the tank; no measurements of the most variable segment, segment 2, were included. This causes the RSDs computed for segment-level data to be too optimistic and also produces a bias in the segment level means.

For example the segment-level estimate for Sr-90 was computed from only 4 segments distributed over two risers and two depth locations (3 and 4). These locations display very little variability between each other. On the other hand, the composite measurements, which contain material from segment 2 and therefore some of the waste crust, are about 150 times higher, indicating that the crust is quite radioactive. Independent confirmation of this comes from the Total β measurements, that happened to be performed on each segment of Core 2. Total β for segment 1 is 1441 μCi/g and for the rest of the segments it is between 10 and 20 μCi/g, a factor of 100 difference!

Given the incompleteness of the segment level data, one would always choose the composite estimates over the segment-level estimates. Even if a complete set of segment level measurements had been taken, one would expect the averages calculated from composite data to be better than their segment level counterparts because homogenization seems to be working well. One should therefore use the average concentrations reported under the composite column in Tables 11 and 12 as the most authoritative estimate of tank contents.

As mentioned in Section 3, 10 constituents were not fitted to the ANOVA models, because more than 85% of their measurements were below detection limits. These constituents are also included in Tables 11 and 12. A simple average is reported for these constituents, with no associated RSD.

4.2 Vertical and Horizontal Concentration Estimates

In Appendix D, the ANOVA fits are used to produce vertical profiles from the segment-level data. Constituents with significant vertical heterogeneity are ^{137}Cs, F, Na, NO_2, NO_3, PO_4, SO_4, ^{90}Sr, TIC, ^{99}Tc, U and Zn. Analytes with marginal vertical heterogeneity are Ag, Ca, ^{60}Co, Fe, Mg, P, Si and TOC. Four

Table 11: Average Concentrations of Radionuclides, Isotopic Ratios, and Below Detection Limit Constituents

Constituent	Composite Mean	Composite RSD	Segment Mean	Segment RSD	Segment 1 Mean
	(μCi/g)				
^{241}Am*	0.072	0.34	0.0072	0.10	NA
^{243,244}Cm	0.0012	0.50	0.0014	0.84	NA
^{60}Co	0.015	0.44	0.10	0.96	0.0050
^{137}Cs	14.9	0.03	13.61	0.03	24.1
^{152}Eu	0.067	0.38	0.014	0.32	NA
^{3}H	0.0021	0.35	NA	NA	NA
^{129}I	0.000036	0.38	0.000057	0.26	NA
^{237}Np*	0.00011	0.24	0.000064	0.34	NA
^{238}Pu	0.0032	0.24	0.0038	0.79	NA
^{90}Sr*	108.4	0.40	0.67	0.26	NA
^{99}Tc	0.016	0.14	0.011	0.31	NA
Total α	0.15	0.10	0.11	0.19	0.33
Total β	183.2	0.36	101.5	0.56	729.6
	(ratio)				
^{238}Pu/^{239}Pu	0.0027	0.78	NA	NA	NA
^{240}Pu/^{239}Pu	0.033	0.10	NA	NA	NA
^{241}Pu/^{239}Pu	0.00074	0.22	NA	NA	NA
^{242}Pu/^{239}Pu	0.00036	0.22	NA	NA	NA
^{234}U/^{238}U	0.000063	0.04	NA	NA	NA
^{235}U/^{238}U	0.0067	0.002	NA	NA	NA
^{236}U/^{238}U	0.00011	0.022	NA	NA	NA
Below Det.	(ppm)				
As	432	$< DL$	504	$< DL$	NA
Be	0.11	$< DL$	0.21	$< DL$	NA
Ce	77	$< DL$	109	$< DL$	NA
Co	121	$< DL$	157	$< DL$	NA
Dy	4.79	$< DL$	7.89	$< DL$	NA
Li	4.93	$< DL$	9.58	$< DL$	NA
Rh	74	$< DL$	106	$< DL$	NA
Sb	156	$< DL$	255	$< DL$	NA
Th	57	$< DL$	89	$< DL$	NA
Tl	923	$< DL$	1292	$< DL$	NA

* = Significant difference between composite and segment data

Table 12: Average Concentrations of Anions and Cations

Constituent	Composite Mean	Composite RSD	Segment Mean	Segment RSD	Segment 1 Mean
(ppm)					
Ag	46.7	0.50	11.51	0.32	NA
Al*	1,133	0.15	383.2	0.31	NA
B	49.4	0.13	115	0.55	NA
Ba	14.14	0.04	12.82	0.04	NA
Bi	18,520	0.06	17,730	0.07	32,029
Ca	809.6	0.07	746.4	0.22	NA
Cd	5.28	0.12	5.25	0.10	NA
Ce	37.14	0.27	NA	NA	NA
Cl	1,234	0.06	1,090	0.05	NA
Cr	810	0.02	821.2	0.03	NA
Cu	42.52	0.27	25.08	0.10	NA
Fe	18,060	0.04	15,750	0.03	36,951
F	1,895	0.06	1,775	0.06	NA
K	311.6	0.04	356.9	0.08	NA
La	31.8	0.29	16.6	0.42	NA
Li	NA	NA	6.97	0.37	NA
Mg	178.5	0.04	159	0.06	NA
Mn	66.7	0.10	54.2	0.05	NA
Mo	13.5	0.39	20.0	0.37	NA
NO_2	10,290	0.03	8,776	0.15	NA
NO_3	187,100	0.08	170,900	0.03	NA
Na	97,730	0.03	92,770	0.01	92,068
Nd	15.8	0.30	20.9	0.33	NA
Ni	18.6	0.04	30.1	0.29	NA
P	16,060	0.04	15,570	0.03	10,571
PO_4	25,250	0.03	24,550	0.05	NA
Pb	528.4	0.22	347.3	0.26	NA
Re	6.5	0.05	8.305	0.22	NA
Ru	111.3	0.24	55.38	0.53	NA
SO_4	11,530	0.06	10,860	0.01	NA
Si	9,358	0.03	8,275	0.04	17,963
Sr	211	0.09	209.2	0.13	NA
TIC	899.5	0.06	807.1	0.19	NA
TOC	381.2	0.06	468.2	0.09	NA
Te	19.26	0.21	27.48	0.37	NA
Ti	8.413	0.16	6.338	0.15	NA
U	208	0.08	142.1	0.36	460.0
V	2.788	0.18	2.557	0.23	NA
Zn	80.51	0.07	87.85	0.15	NA
Zr	6.25	0.12	7.01	0.15	NA

* = Significant difference between composite and segment data.

Table 13: Numbers of Significant Differences between Segment and Composite Estimates

	Not Sig.	Sig.	Percent Not Sig.
metals	17	98	15%
anions	2	34	6%
radionuclides	5	22	19%
Total	24	154	13%

constituents, NO_2, TIC, U, and Zn, exhibit the clearest vertical patterns; The concentrations of these constituents are monotonically related to depth. As one would expect, those constituents that exhibit vertical patterns also had large segment RSDs from the ANOVA fits described in Section 3. For example, the segment RSD for NO_2, TIC, and Zn were all over 50%.

The segment 1 data also is relevant to vertical heterogeneity. Very little segment 1 data was produced, and most of it came from riser 1 (See Table 5). Because the segment 1 data was so incomplete, it was dropped from the ANOVA analyses and does not appear in the Appendix D plots. However, we did examine the segment 1 data that was available and found that it seemed to differ from the rest of the tank contents. The last column in Tables 11 and 12 lists the average concentration within segment 1. By comparing this number to the other average concentrations, one can see that segment 1 concentration frequently differs from the average by about 100%. In other words, the "crust" on the surface of the tank seems to have different composition than the main portion of the tank. Since the segment 1 measurements were taken at essentially one location, we can not determine whether these differences exist at other locations in the tank.

Appendix E contains plots that display the horizontal (i.e., riser-to-riser) heterogeneity in the tank. Riser to riser concentrations can be estimated from both the composite and segment-level data sets, and both estimates are presented in the plots, along with associated confidence bounds. From the plots, one can determine that significant horizontal variations exist in Ag, ^{241}Am, NO_3, ^{137}Cs, Cu, SO_4, Sr, and ^{90}Sr (using composite estimates).

Over half of these constituents (i.e Ag, NO_3, ^{137}Cs, Cu and SO_4) had a significantly larger value at riser 3. The other significant constituents displayed no obvious pattern in their horizontal variations. Given the fact that risers are clustered together as illustrated in Figure 1, one would expect to see a significant difference between risers 1,2 and 3,4; None of the constituents exhibit such a pattern.

It would be reasonable to conclude that the riser variability present in this data is caused by the crust; Some of the risers contain more of the crust than others causing the horizontal variability between risers. If segment 1 material had been included in the composites, the differences between risers may have been less. Therefore, it is reasonable to conclude that horizontal variability is generally low *at the risers sampled in B110*. One should note that the riser locations chosen for B110 may not provide the best estimate of horizontal variability.

Since vertical variability is also generally low, except for segments that contain waste crust, one can conclude that the waste below the crust is fairly homogeneous.

4.3 Comparison of Composite and Segment-Level Estimates

Appendix E also allows one to compare segment-level and composite data in detail. If both sampling methods provided unbiased estimates of the same quantity, one would expect almost all segment and composite confidence bounds to intersect in the plots. The majority of the confidence bounds do, but there are some cases where significant differences occur.

In Section 3, we have already discussed the most probable cause for these differences; incomplete segment level measurements. The composite samples always contain material from segment 2, which contains some crustal material. The segment level measurements never include all of the segment 2 samples. In fact for many constituents, no segment 2 samples are included. The effect of the incomplete segment-level measurements

can be dramatic (see the plots of Al and ^{90}Sr in Appendix E).

Table 13 presents a summary of the significant differences (at the 5% level) that exist between segment and composite measurements. From the table, one can see that 24 of a possible 178 measurements, or 13%, are significantly different. With a test conducted at the 5% level, one would expect 9 significant differences to occur by chance, so 13% shows that most of the composite and segment-level data agrees. When one also considers the fact that the segment level data is quite unbalanced for some constituents (particularly the radionuclides), the agreement between composite and segment level samples should be considered quite good. From this data set, one would conclude that the two sampling methods generally agree.

5 Analysis of Holding Time Effects

The objective of the "holding time effects" measurements analyzed in this section is to determine whether certain analyte samples may degrade with time. Due to backlogs of core samples to be analyzed, a substantial time interval may occur between the time the sample is taken and when it is run through the laboratory.

Since there are regulatory limits for the duration that sample material may be held before analysis is completed, and these limits are shorter than the typical process time required for analysis, a variance to compliance with the holding-time requirements was requested. This variance permits non-compliance with the provision that there are no effects of holding time. The present analysis was performed to verify that no significant effects do indeed occur.

A special set of samples were drawn from homogenized, segment-level waste for this study. Three sets of measurements were made on each sample: a set at 20 days after sampling, a set at 60 days after sampling, and finally a set at 120 days after sampling. The observations also included replicate measurements, so that different sources of measurement variability could be established.

The data from the holding time study are given in Table 14 and plotted against time in Figures 4 through 6. Each line in Table 14 describes a replicate measurement taken from a particular segment (on core 4) at a particular holding time (batch).

5.1 Statistical Model

Given observations with a structure such as this, it is possible to determine the following forms of variability within the measurements:

- pure replicate variability σ_e^2
- segment by batch variability σ_{sb}^2
- batch variability σ_b^2
- segment variability σ_s^2

In other words, a typical measurement Y_{ijk}, where i represents the segment, j the batch, and k the replicate, is described according to the following ANOVA model:

$$Y_{ijk} = \mu + \beta T_j + S_i + B_j + SB_{ij} + E_{ijk} \tag{8}$$

where

$i = 1, 2, 3, 4$, $j = 1, 2, 3$, $k = 1, 2$, and

$var(S_i) = \sigma_s^2$,

$var(B_j) = \sigma_b^2$,

$var(SB_{ij}) = \sigma_{sb}^2$, and

$var(E_{ijk}) = \sigma_e^2$.

In this model, the term βT_j has been added to account for the possible "holding time" effect, which should result in a systematic (i.e. monotonic) increase or decrease in constituent concentration over time. The term T_j represents the holding time associated with batch j. If the slope parameter, β, is not significantly different from 0, then no evidence exists for a systematic effect over time.

Since the data is balanced, except for one missing observation associated with Cr, it is easy to produce simple estimates for the variance components, the intercept, μ, and the slope parameter β using standard ANOVA procedures.

Table 14: Raw Holding Time Data (ppm)

days	batch	seg	Cl	F	NO_2	NO_3	PO_4	SO_4	TIC	TOC	Cr
19	1	2	1630	799	13800	139000	18100	10000	1520	595	78
19	1	2	959	805	13500	146000	19100	9680	1650	579	87
19	1	3	1290	1570	11200	184000	22300	11700	755	489	53
19	1	3	1030	1530	11000	162000	21100	11100	901	460	61
20	1	4	934	1610	6750	175000	22000	11000	399	399	40
21	1	4	848	1550	6450	177000	21500	10900	413	383	36
21	1	5	848	1550	4030	196000	22600	11500	177	353	21
21	1	5	872	1530	3920	201000	23500	11600	174	356	23
60	2	2	976	908	15300	149000	21600	8840	1870	476	92
60	2	2	976	910	14900	148000	20700	9490	2070	344	88
55	2	3	1030	1670	10600	184000	24900	11700	918	368	67
55	2	3	1000	1750	10700	168000	22800	11700	898	398	64
48	2	4	1240	2050	7490	197000	28000	9650	474	485	16
49	2	4	1180	2020	7540	142000	19200	8570	453	443	17
54	2	5	1130	2640	4050	215000	27300	11800	476	100	33
54	2	5	1150	2450	4050	229000	28500	15000	469	100	32
109	3	2	1030	956	16400	153000	18400	9940	2430	468	65
110	3	2	1030	838	16500	154000	17300	10000	1630	488	NA
110	3	3	1000	1680	10000	160000	19200	11300	974	501	24
111	3	3	1050	1950	11100	179000	24600	11900	1000	515	25
127	3	4	993	1750	6880	176000	20000	10700	453	357	11
127	3	4	1040	1750	6860	190000	23300	11300	457	606	11
131	3	5	1070	2280	3590	198000	24100	11100	407	271	11
132	3	5	1070	2200	3650	193000	24000	11000	392	274	7

Table 15: Summary of ANOVA Fits

Consti tuent	μ	RSD S_i	B_j	SB_{ij}	E_{ijk}	β	$sd(\beta)$	Z-stat
Cl	1057.3	0.0000	0.0000	0.1179	0.1413	-0.240	1.315	-0.1821
F	1614.4	0.3175	0.1475	0.1305	0.0477	2.424	3.754	0.6457
NO2	9177.5	0.5239	0.0000	0.0857	0.0284	4.795	6.504	0.7372
NO3	175625.0	0.1294	0.0000	0.0000	0.0790	17.707	78.991	0.2242
PO4	22254.2	0.0979	0.0949	0.0000	0.1041	-4.798	32.273	-0.1487
SO4	10894.6	0.0843	0.0000	0.0764	0.0677	-0.138	7.905	-0.0174
TIC	890.0	0.7739	0.0944	0.0000	0.1946	1.936	1.531	1.2645
TOC	408.7	0.2548	0.1891	0.1505	0.1448	0.047	1.233	0.0381
Cr	42.8	0.6324	0.1303	0.2114	0.0714	-0.244	0.108	-2.2658

5.2 Results

Figures 4 through 6 present the segment adjusted data (i.e. $Y_{ijk} - S_i$) and the batch effects (the batch effects are simply $\mu + \beta T_j + B_j$). The data has been segment adjusted to reduce the scatter in the data so that the viewer will be better able to visually compare the scatter in the data with the batch effects.

From these plots, it is intuitively apparent that no large systematic time trend exists for any of the constituents, except possibly Cr. Visually, the concentration of Cr in the third batch does seem to be significantly less than the other two. However, only three time groups exist, so it is not clear whether this "low" batch is due to measurement bias or a true systematic time trend; we would certainly be more likely to believe this low batch was due to a systematic time trend if batch 2 was also lower than batch 1, but it is not.

From these figures, we do see some evidence for a batch effect, but it does not seem to be a systematic batch effect. In other words, the batch effect is caused by factors that randomly change from one measurement time to the next (instrument calibration, operator vigilance, etc.). The term B_j and its variance σ_b^2 measures this sort of effect.

If a systematic effect does occur, concentration may either be decreasing or increasing (With only 3 points in time, we cannot consider more exotically shaped systematic effects). Of course, a decreasing time trend would be of most concern, because that would mean that current procedures underestimate the concentrations of important constituents. It is also possible to have the measurements display an increasing time trend, which could be caused by evaporation, redox changes, or gas (e.g. CO_2) escape.

The essential results of the fits of ANOVA model (1) to the data are presented in Table 15. The most critical column in the table is the last, which contains a z-statistic to test whether $\beta = 0$ (this is simply the estimate divided by its standard deviation). When the absolute value of this statistic is greater than 2, the result would be significant at the 5% level. As one can see from the table, there is no significant time trend except possibly for Cr. At a 1% level of significance, Cr would not be significant. Therefore, one can conclude that there is no evidence for a time trend except possibly for Cr, and that evidence is weak.

An examination of the variability within the data reveals little consistency from one constituent to the next. Some constituents have significant batch-to-batch variability; others have none. The variability associated with batches was found to be statistically significant in more than half of the analytes examined. The variability between segments was found to be significant for all analytes other than Cl.

Figure 4: Segment-Adjusted Data Versus Time

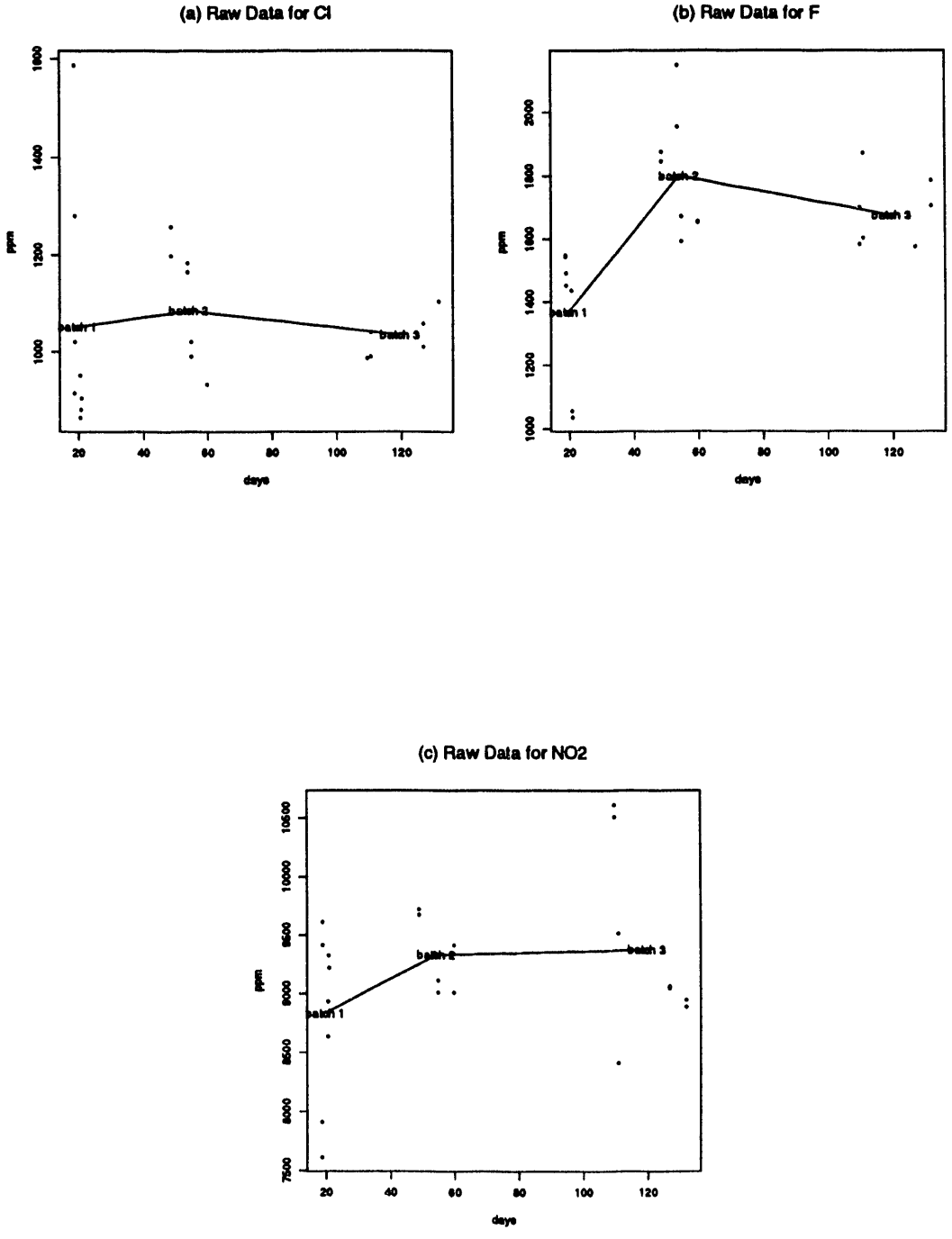

Figure 5: Segment-Adjusted Data Versus Time (cont)

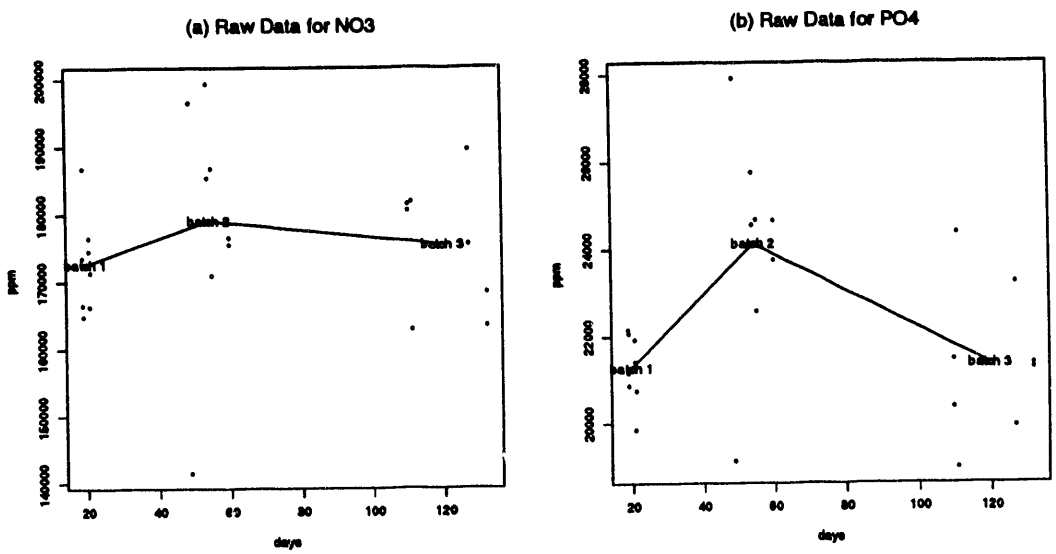

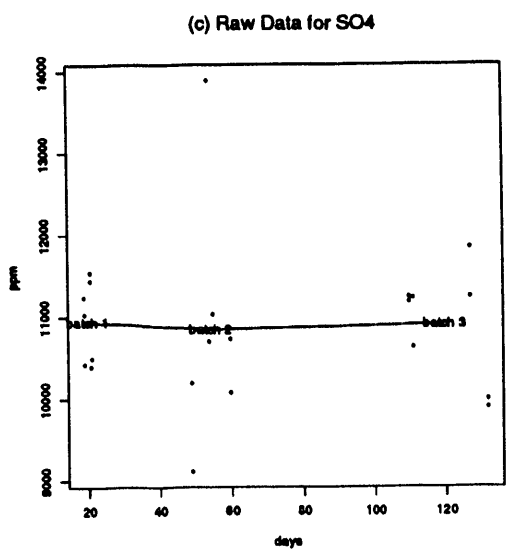

Figure 6: Segment-Adjusted Data Versus Time (cont)

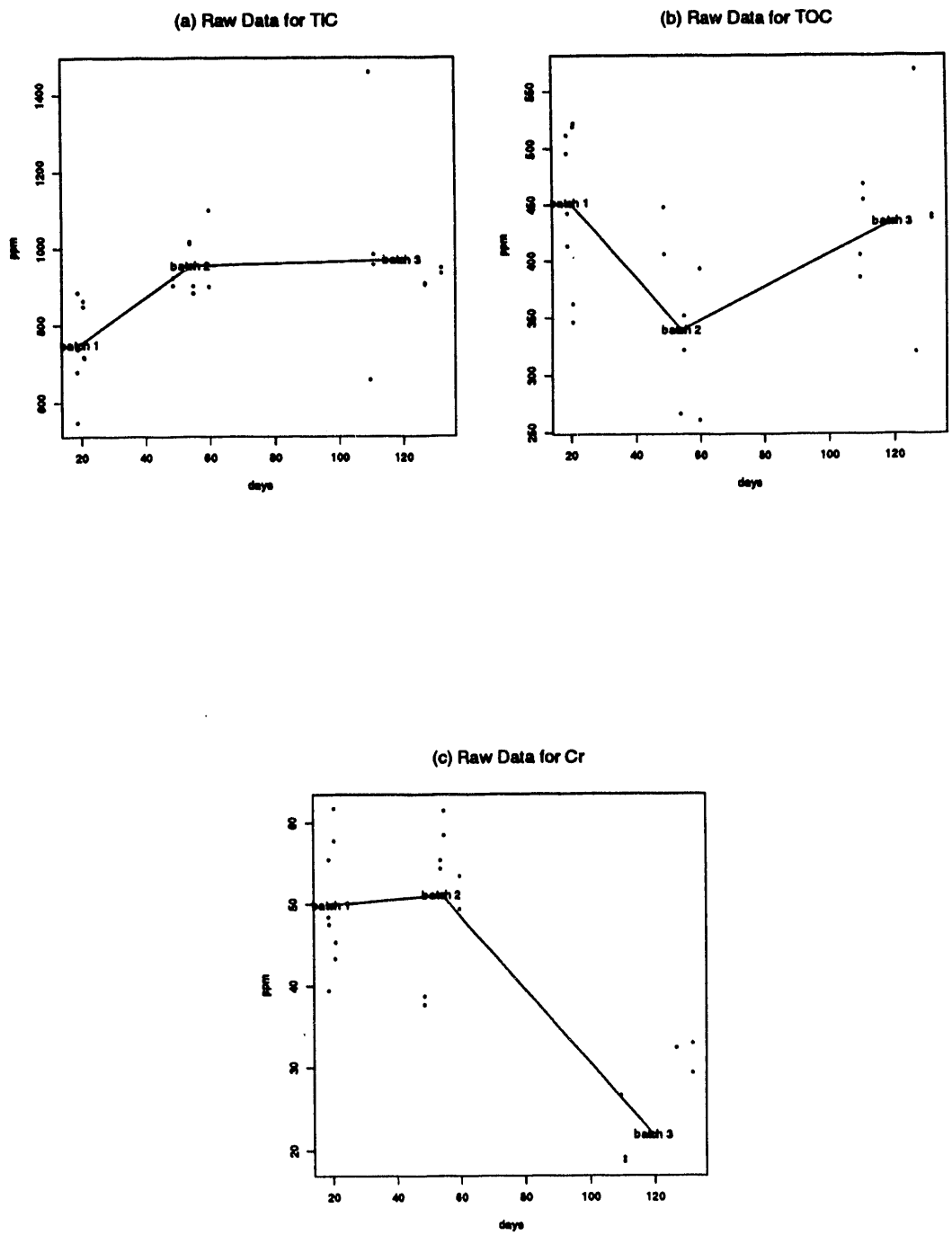

6 Conclusions

The B110 data has been used to calculate inventory estimates for approximately 70 constituents, which are listed in Table 2 and graphically displayed in Appendices D and E. The data also provides estimates for several types of spatial, sampling, mixing, and measurement variabilities using ANOVA procedures. These results are presented in Appendix C.

The average concentration of a typical constituent has a relative standard deviation of about 10%. However, the uncertainty ranges from a few percent up to about 100%. One factor that affects this uncertainty is the number of measurements made on each constituent. Some constituents were measured quite extensively, other constituents had little data.

It is difficult to make any strong generalizations about the relative magnitudes of spatial, sampling, mixing, and measurement variabilities. In the results, one can find examples for which each type of variability is dominant. However, if one had to summarize the sources of variability, one would say that mixing (homogenization) variability is generally the smallest source of variability, measurement variability is next, followed by spatial variability, and sampling variability (i.e. core and segment replication error) is the largest.

6.1 Adequacy of Sample Homogenization (Mixing)

The data allows us to determine the variability within a homogenized (or blended) sample. An acceptable homogenization procedure should exhibit sampling variabilities that are less than laboratory measurement variabilities. For both types of sampling (composite and segment-level), nomogenization variability was usually the smallest type of variability measured. One can therefore conclude that sample homogenization procedures are adequate, at least for B110 waste.

6.2 Spatial Variability

Two types of spatial variability could be measured in the data, horizontal (riser to riser) and vertical (segment to segment). Horizontal variations were less significant than vertical variations. In fact, for most constituents horizontal variations were not significantly different from zero. This result does depend on the riser locations chosen for the B110 coring. A different choice of riser locations may have produced more horizontal variations.

Evaluation of vertical variability was hampered by incomplete segment-level measurements. For many constituents, the crust of the waste was not measured; This made the constituent appear vertically homogeneous when it was not. Nevertheless, the basic vertical pattern is present in the data. The waste is fairly homogeneous vertically, except for the crust at the top. The crust at the top is quite different chemically from the waste beneath it.

6.3 Comparison of Segment and Composite Sampling

In Section 4.3, concentration estimates calculated from composite samples were compared to segment-level estimates. In the majority of cases (87%) no significant differences were found. In the 13% of the cases in which significant differences were found, many were due to the fact that the segment-level data was unbalanced and therefore did not produce unbiased estimates.

6.4 Holding Time Results

The holding time data exhibited significant between-batch variability. In other words, there were significant differences between analyses performed at one time period when compared to another. This between-batch variability may indicate that laboratory measurements are not in statistical control.

However, these differences did not exhibit any systematic pattern or trend. From the analysis of the holding time data presented in Section 5, only one constituent, Cr, displays a marginally significant (at 5% level) time trend. The other eight constituents exhibit no strong relationship to time.

7 References

[1] Beckman RJ, Nachtsheim CJ, Cook RD, "Diagnostics for Mixed-Model Analysis of Variance", Technometrics, Vol. 29, No 4, Nov. 1987.

[2] Corbeil RR, Searle SR, "Restricted Maximum Likelihood (REML) Estimation of Variance Components in the Mixed Model", Technometrics, Vol. 18, No 1, Feb. 1976.

[3] Dempster AP, Laird NM, Rubin DB, "Maximum Likelihood from Incomplete Data via the EM Algorithm", Royal Stat. Society Meeting, Dec. 8, 1976.

[4] Dempster AP, Rubin DB, Tsutakawa RK, "Estimation in Covariance Components Models", JASA, Vol 76, No 374, June 1981.

[5] Jensen L, Liebetrau AM, "Statistical Techniques for Characterizing Single-Shell Tank Wastes", Westinghouse, WHC-SA-0348-FP, July 1988.

[6] McLean RA, Sanders WL, Stroup WW, "A Unified Approach to Mixed Linear Models", The American Statistician, Vol. 45, No 1, Feb. 1991.

[7] Milliken GA, Johnson DE, "Analysis of Messy Data, Vol 1: Designed Experiments", Wadsworth Inc. 1984.

[8] SAS/STAT User's Guide, Version 6, Fourth Edition, Volumes 1 and 2, SAS Institute Inc., Cary, NC, ISBN 1-55533-376, 1990. SAS Manual

[9] S-PLUS Version 3.1 Supplement, Statistical Sciences, Inc., Seattle, Wa., 1992.

[10] Winters WI, Jensen L, Sasaki LM, Weiss RL, Keller JF, Schmidt AJ, Woodruff MG, "Waste Characterization Plan for the Hanford Site Single-Shell Tanks", WHC-EP-0210, May 1989.

APPENDIX A

B110 DATA SET FORMAT

Appendix A - B110 Data Set Format

This appendix describes the format of the B110 data set used to produce the results discussed in this report. The data set contains chemical measurements made by the 324 Lab on B110 cores in 1990. The data was assembled from laboratory spreadsheets by Brenda Thorton and Rick Walling at PNL for the SST Characterization Program in 1991.

Each row in the data-base represents a single observation. The columns in the data-set are defined in Table 16 and Table 17. An excerpt from the data base is provided in Table 18 as an example.

Table 16: Description of B110 Data Base Fields

Field	Description
1	Name of Tank measured
2	Core ID associated with sample
3	Segment Sampled. If "Comp" is in this field, then the measurement was on a composite sample
4	Constituent Measured
5	Homogenization Sample Replication Number
6	Aliquot Sample Replication Number
7	Measured value
8	Detection limit associated with the measured value
9	Units associated with columns 7 and 8
10	Measured value in "EPA-preferred" units
11	Detection Limit in "EPA-preferred" units
12	Units associated with columns 10 and 11
13	Master Sample Identifier
14	Method of chemical analysis utilized (See Table 17 for description)
15	Status of the observation in the analysis (0 - not included in the analysis, 1 - included in the analysis)

Table 17: Explanation of Analysis Method Codes

	Detector Codes
ICP:	inductively coupled plasma emission spectroscopy
GEA:	gamma energy analysis using either Ge(Li) or intrinsic Ge detectors
GP:	gas proportional counter
LF:	laser fluorescence
AEA:	alpha energy analysis on surface barrier (Si) detectors
MS:	mass spectrometry
AAGF:	atomic absorption graphite furnace
CVAA:	cold vapor atomic absorption
UV-VIS:	ultra violet-visible spectrometry
IC:	ion chromatography
CA:	carbon analyzer
LS:	liquid scintillation
	Pre-treatment Codes
F:	KOH fusion with HCl dissolve
A:	Acid Leach
W:	Water Leach

Table 18: Excerpt from B110 Data Base

Field 1	Field 2	Field 3	Field 4	Field 5	Field 6	Field 7	Field 8
	Field 9	Field 10	Field 11	Field 12	Field 13	Field 14	Field 15
B110	core01	comp	Ag	sampl	al-1	133.836233	121.826402
	mg/kg.dry	0.0055	0.0050	wgt.%.wet	90-1125a1	ICP:F	0
B110	core01	comp	Ag	sampl	al-1	21.900475	76.360238
	mg/kg.dry	0.0009	0.0031	wgt.%.wet	89-0621c1	ICP:W	0
B110	core01	comp	Ag	sampl	al-1	58.401265	37.044215
	mg/kg.dry	0.0024	0.0015	wgt.%.wet	89-0621a1	ICP:A	1
B110	core01	comp	Al	sampl	al-1	248.205378	511.709648
	mg/kg.dry	0.0102	0.0210	wgt.%.wet	89-0621c1	ICP:W	0
B110	core01	comp	Al	sampl	al-1	2791.093807	260.485509
	mg/kg.dry	0.1147	0.0107	wgt.%.wet	89-0621a1	ICP:A	1
B110	core01	comp	Al	sampl	al-1	2890.862635	852.784816
	mg/kg.dry	0.1188	0.0350	wgt.%.wet	90-1125a1	ICP:F	0
B110	core01	comp	Am-241	sampl	al-1	12000	0
	dpm/g.wet	5.4054	0	nano-Ci/g.wet	89-0621-C-1	RAD:W	0
B110	core01	comp	Am-241	sampl	al-1	305000	0
	dpm/g.wet	137.3873	0	nano-Ci/g.wet	89-0622-A-2	RAD:F	0
B110	core01	comp	Am-241	sampl	al-1	0.1362	0
	micro-Ci/g	136.2000	0	nano-Ci/g.wet	89-0622a2	GEA:F	1
B110	core01	comp	Am-241	samp3	al-1	0.2355	0
	micro-Ci/g	235.5000	0	nano-Ci/g.wet	90-1125-A-1	GEA:F	1

APPENDIX B

BOX PLOTS OF THE RAW DATA

Appendix B - Box Plots of the Raw Data

This appendix presents summaries of the raw B110 data. For each constituent grouping (radionuclides, cations, anion, and mass spectrometer) box plots and tables of summary statistics are provided. Box plots provide a graphical summary of the data. The box in a boxplot contains the middle half of the data (the 25th percentile and 75th percentile define the box, the mean is also displayed); the whiskers extending from the box show the range of the data. The numbers used to create the box plots are provided in the accompanying tables. For each constituent, the tables contain the overall mean, the min and max, the 25th and 75th quantiles, the number of observations, and the overall standard deviation.

Separate plots are presented for segment-level and composite data and for anions, cations, radionuclides and mass-spec ratios.

Table 19: Segment Level Radionuclides

Cons	# Obs	Max	75% Quant	Mean	25% Quant	Min	Std Dev
^{241}Am	12	0.0097	0.0078	0.0070	0.0056	0.0050	0.0747
^{243,244}Cm	11	5.7e-03	1.5e-03	1.2e-03	2.0e-04	9.4e-05	1.4e-02
^{60}Co	36	1.2e+00	1.5e-02	1.2e-01	1.6e-03	6.4e-04	4.0e-02
^{137}Cs	74	37.9	15.3	14.4	12.1	10.3	3.5
^{152}Eu	4	0.0270	0.0176	0.0143	0.0090	0.0054	0.0947
^{129}I	12	8.0e-05	6.9e-05	5.2e-05	4.2e-05	3.8e-05	6.5e-03
^{237}Np	12	1.1e-04	9.2e-05	7.1e-05	5.2e-05	3.0e-05	7.2e-03
^{238}Pu	12	1.2e-02	5.5e-03	3.8e-03	9.2e-04	8.0e-05	3.0e-02
^{90}Sr	12	1.36	0.68	0.62	0.43	0.28	0.65
^{99}Tc	12	0.0197	0.0170	0.0111	0.0045	0.0040	0.0669
Total α	56	0.635	0.176	0.160	0.077	0.049	0.278
Total β	60	1653.2	143.2	228.2	13.2	9.7	3.6
^{14}C	0	0	0	0	0	0	0
^{3}H	0	0	0	0	0	0	0

Table 20: Composite Level Radionuclides

Cons	# Obs	Max	75% Quant	Mean	25% Quant	Min	Std Dev
^{241}Am	23	0.141	0.086	0.062	0.027	0.013	0.165
^{243,244}Cm	15	3.3e-03	9.0e-04	8.6e-04	3.3e-04	1.8e-04	1.8e-02
^{60}Co	25	0.3210	0.0086	0.0268	0.0029	0.0012	0.0540
^{137}Cs	52	16.9	14.8	14.0	13.6	3.7	3.7
^{152}Eu	5	0.118	0.099	0.080	0.068	0.037	0.261
^{129}I	22	1.3e-04	3.8e-05	3.0e-05	1.5e-05	6.3e-06	3.9e-03
^{237}Np	22	5.0e-04	1.1e-04	1.2e-04	7.3e-05	2.7e-05	8.5e-03
^{238}Pu	22	0.0075	0.0034	0.0029	0.0019	0.0012	0.0439
^{90}Sr	22	235.6	132.4	91.7	32.1	6.4	5.7
^{99}Tc	18	0.025	0.020	0.016	0.012	0.011	0.112
Total α	24	0.24	0.16	0.16	0.13	0.11	0.36
Total β	26	523	244	198	107	28	10
^{14}C	9	3.6e-03	2.5e-10	4.0e-04	3.9e-17	2.7e-17	6.3e-09
^{3}H	14	7.1e-03	3.3e-03	2.2e-03	9.8e-04	3.5e-06	3.1e-02

Table 21: Segment Level Cations

Cons	# Obs	Max	75% Quant	Mean	25% Quant	Min	Std Dev
Ag	36	63.0	13.2	11.6	2.0	0.0	1.4
Al	36	2077	289	383	123	28	11
As	74	2330.0	234.0	181.1	40.8	1.0	6.4
B	36	325.0	71.2	80.4	42.5	16.0	6.5
Ba	36	19.0	14.2	12.8	11.0	8.0	3.3
Be	36	0	0	0	0	0	0
Bi	74	33249	19335	18557	15939	13320	126
Ca	36	2202	651	678	506	355	22
Cd	36	9.0	7.0	5.2	3.0	2.0	1.7
Ce	36	261.0	57.8	46.1	9.8	3.0	3.1
Co	36	119.0	64.2	41.1	10.0	2.0	3.2
Cr	36	977	887	821	746	640	27
Cu	36	64.0	29.0	25.1	18.0	14.0	4.2
Dy	36	7.0	2.2	2.0	1.0	0.0	1.0
Fe	74	39045	16707	17164	15012	12966	123
K	36	706	388	354	278	158	17
La	36	130.0	13.5	16.7	3.0	1.0	1.7
Li	36	42.0	10.5	7.3	1.0	0.0	1.0
Mg	36	256	169	158	137	81	12
Mn	36	95.0	61.3	54.4	47.7	38.0	6.9
Mo	36	107.0	18.2	20.6	5.0	1.0	2.2
Na	74	106543	96374	93055	90220	65001	300
Nd	36	146	24	21	4	0	2
Ni	36	143.0	24.2	32.6	13.8	12.0	3.7
P	74	18651	16534	15406	14851	10107	122
Pb	36	1636	460	347	128	38	11
Re	36	19.0	9.2	8.2	5.0	0.0	2.2
Rh	36	81	46	26	9	0	3
Ru	36	155.0	51.8	52.6	16.8	9.0	4.1
Sb	36	189.0	91.2	58.3	17.8	2.0	4.2
Si	74	19068	8862	8935	8074	6553	90
Sr	36	319	224	199	167	125	13
Te	36	94.0	33.5	27.1	12.0	3.0	3.5
Th	36	93.0	35.2	27.8	12.8	1.0	3.6
Ti	36	18.0	8.2	6.3	4.0	0.0	2.0
Tl	36.0	1282.0	468.2	339.4	85.8	13.0	9.3
U	60	797.7	212.5	196.9	46.7	6.8	6.8
V	36	6.0	4.0	2.5	1.0	0.0	1.0
Zn	36	184.0	130.2	89.1	45.5	32.0	6.7
Zr	36	31.0	11.0	7.8	3.8	0.0	1.9

(Units are ppm)

Table 22: Composite Level Cations

Cons	# Obs	Max	75% Quant	Mean	25% Quant	Min	Std Dev
Ag	14	119.0	42.2	37.1	14.5	7.0	3.8
Al	14	1766	1416	1133	858	329	29
As	42	556.0	216.0	166.2	67.2	7.0	8.2
B	14	87.0	51.5	49.4	39.0	29.0	6.2
Ba	14	17.0	15.8	14.1	13.0	12.0	3.6
Be	14	0.0116	0.0000	0.0014	0.0000	0.0000	0.0000
Bi	42	23643	21978	19577	17415	14094	132
Ca	14	1012	944	810	673	592	26
Cd	14	8.0	6.8	5.3	4.0	2.0	2.0
Ce	14	74.0	61.8	37.1	16.8	3.0	4.1
Co	14	174.0	57.0	51.1	22.8	12.0	4.8
Cr	14	1925	833	885	803	712	28
Cu	14	93.0	61.0	44.0	24.0	18.0	4.9
Dy	14	6.0	1.0	1.3	1.0	0.0	1.0
Fe	42	28417	18562	18293	17700	14256	133
K	14	1146	359	372	277	252	17
La	14	65.0	46.5	30.5	15.2	6.0	3.9
Li	14	14.000	3.000	2.527	0.094	0.000	0.307
Mg	14	251	194	182	162	154	13
Mn	14	195.0	76.8	75.1	54.2	49.0	7.4
Mo	14	47.0	18.8	15.7	6.2	3.0	2.5
Na	42	123063	96703	96219	91887	88036	303
Nd	14	33.0	25.8	15.4	5.5	1.0	2.3
Ni	14	610.0	20.0	60.9	17.2	15.0	4.2
P	42	21695	17994	16710	15362	12532	124
Pb	14	1165	598	527	306	274	17
Re	14	9.0	7.0	6.5	6.0	5.0	2.4
Rh	14	125	11	24	4	1	2
Ru	14	187.0	173.8	111.3	35.2	28.0	5.9
Sb	14	563.0	65.0	85.4	11.5	2.0	3.4
Si	42	11910	9660	9383	8994	8082	95
Sr	14	269	252	215	186	172	14
Te	14	39.0	22.0	19.4	14.2	6.0	3.8
Th	14	80.0	31.2	25.4	9.5	2.0	3.1
Ti	14	16.0	10.0	8.4	7.0	4.0	2.6
Tl	14	961.0	154.2	176.9	42.8	16.0	6.5
U	26	283	233	213	180	136	13
V	14	8.0	4.0	3.2	2.0	0.0	1.4
Zn	14	95.0	89.8	80.3	76.8	52.0	8.8
Zr	14	20.0	8.0	7.4	5.0	4.0	2.2

(units are ppm)

Table 23: Segment Level Anions

Cons	# Obs	Max	75% Quant	Mean	25% Quant	Min	Std Dev
Cl	52	1630	1172	1078	989	844	31
F	52	2940	1968	1733	1548	799	39
NO_2	52	17400	12000	8895	4050	3050	64
NO_3	52	229000	186250	171788	153750	127000	392
PO_4	52	37900	24925	23640	21750	17300	147
SO_4	52	15000	11500	10921	10375	8570	102
TIC	52	2430	980	828	400	174	20
TOC	52	798	533	465	380	94	20

Table 24: Composite Level Anions

Cons	# Obs	Max	75% Quant	Mean	25% Quant	Min	Std Dev
Cl	14	1500	1397	1226	1050	987	32
F	14	2290	2032	1875	1703	1360	41
NO_2	14	12300	10875	10288	9392	8870	97
NO_3	14	235000	188500	181000	166250	155000	408
PO_4	14	28500	26150	24914	23725	21800	154
SO_4	14	14000	11275	11236	10525	10100	103
TIC	14	1200	986	899	835	618	29
TOC	14	463	434	381	316	298	18

Table 25: Composite Level Isotopic Mass Ratios

Cons	# Obs	Max	75% Quant	Mean	25% Quant	Min	Std Dev
$^{238}Pu/^{239}Pu$	6	0.00515	0.00367	0.00202	0.00050	0.00026	0.02232
$^{240}Pu/^{239}Pu$	6	0.038	0.034	0.032	0.030	0.029	0.172
$^{241}Pu/^{239}Pu$	6	0.00103	0.00077	0.00070	0.00057	0.00051	0.02388
$^{242}Pu/^{239}Pu$	6	0.00049	0.00040	0.00034	0.00025	0.00019	0.01568
$^{234}U/^{238}U$	6	7.8e-05	6.3e-05	6.4e-05	6.1e-05	5.6e-05	7.8e-03
$^{235}U/^{238}U$	6	0.0068	0.0068	0.0068	0.0067	0.0067	0.0821
$^{236}U/^{238}U$	6	0.00012	0.00012	0.00011	0.00011	0.00011	0.01050

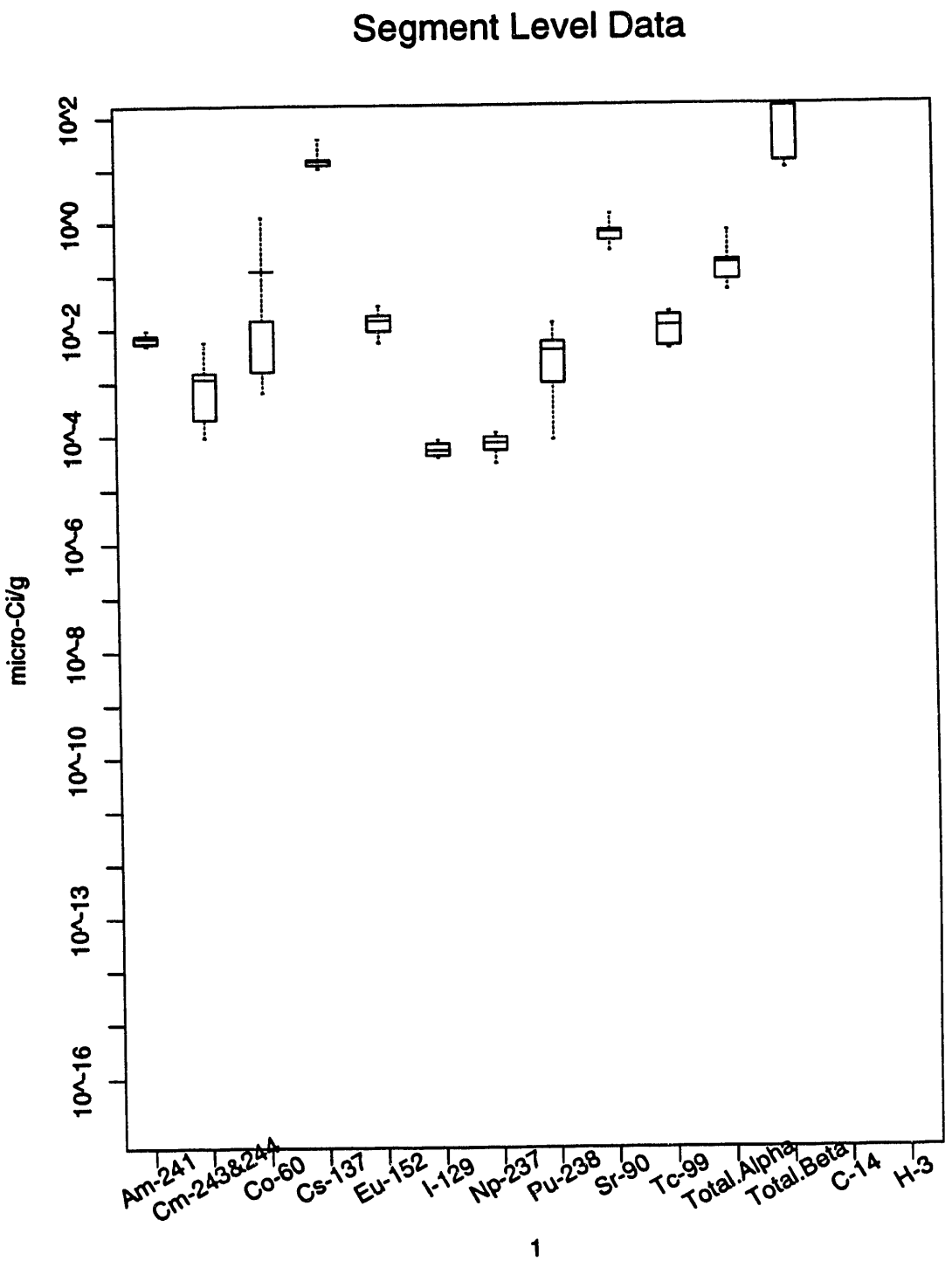

Figure 7: Box Plots of Segment Level Radionuclides

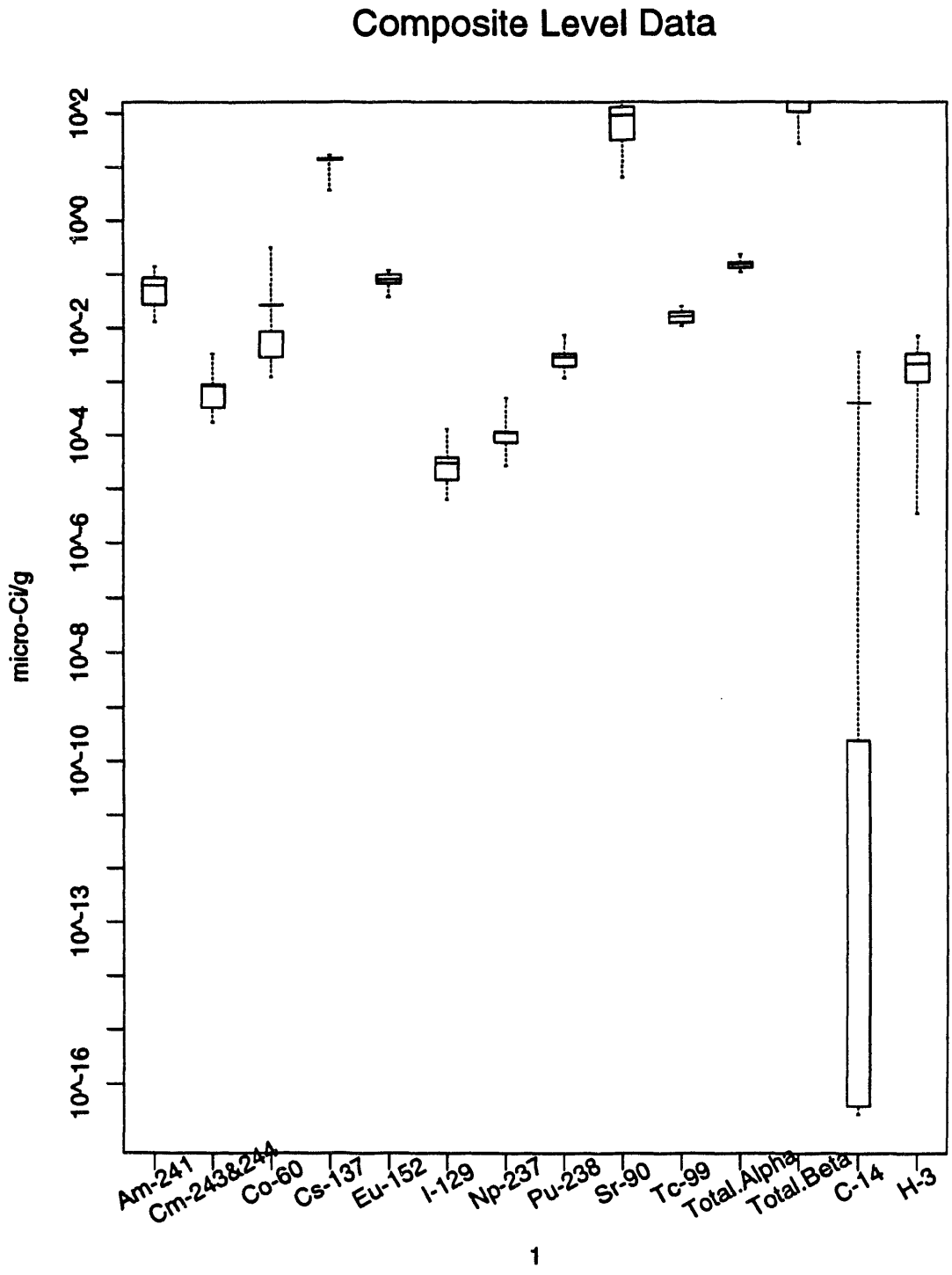

Figure 8: Box Plots of Composite Level Radionuclides

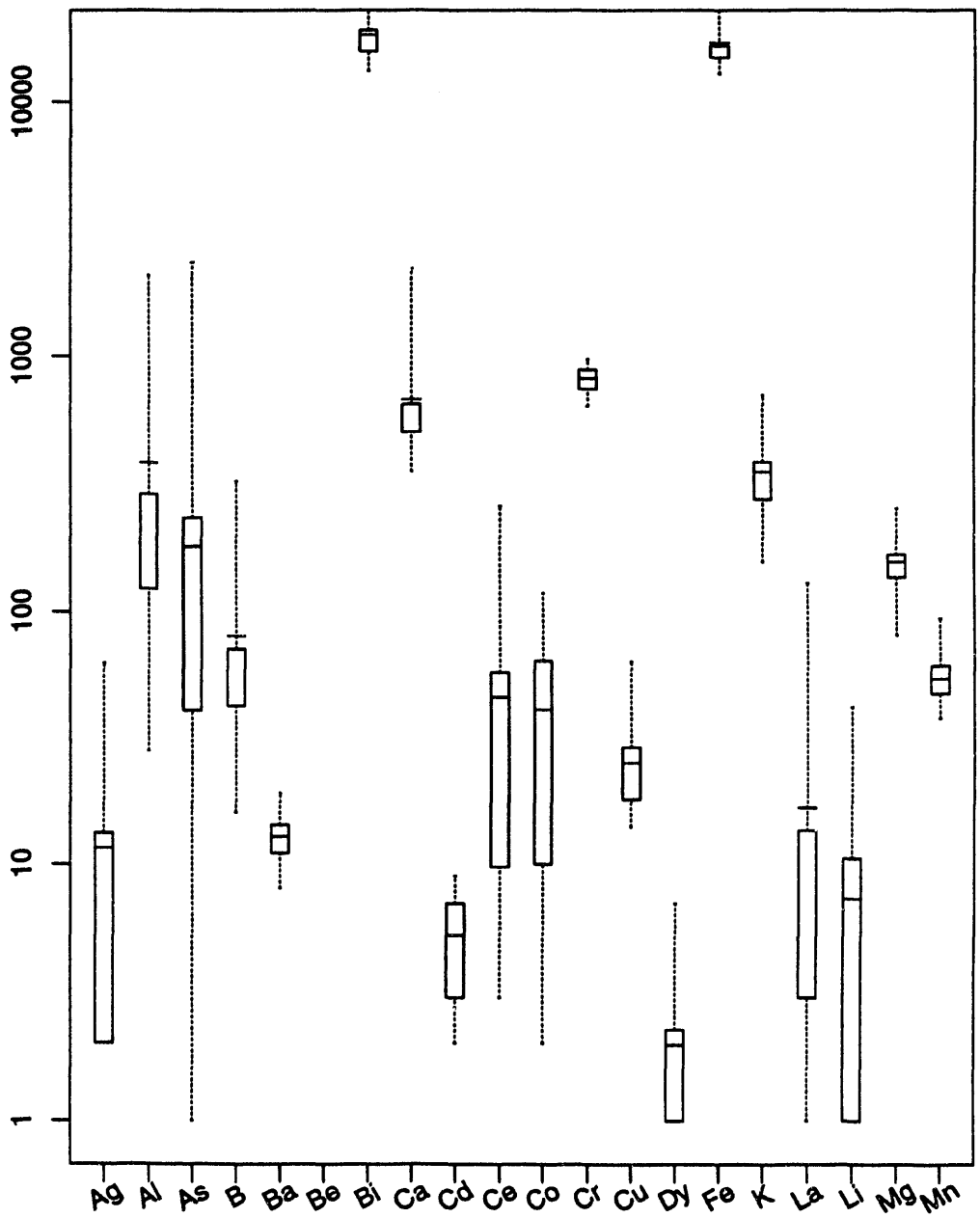

Figure 9: Box Plots of Segment Level Cations

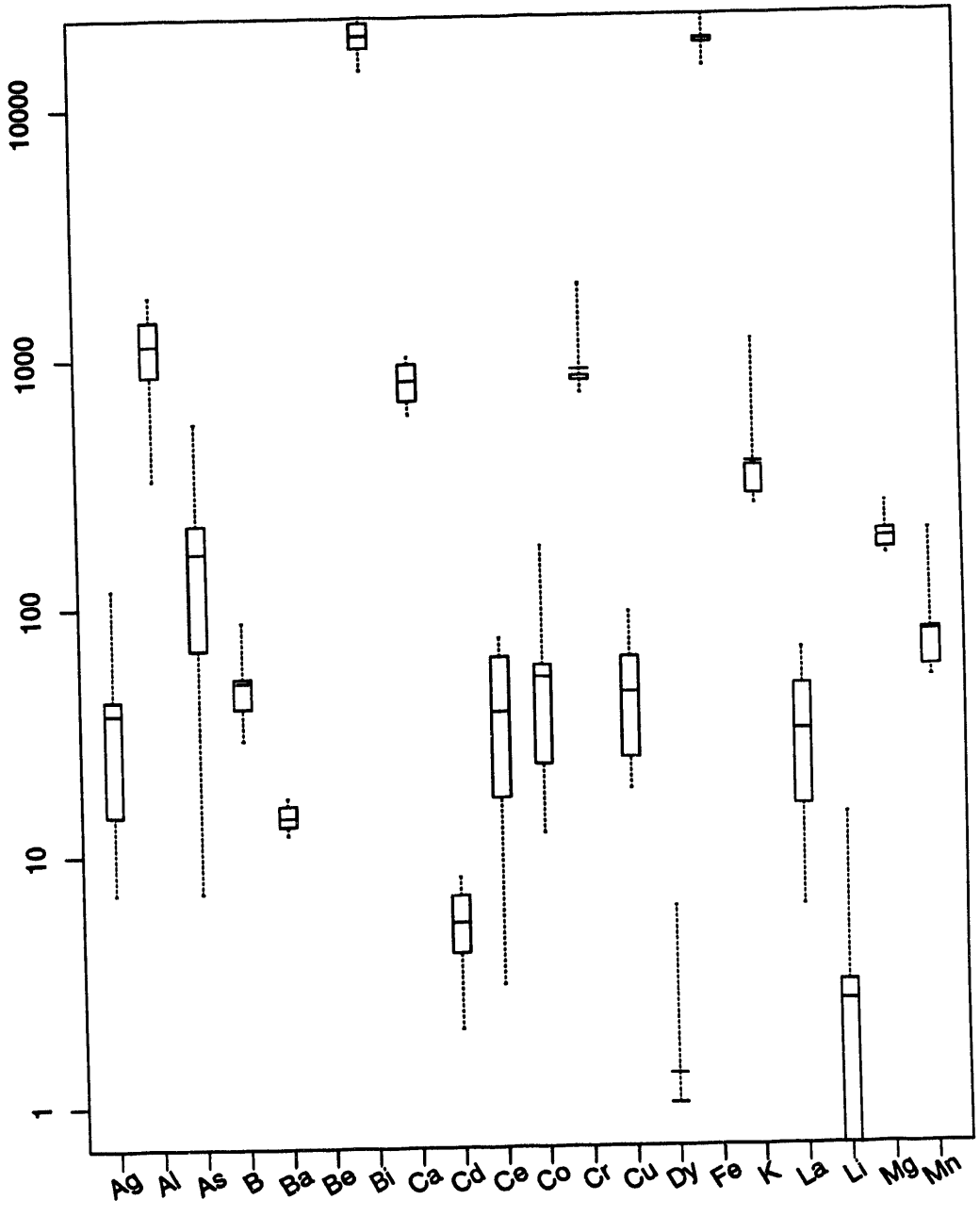

Figure 10: Box Plots of Composite Level Cations

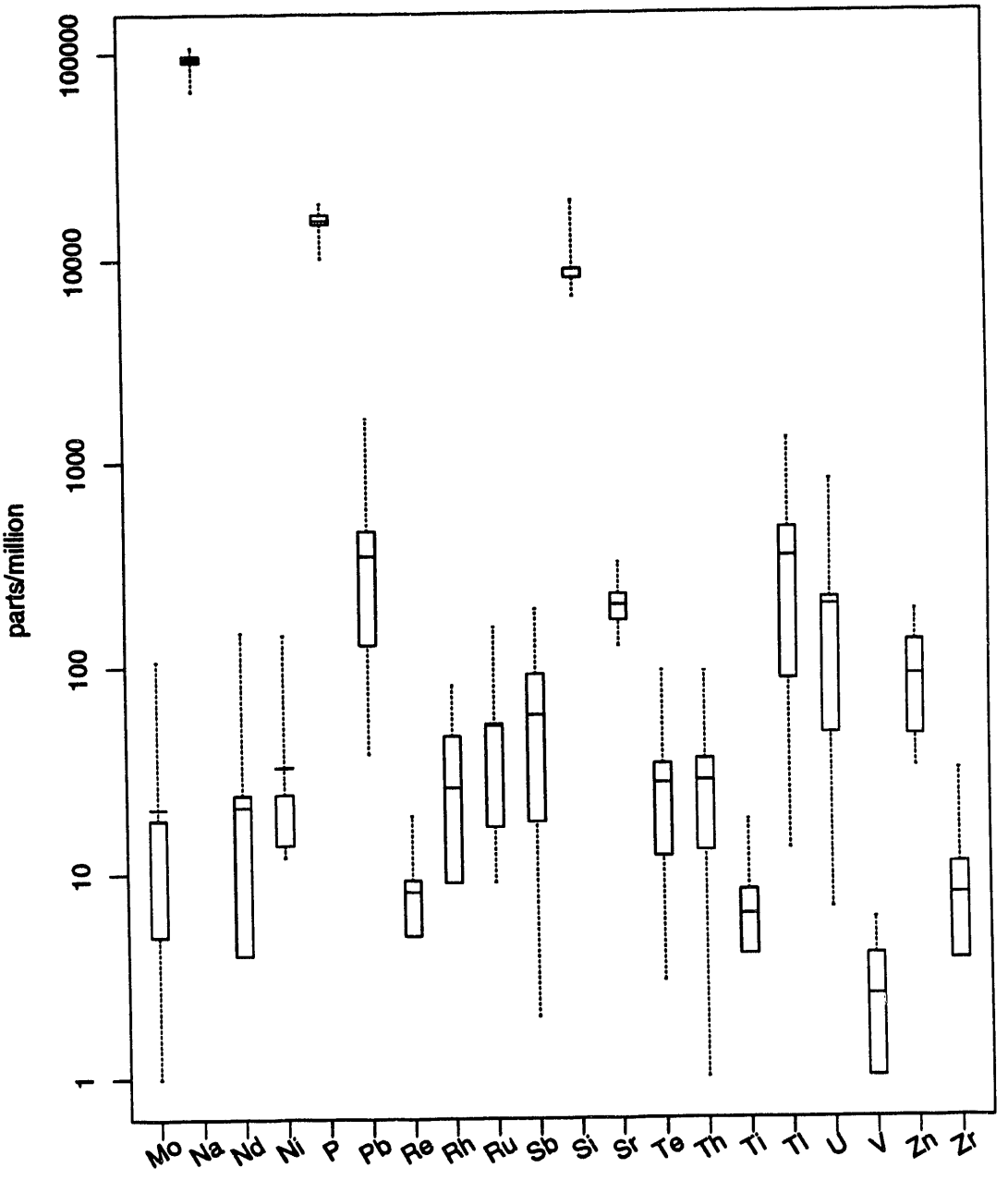

Figure 11: Box Plots of Segment Level Cations

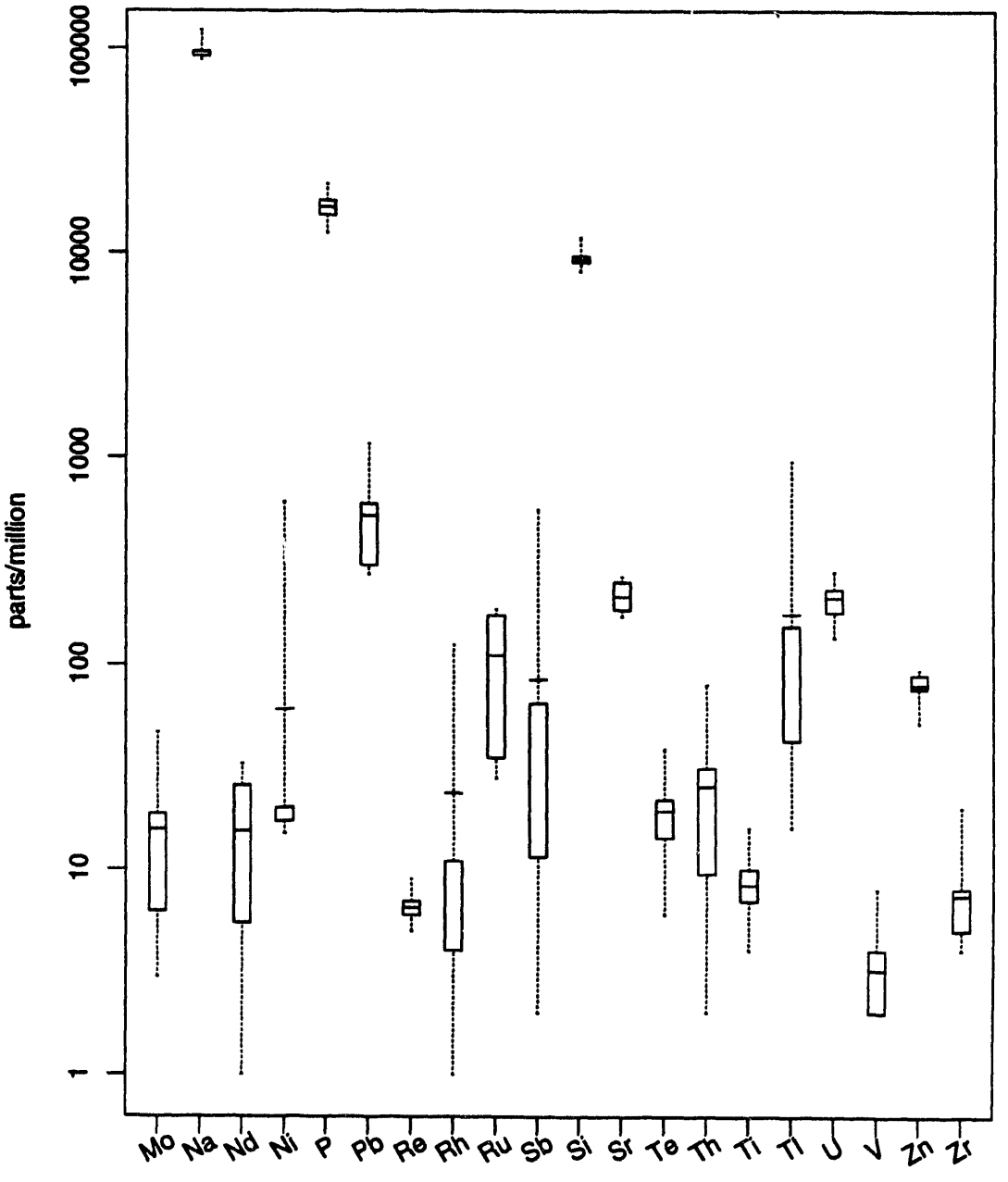

Figure 12: Box Plots of Composite Level Cations

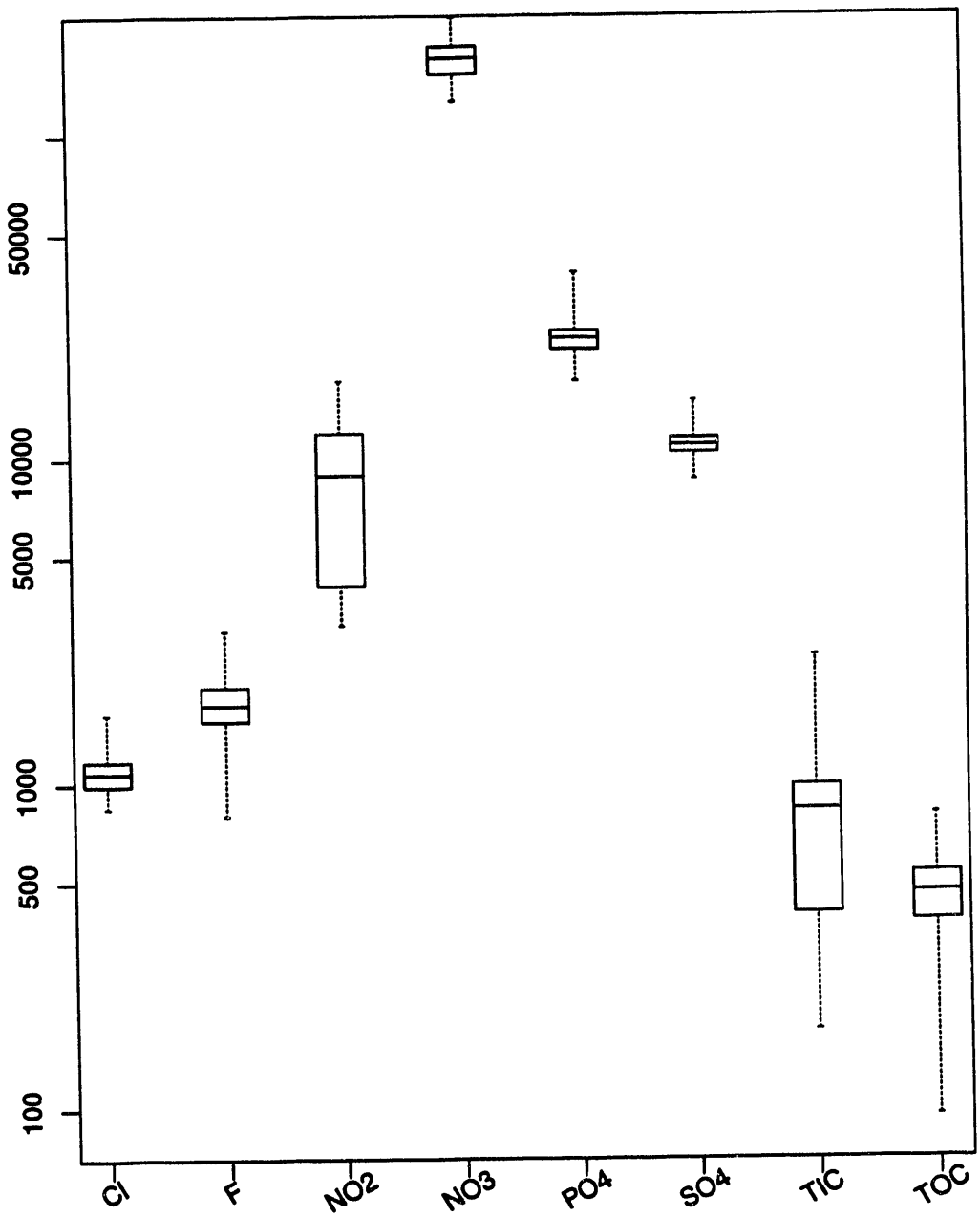

Figure 13: Box Plots of Segment Level Anions

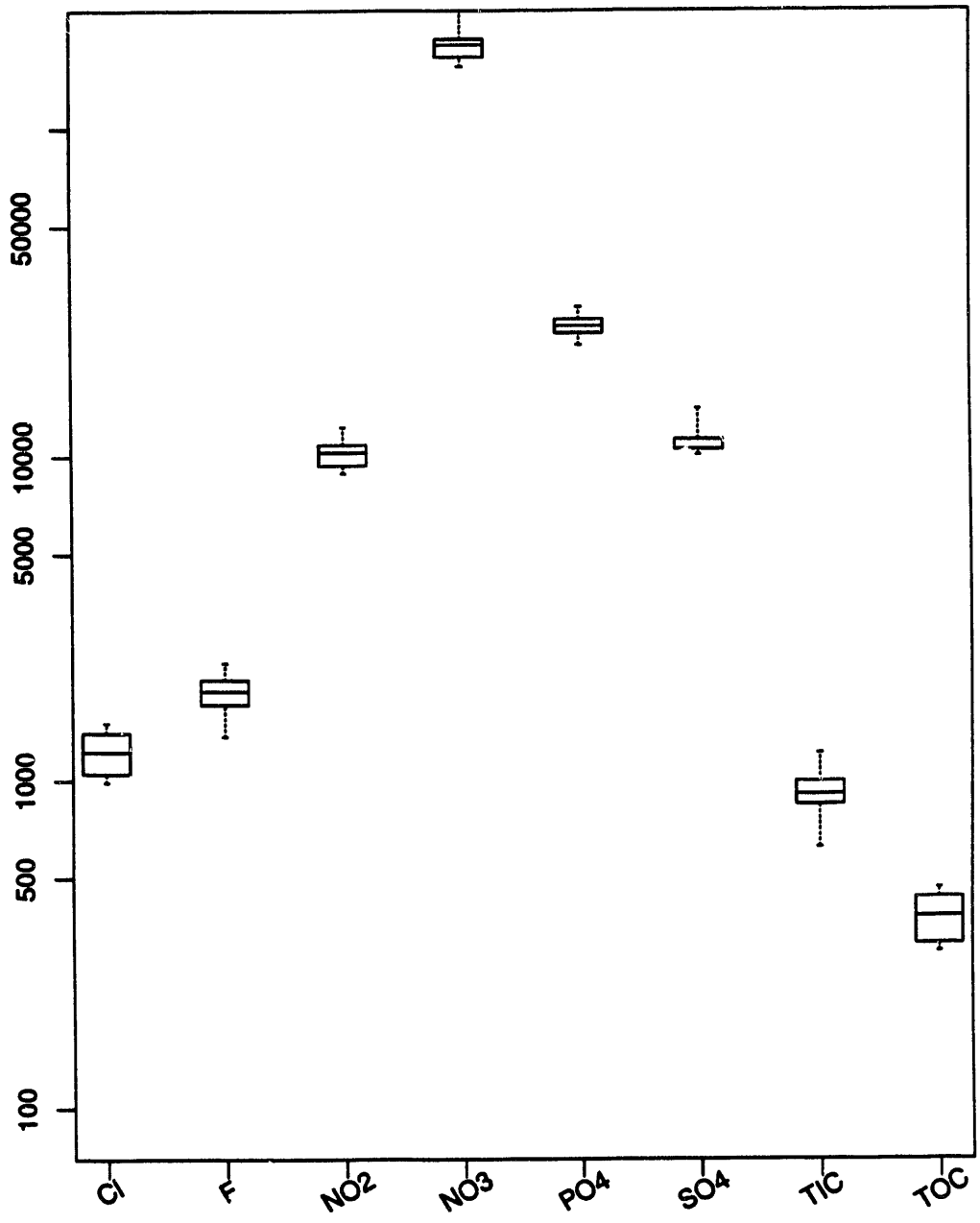

Figure 14: Box Plots of Composite Level Anions

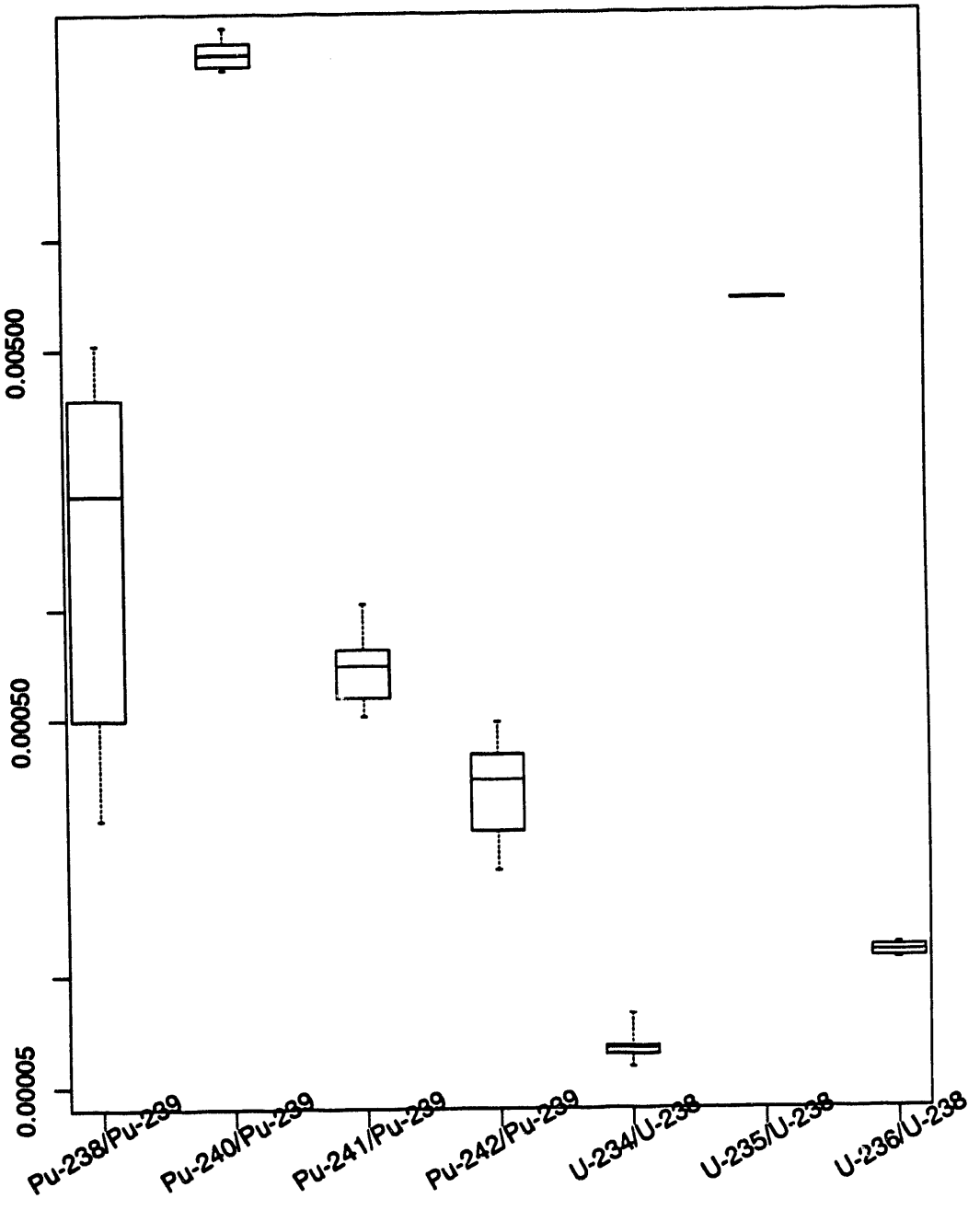

Figure 15: Box Plots of Composite Level Isotopic Mass Ratios

APPENDIX C

RESULTS OF REML ANOVA FITS

Appendix C - Results of REML ANOVA Fits

C.1 Segment-Level Results

The relative standard deviations for the segment-level data are reported in Tables 26, 28, and 29 for cations, anions, and radionuclides constituents, respectively. The first column identifies the constituent, the next five columns contain the relative standard deviations for each variance component. Columns 7 and 8 contain the estimated mean concentration and the overall RSD. Column 9 contains the number of observations that were reported in the core reports as less-than values, and column 10 contains the total number of observations.

Relative standard deviations (RSD) are used to represent the variance components for the model terms. An RSD is the ratio of a standard deviation to a mean. It is a unitless measurement of variability and allows comparisons of variability across constituents whose magnitudes might widely differ. For individual variance components, the RSD is computed by dividing the square root of the variance component by the estimated mean concentration. An overall RSD was computed for each constituent by dividing the square root of the predicted variance of the mean by the estimated mean. The variance components are defined in terms of the ANOVA model;

$$Y_{ijkmp} = \mu + Riser_i + Seg_{ij} + Rep_{ijk} + Hom_{ijkm} + Error_{ijkmp} \tag{9}$$

see Section 2.3 for a complete description of all terms in the model.

The tables also contain the degrees of freedom associated with the segment-level data. The degrees of freedom indicate how much information is available for each estimate. For example, in Table 26 the degrees of freedom for riser is usually 3. This means that the riser RSD is estimated with the equivalent of 4 individual observations.

Table 26: Segment Data: Relative Standard Deviations for Cations (ppm)

	Riser	Seg	Seg-Rep	Hom	Lab	Mu	RSD(Mu)	Less Than	Obs
Ag	0	0.7148	1.022	**	0.2724	11.51	0.3249	15	36
	3*	8	6	0	18				
Al	0	0	1.324	**	0.07756	383.2	0.3124	4	36
	3	8	6	0	18				
As								71	74
B	1.109	0	0.1084	**	0.09355	115	0.5557	15	36
	3	8	6	0	18				
Ba	0	0.1001	0.1635	**	0.06234	12.82	0.04992	0	36
	3	8	6	0	18				
Be								36	36
Bi	0.1385	0.04818	0.101	0.03075	0.04573	17,730	0.07505	0	74
	3	8	8	14	36				
Ca	0.3376	0.4218	0.2689	**	0.07759	746.4	0.2221	0	36
	3	8	6	0	18				
Cd	0	0	0.4064	**	0.1931	5.25	0.1011	14	36
	3	8	6	0	18				
Ce								31	36
Co								36	36
Cr	0.03797	0	0.09814	**	0.02899	821.2	0.03117	0	36
	3	8	6	0	18				
Cu	0	0.1229	0.4042	**	0.2391	25.08	0.1098	2	36
	3	8	6	0	18				
Dy								35	36
Fe	0.05226	0.05949	0.05331	0.008386	0.03735	15,750	0.03437	0	74
	3	8	8	14	36				
K	0	0.1473	0.2677	**	0.2081	356.9	0.08453	8	36
	3	8	6	0	18				
La	0	0	1.8	**	0.09055	16.67	0.4245	18	36
	3	8	6	0	18				
Li	0.3791	0	1.326	**	0.207	6.974	0.3753	25	36
	3	8	6	0	18				
Mg	0	0.1458	0.1796	**	0.0409	159	0.06095	0	36
	3	8	6	0	18				

* = Degrees of Freedom, ** = Data was not available to estimate this effect

Table 27: Segment Data: Relative Standard Deviations for Cations (ppm, Continued)

	Riser	Seg	Seg-Rep	Hom	Lab	Mu	RSD(Mu)	Less Than	Obs
Mn	0.039	0	0.2327	**	0.05593	54.29	0.05961	0	36
	3*	8	6	0	18				
Mo	0.3843	0	1.287	**	0.2598	20.09	0.3701	22	36
	3	8	6	0	18				
Na	0	0.04462	0.024	0.02666	0.03183	92,770	0.01552	0	74
	3	8	8	14	36				
Nd	0	0	1.389	**	0.4304	20.97	0.3352	28	36
	3	8	6	0	18				
Ni	0.1929	0	1.159	**	0.2176	30.13	0.2953	2	36
	3	8	6	0	18				
P	0.04558	0.07064	0.05263	0.02974	0.04486	15,570	0.0343	0	74
	3	8	8	14	36				
Pb	0	0	1.118	**	0.04355	347.3	0.2637	2	36
	3	8	6	0	18				
Re	0.4017	0.2272	0.2382	**	0.3322	8.305	0.2293	12	36
	3	8	6	0	18				
Rh								33	36
Ru	1.07	0	0.2453	**	0.06348	55.38	0.5391	7	36
	3	8	6	0	18				
Sb								36	36
Si	0.08558	0.03776	0.03075	0.007794	0.03536	8,275	0.04516	0	74
	3	8	8	14	36				
Sr	0.2612	0.1252	0.04699	**	0.02754	209.2	0.1367	0	36
	3	8	6	0	18				
Te	0.6885	0.3011	0.3765	**	0.4672	27.48	0.3793	25	36
	3	8	6	0	18				
Th								34	36
Ti	0	0.178	0.5849	**	0.2071	6.338	0.152	7	36
	3	8	6	0	18				
Tl								36	36
U	0	0.9993	0.3055	0	0.1423	142.1	0.3631	0	60
	2	5	7	10	27				
V	0.3727	0	0.5088	**	0.3745	2.557	0.2364	20	36
	3	8	6	0	18				
Zn	0	0.5068	0.2034	**	0.05521	87.85	0.1551	0	36
	3	8	6	0	18				
Zr	0	0	0.6252	**	0.2676	7.017	0.1543	9	36
	3	8	6	0	18				

* = Degrees of Freedom, ** = Data was not available to estimate this effect

Table 28: Segment Data: Relative Standard Deviations for Anions (ppm)

	Riser	Seg	Seg-Rep	Hom	Lab	Mu	RSD(Mu)	Less Than	Obs
Cl	0.09715	0	0	0.09518	0.04937	1,090	0.05406	0	52
	3*	8	6	8	26				
F	0	0.2083	0	0.1248	0.06529	1,775	0.06613	0	52
	3	8	6	8	26				
NO_2	0	0.524	0	0.07964	0.03434	8,776	0.1523	0	52
	3	8	6	8	26				
NO_3	0	0.1157	0	0.03013	0.04552	170,900	0.03465	0	52
	3	8	6	8	26				
PO_4	0.07071	0.1386	0	0.02605	0.07572	24,550	0.05571	0	52
	3	8	6	8	26				
SO_4	0	0.05019	0	0.04405	0.02779	10,860	0.01753	0	52
	3	8	6	8	26				
TIC	0	0.6502	0	0.1509	0.06892	807.1	0.1906	0	52
	3	8	6	8	26				
TOC	0.1197	0.2207	0	0.1673	0.112	468.2	0.09731	0	52
	3	8	6	8	26				

* = Degrees of Freedom, ** = Data was not available to estimate this effect

Table 29: Segment Data: Relative Standard Deviations for Radionuclides (μCi/g)

	Riser	Seg	Seg-Rep	Hom	Lab	Mu	RSD(Mu)	Less Than	Obs
^{241}Am	0.08313	0.1746	**	0	0.1011	0.007287	0.1097	0	12
	1*	2	0	2	6				
^{243,244}Cm	1.074	0.6188	**	0	0.6972	0.001483	0.8485	0	11
	1	2	0	2	5				
^{60}Co	1.514	1.74	0.3083	0.3323	0.8203	0.1051	0.9647	0	36
	3	6	3	7	13				
^{137}Cs	0	0.1141	0	0.05098	0.05203	13.61	0.03514	0	74
	3	8	8	14	36				
^{152}Eu	**	0	**	**	0.6478	0.01426	0.3239	0	4
	0	1	0	0	2				
^{129}I	0.3788	0	**	0	0.06922	0.00005749	0.2687	0	12
	1	2	0	2	6				
^{237}Np	0.4668	0	**	0	0.2901	0.00006457	0.3417	0	12
	1	2	0	2	6				
^{238}Pu	1.104	0	**	0	0.5536	0.003846	0.7999	0	12
	1	2	0	2	6				
^{90}Sr	0	0.5269	**	0	0.1496	0.6725	0.2674	0	12
	1	2	0	2	6				
^{99}Tc	0	0.6184	**	0	0.07283	0.01148	0.31	0	12
	1	2	0	2	6				
Total α	0	0.2434	0.6425	0.01034	0.08681	0.1182	0.1998	0	56
	2	5	5	10	25				
Total β	0	0	2.183	0	0.1238	101.5	0.564	0	60
	2	5	7	10	27				

* = Degrees of Freedom, ** = Data was not available to estimate this effect

C.2 Composite Results

The relative standard deviations for the composite data are reported in Tables 30, 32, 33, and 34 for cations, anions, radionuclides, and mass spectrometer constituents, respectively. The first column identifies the constituent, the next four columns contain the relative standard deviations for each variance component. Columns 5 and 6 contain the estimated mean concentration and the overall RSD. Column 7 contains the number of observations that were reported in the core reports as less than values, and column 8 contains the total number of observations.

Relative standard deviations (RSD) are used to represent the variance components for the model terms. An RSD is the ratio of a standard deviation to a mean. It is a unitless measurement of variability and allows comparisons of variability across constituents whose magnitudes might widely differ. For individual variance components, the RSD is computed by dividing the square root of the variance component by the estimated mean concentration. An overall RSD was computed for each constituent by dividing the square root of the predicted variance of the mean by the estimated mean. The variance components are defined in terms of the ANOVA model;

$$Y'_{ijmp} = \mu' + Riser'_i + Rep'_{ij} + Hom'_{ijm} + Error'_{ijmp} \tag{10}$$

see section 2.3 for a more complete description of the model.

Table 30: Composite Data: Relative Standard Deviations for Cations (ppm)

	Riser	Core	Hom	Lab	Mu	RSD(Mu)	Less Than	Obs
Ag	0.9958	0.148	**	0.0647	46.73	0.5017	0	14
	3*	3	0	7				
Al	0	0.4132	**	0.01097	1,133	0.1562	0	14
	3	3	0	7				
As							41	42
B	0	0.333	**	0.1762	49.43	0.1344	3	14
	3	3	0	7				
Ba	0	0.1152	**	0.02672	14.14	0.04413	0	14
	3	3	0	7				
Be							14	14
Bi	0.122	0.0679	0.01977	0.06739	18,520	0.06785	0	42
	3	3	8	27				
Ca	0	0.1852	**	0.02721	809.6	0.07036	0	14
	3	3	0	7				
Cd	0	0.2905	**	0.2261	5.286	0.1253	4	14
	3	3	0	7				
Ce	0	0.727	**	0.1489	37.14	0.2777	9	14
	3	3	0	7				
Co							13	14
Cr	0.03903	0.04174	**	0.005823	810	0.02539	0	14
	3	3	0	7				
Cu	0.5264	0.1843	**	0.2165	42.52	0.2795	1	14
	3	3	0	7				
Dy							11	14
Fe	0.05518	0.07483	0	0.04885	18,060	0.04081	0	42
	3	3	8	27				
K	0	0.09467	**	0.115	311.6	0.0482	2	14
	3	3	0	7				
La	0.4448	0.5102	**	0.03663	31.81	0.2973	0	14
	3	3	0	7				
Li							13	14
Mg	0	0.1045	**	0.02441	178.5	0.04011	0	14
	3	3	0	7				
Mn	0	0.2865	**	0.01144	66.78	0.1083	0	14
	3	3	0	7				
Mo	0.2217	0.9941	**	0.1757	13.54	0.3959	3	14
	3	3	0	7				

* = Degrees of Freedom, ** = Data was not available to estimate this effect

Table 31: Composite Data: Relative Standard Deviations for Cations (ppm, continued)

	Riser	Core	Hom	Lab	Mu	RSD(Mu)	Less Than	Obs
Na	0.05515	0.03853	0.008702	0.05231	97,730	0.03285	0	42
	3*	3	8	27				
Nd	0.3433	0.6317	**	0.1936	15.86	0.3009	10	14
	3	3	0	7				
Ni	0	0.0959	**	0.08494	18.63	0.04346	2	14
	3	3	0	7				
P	0	0.1087	0	0.08798	16,060	0.04381	0	42
	3	3	8	27				
Pb	0.2017	0.5283	**	0.03614	528.4	0.2251	0	14
	3	3	0	7				
Re	0	0.1035	**	0.1482	6.5	0.05567	2	14
	3	3	0	7				
Rh							13	14
Ru	0	0.6444	**	0.02717	111.3	0.2437	0	14
	3	3	0	7				
Sb							13	14
Si	0.06073	0.04242	0.004126	0.05226	9,358	0.03584	0	42
	3	3	8	27				
Sr	0.1868	0.04684	**	0.005067	211	0.09523	0	14
	3	3	0	7				
Te	0.3583	0.2783	**	0.2268	19.26	0.2183	4	14
	3	3	0	7				
Th							11	14
Ti	0.1434	0.3669	**	0.123	8.413	0.1604	2	14
	3	3	0	7				
Tl							14	14
U	0.1019	0.1807	0.02521	0.03889	208	0.08654	0	26
	3	3	6	13				
V	0	0.4786	**	0.1034	2.788	0.1833	3	14
	3	3	0	7				
Zn	0.1049	0.1425	**	0.02151	80.51	0.07609	0	14
	3	3	0	7				
Zr	0	0.2921	**	0.04619	6.25	0.12	1	14
	3	3	0	7				

* = Degrees of Freedom, ** = Data was not available to estimate this effect

Table 32: Composite Data: Relative Standard Deviations for Anions (ppm)

	Riser	Core	Hom	Lab	Mu	RSD(Mu)	Less Than	Obs
Cl	0.07462	0.1345	**	0.0233	1,234	0.06385	0	14
	3*	3	0	7				
F	0.0906	0.1114	**	0.04075	1,895	0.06338	0	14
	3	3	0	7				
NO_2	0	0.1013	**	0.02096	10,290	0.0387	0	14
	3	3	0	7				
NO_3	0.1618	0.007428	**	0.03104	187,100	0.08139	0	14
	3	3	0	7				
PO_4	0.07181	0	**	0.04451	25,250	0.03798	0	14
	3	3	0	7				
SO_4	0.1242	0.03478	**	0.0175	11,530	0.06378	0	14
	3	3	0	7				
TIC	0.03339	0.1693	**	0.06671	899.5	0.0686	0	14
	3	3	0	7				
TOC	0	0.1505	**	0.08055	381.2	0.06082	0	14
	3	3	0	7				

= Degrees of Freedom, ** = Data was not available to estimate this effect

Table 33: Composite Data: Relative Standard Deviations for Radionuclides (μCi/g)

	Riser	Core	Hom	Lab	Mu	RSD(Mu)	Less Than	Obs
^{241}Am	0.6807	0.1498	0	0.08984	0.07254	0.347	0	23
	3*	2	5	12				
^{243,244}Cm	0.8885	0.4224	0	0.3787	0.001279	0.5002	0	15
	3	1	3	7				
^{60}Co	0	0	1.022	1.71	0.01527	0.445	0	25
	2	2	10	10				
^{137}Cs	0.07155	0.02767	0.01376	0.02044	14.9	0.03775	0	52
	3	3	15	30				
^{152}Eu	0.4825	**	0	0.3368	0.06748	0.3858	0	5
	1	0	1	2				
^{3}H	0.06136	0.9017	**	0.3091	0.002167	0.3521	0	14
	3	3	0	7				
^{129}I	0	0.929	0	0.2896	0.00003606	0.3846	0	22
	3	2	5	11				
^{237}Np	0.3985	0	0.4422	0.2405	0.0001122	0.2483	0	22
	3	2	5	11				
^{238}Pu	0	0.5866	0.1344	0.138	0.003212	0.245	0	22
	3	2	5	11				
^{90}Sr	0.8082	0.08334	0	0.1726	108.4	0.4075	0	22
	3	2	5	11				
^{99}Tc	0.2537	0.1033	0.07417	0.08586	0.01648	0.1402	0	18
	3	1	4	9				
Total α	0	0.2429	0	0.06539	0.1555	0.1	0	24
	3	2	6	12				
Total β	0.4328	0.7805	0	0.03599	183.2	0.3688	0	26
	3	3	6	13				

* = Degrees of Freedom, ** = Data was not available to estimate this effect

Table 34: Composite Data: Relative Standard Deviations for Isotopic Mass Ratios

	Riser	Core	Hom	Lab	Mu	RSD(Mu)	Less Than	Obs
$^{238}Pu/^{239}Pu$	1.105	**	0	0.1235	0.002729	0.7831	0	6
	1*	0	1	3				
$^{240}Pu/^{239}Pu$	0.1526	**	0	0.02409	0.03323	0.1084	0	6
	1	0	1	3				
$^{241}Pu/^{239}Pu$	0.3029	**	0	0.1303	0.0007494	0.2215	0	6
	1	0	1	3				
$^{242}Pu/^{239}Pu$	0.2784	**	0	0.2534	0.00036	0.2247	0	6
	1	0	1	3				
$^{234}U/^{238}U$	0	**	0	0.1178	0.00006367	0.0481	0	6
	1	0	1	3				
$^{235}U/^{238}U$	0.003789	**	0	0.001665	0.006757	0.002774	0	6
	1	0	1	3				
$^{236}U/^{238}U$	0	**	0.03378	0.02812	0.0001143	0.02263	0	6
	1	0	1	3				

* = Degrees of Freedom, ** = Data was not available to estimate this effect

APPENDIX D

PLOTS OF CONSTITUENTS BY RISER AND SEGMENT

Appendix D - Plots of Constituents by Riser and Segment

This appendix contains "vertical profile" plots for each constituent. These are plots of the term

$$\mu + \frac{1}{n_i} \sum_i (Riser_i + Seg_{ij}) \,, \tag{11}$$

for each constituent. The vertical profiles are surrounded by 95% confidence bounds.

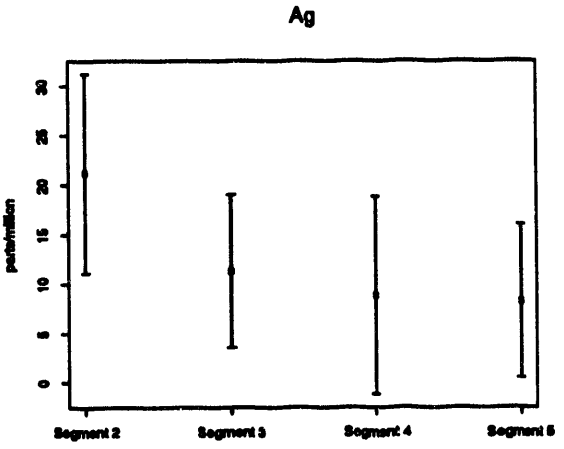
Ag
parts/million
0
5
10
15
20
25
30
Segment 2
Segment 3
Segment 4
Segment 5

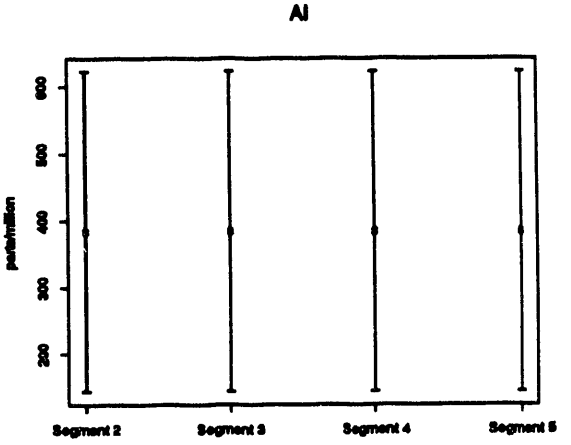
Al
parts/million
200
300
400
500
600
Segment 2
Segment 3
Segment 4
Segment 5

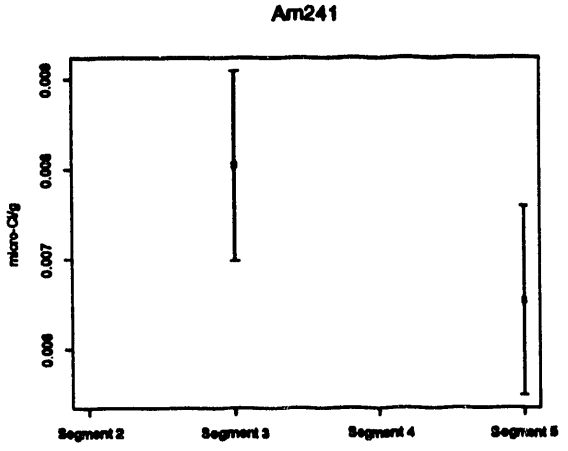
Am241
micro-Ci/g
0.006
0.007
0.008
0.009
Segment 2
Segment 3
Segment 4
Segment 5

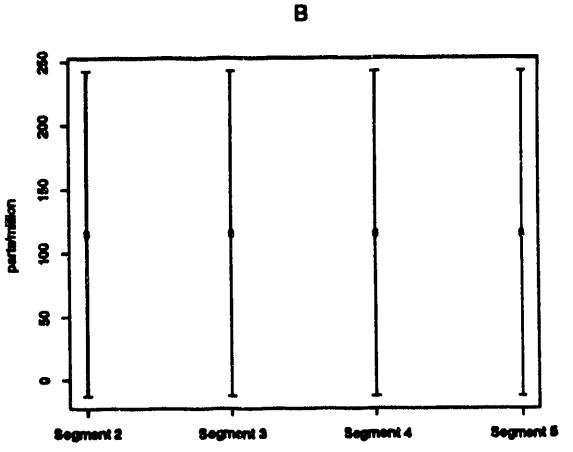
B
parts/million
0
50
100
150
200
250
Segment 2
Segment 3
Segment 4
Segment 5

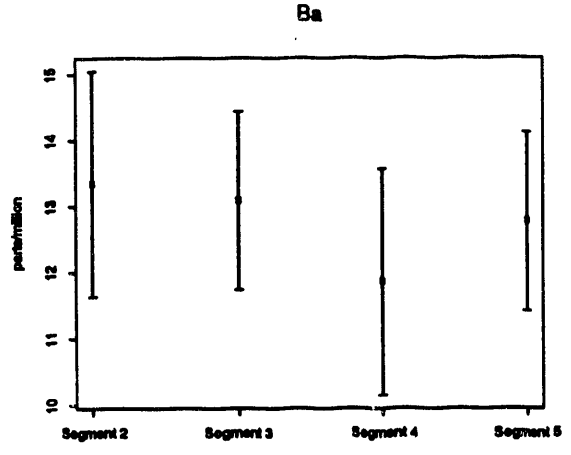
Ba
parts/million
10
11
12
13
14
15
Segment 2
Segment 3
Segment 4
Segment 5

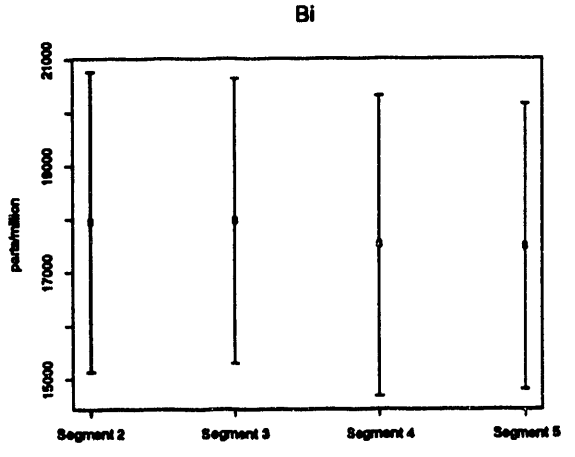
Bi
parts/million
15000
17000
19000
21000
Segment 2
Segment 3
Segment 4
Segment 5

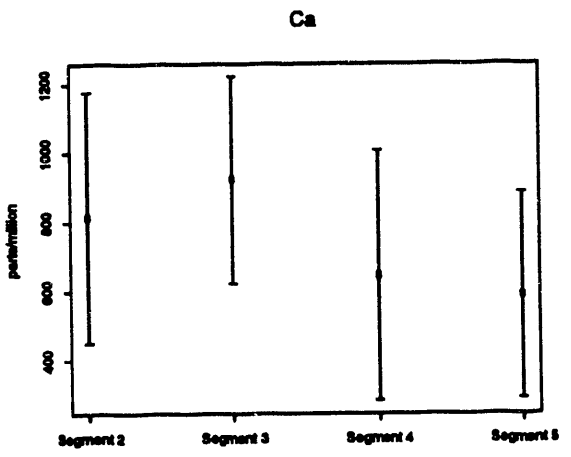
Ca
parts/million
400
600
800
1000
1200
Segment 2
Segment 3
Segment 4
Segment 5

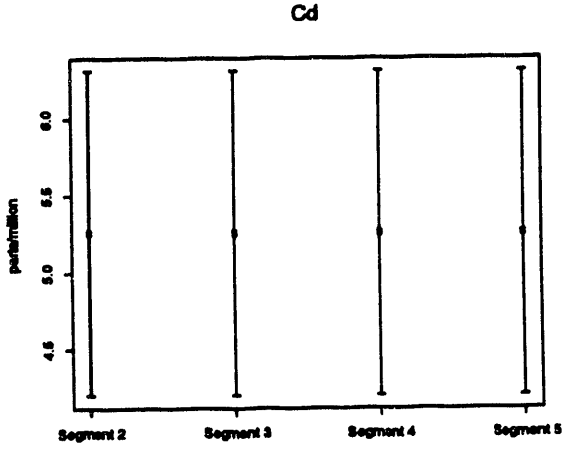
Cd
parts/million
4.5
5.0
5.5
6.0
Segment 2
Segment 3
Segment 4
Segment 5

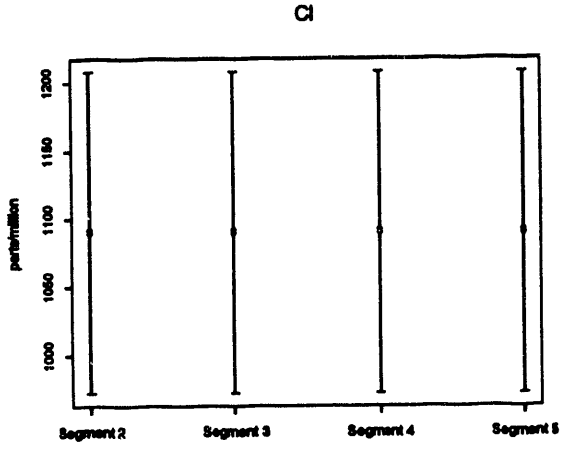
Cl
parts/million
1000
1050
1100
1150
1200
Segment 2
Segment 3
Segment 4
Segment 5

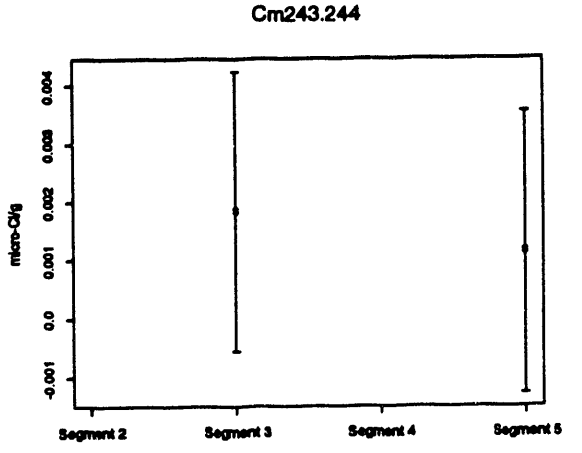
Cm243.244
micro-Ci/g
-0.001
0.0
0.001
0.002
0.003
0.004
Segment 2
Segment 3
Segment 4
Segment 5

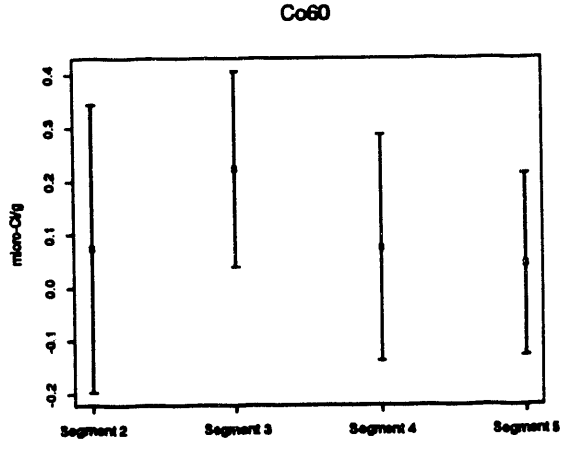
Co60
micro-Ci/g
-0.2
-0.1
0.0
0.1
0.2
0.3
0.4
Segment 2
Segment 3
Segment 4
Segment 5

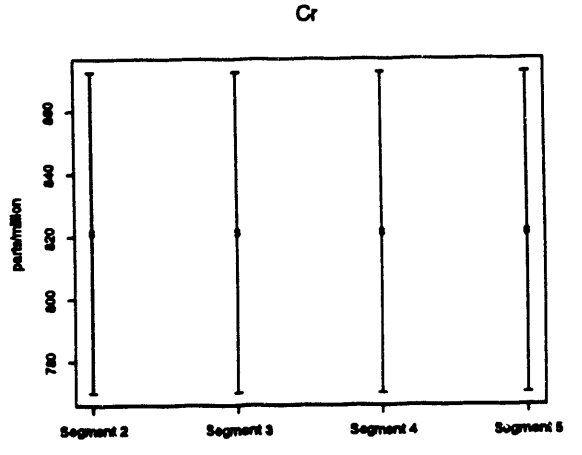
Cr
parts/million
780
800
820
840
860
Segment 2
Segment 3
Segment 4
Segment 5

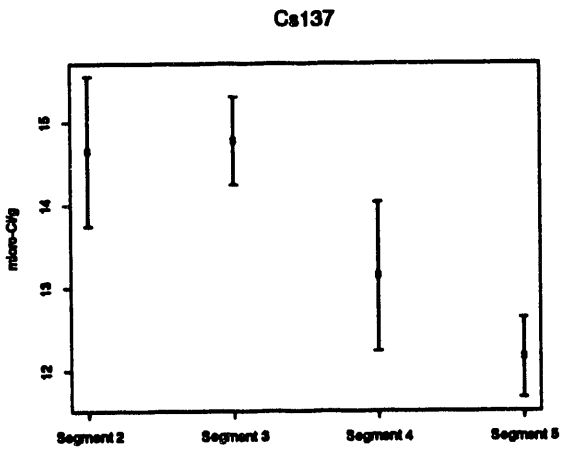
Cs137
micro-Ci/g
12
13
14
15
Segment 2
Segment 3
Segment 4
Segment 5

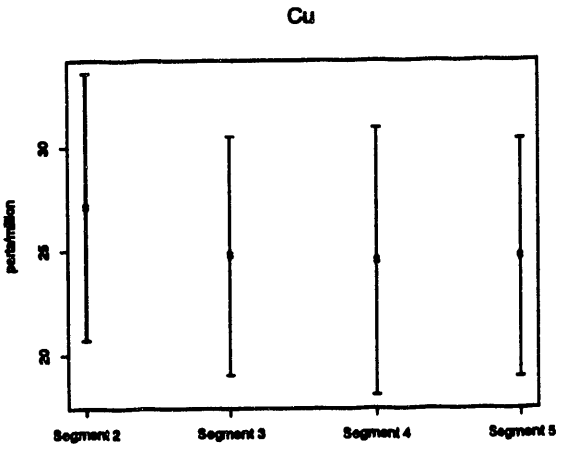
Cu
parts/million
20
25
30
Segment 2
Segment 3
Segment 4
Segment 5

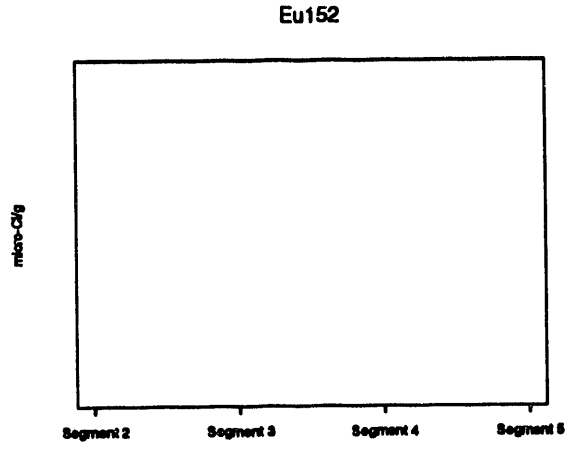
Eu152
micro-Ci/g
Segment 2
Segment 3
Segment 4
Segment 5

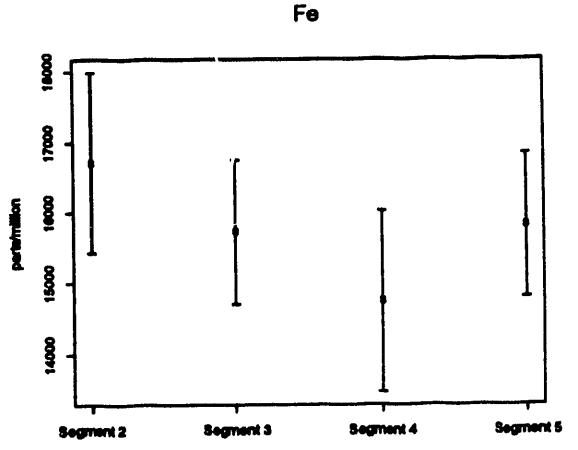
Fe
parts/million
14000
15000
16000
17000
18000
Segment 2
Segment 3
Segment 4
Segment 5

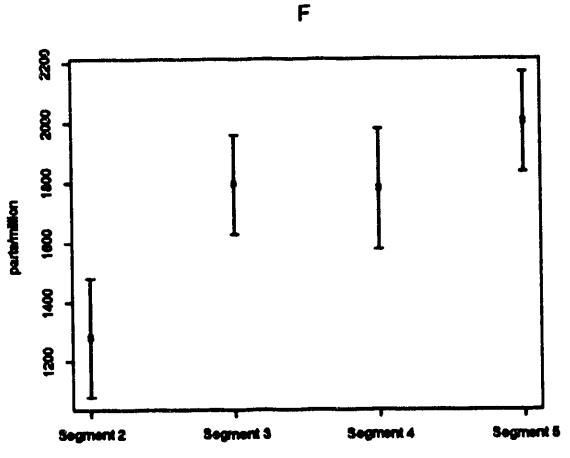
F
parts/million
1200
1400
1600
1800
2000
2200
Segment 2
Segment 3
Segment 4
Segment 5

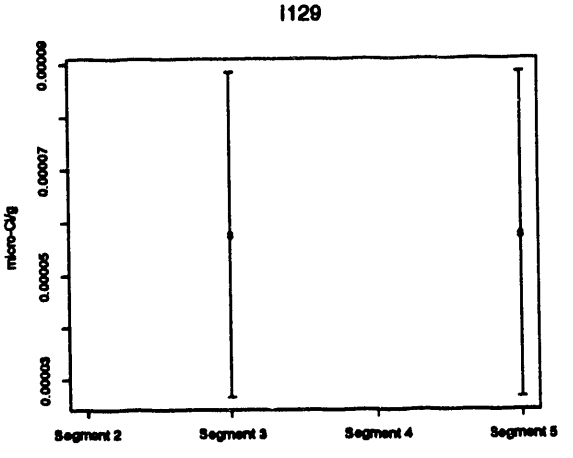
I129
micro-Ci/g
0.00003
0.00005
0.00007
0.00009
Segment 2
Segment 3
Segment 4
Segment 5

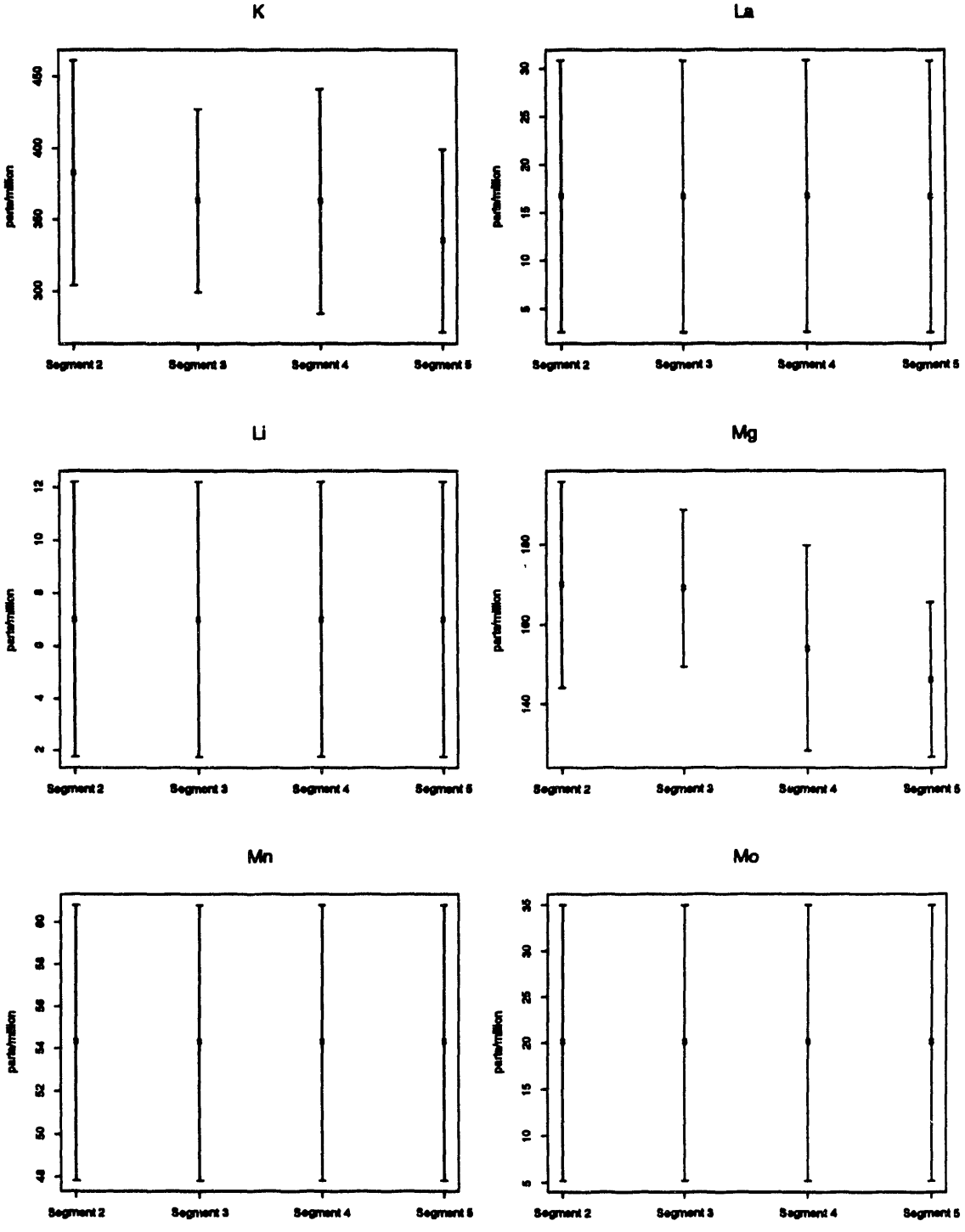
K
La
Li
Mg
Mn
Mo
parts/million
Segment 2
Segment 3
Segment 4
Segment 5

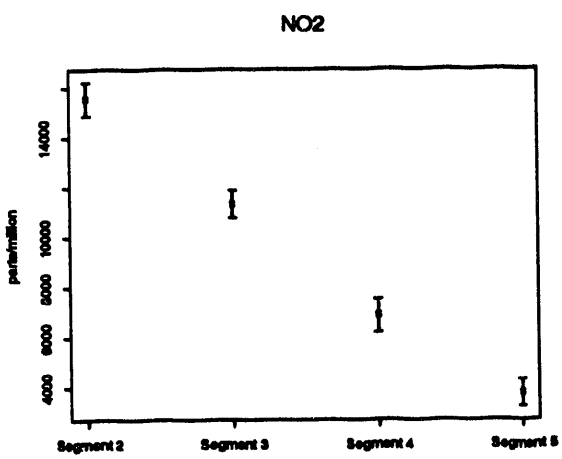
NO2
parts/million
4000
6000
8000
10000
14000
Segment 2
Segment 3
Segment 4
Segment 5

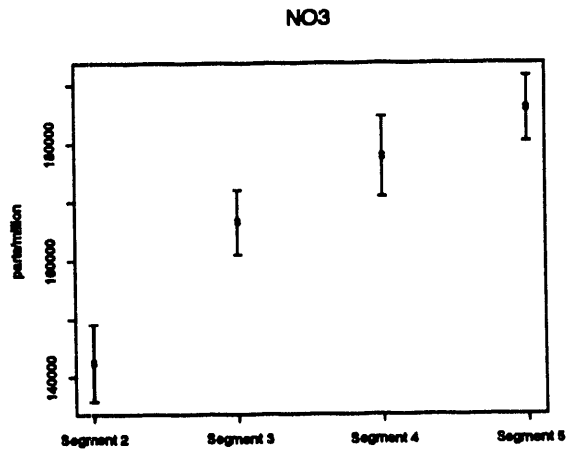
NO3
parts/million
140000
160000
180000
Segment 2
Segment 3
Segment 4
Segment 5

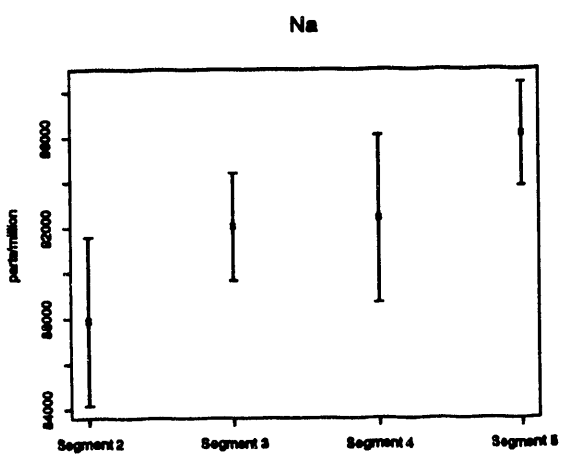
Na
parts/million
84000
88000
92000
96000
Segment 2
Segment 3
Segment 4
Segment 5

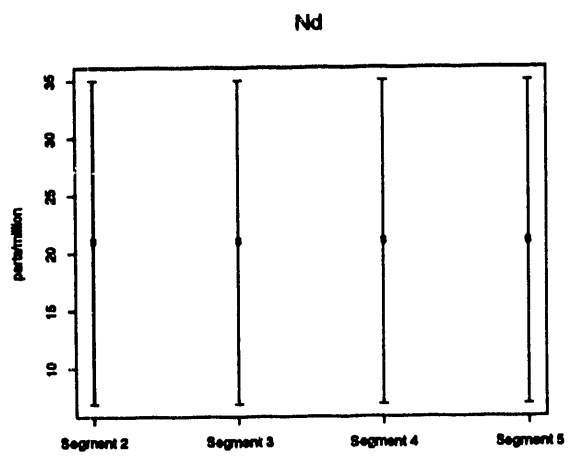
Nd
parts/million
10
15
20
25
30
35
Segment 2
Segment 3
Segment 4
Segment 5

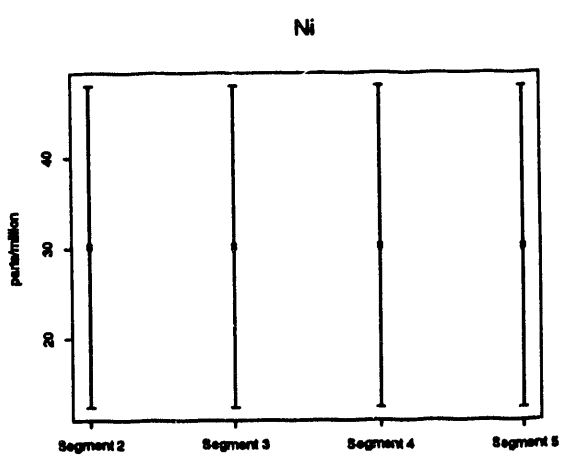
Ni
parts/million
20
30
40
Segment 2
Segment 3
Segment 4
Segment 5

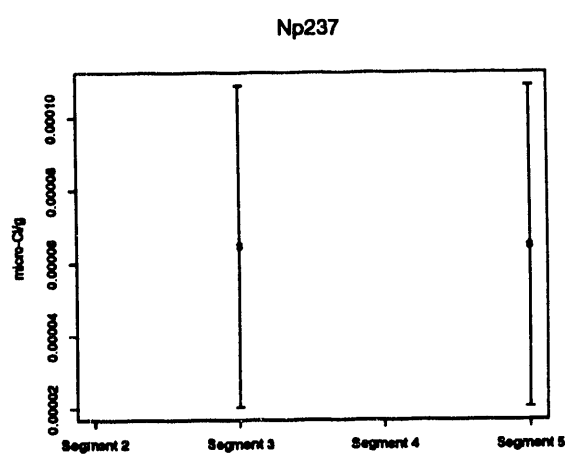
Np237
micro-Ci/g
0.00002
0.00004
0.00006
0.00008
0.00010
Segment 2
Segment 3
Segment 4
Segment 5

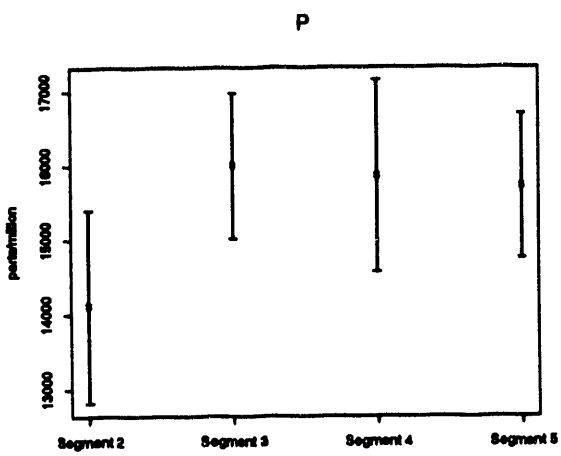
P
parts/million
13000
14000
15000
16000
17000
Segment 2
Segment 3
Segment 4
Segment 5

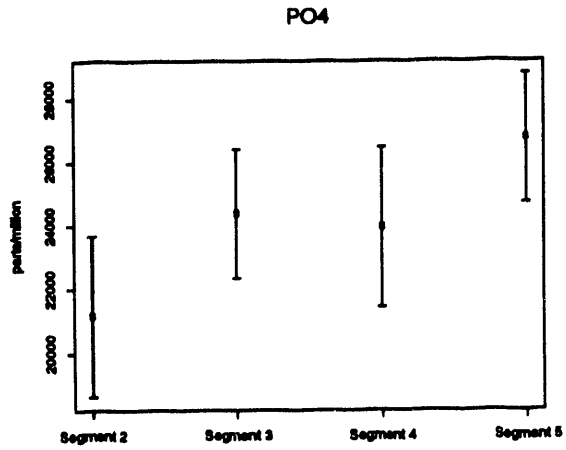
PO4
parts/million
20000
22000
24000
26000
28000
Segment 2
Segment 3
Segment 4
Segment 5

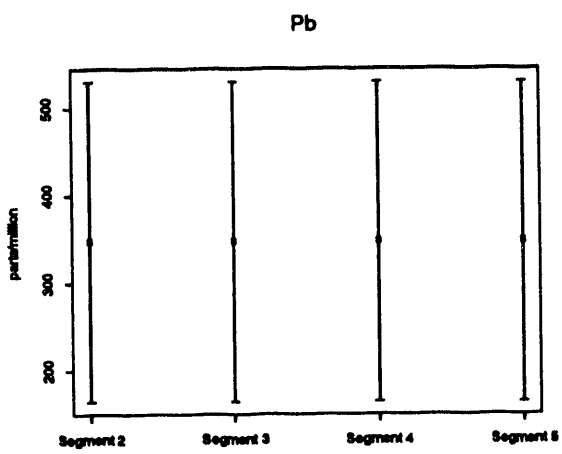
Pb
parts/million
200
300
400
500
Segment 2
Segment 3
Segment 4
Segment 5

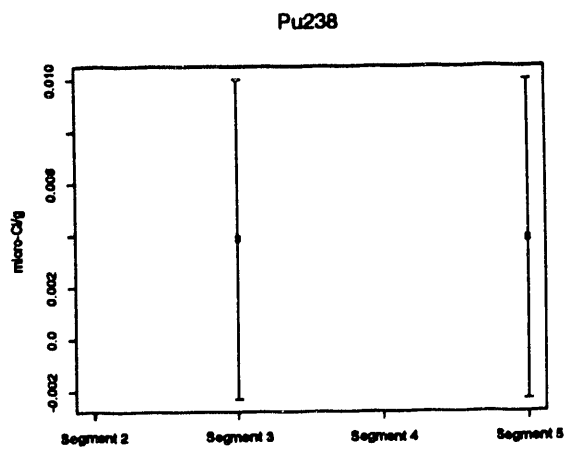
Pu238
micro-Ci/g
-0.002
0.0
0.002
0.006
0.010
Segment 2
Segment 3
Segment 4
Segment 5

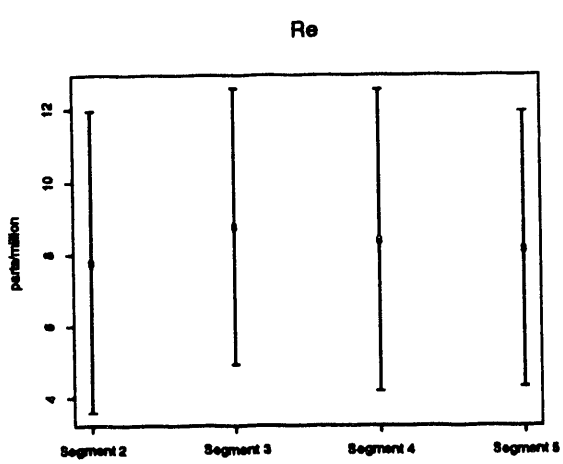
Re
parts/million
4
6
8
10
12
Segment 2
Segment 3
Segment 4
Segment 5

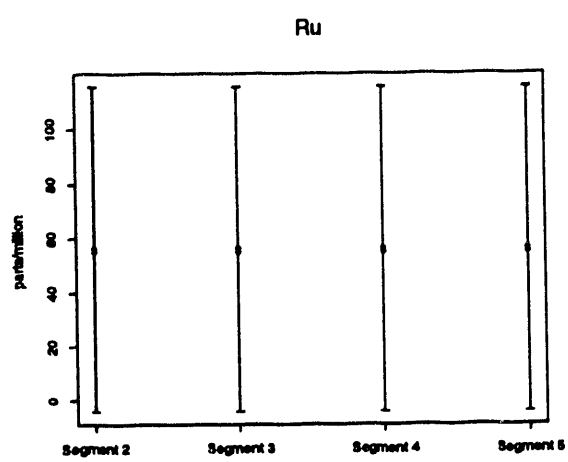
Ru
parts/million
0
20
40
60
80
100
Segment 2
Segment 3
Segment 4
Segment 5

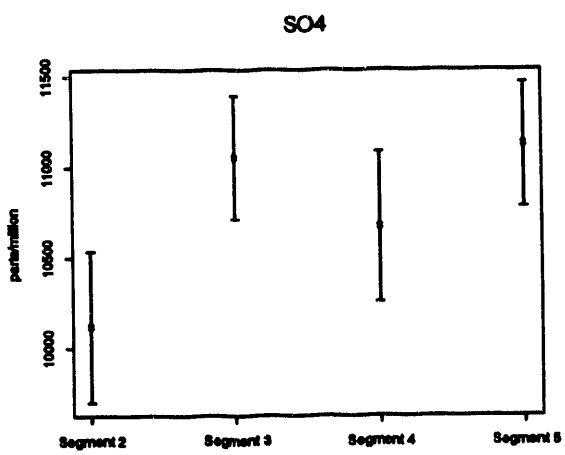
SO4
parts/million
10000
10500
11000
11500
Segment 2
Segment 3
Segment 4
Segment 5

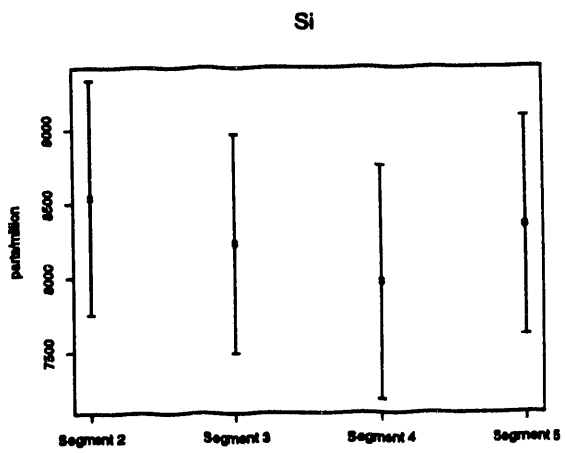
Si
parts/million
7500
8000
8500
9000
Segment 2
Segment 3
Segment 4
Segment 5

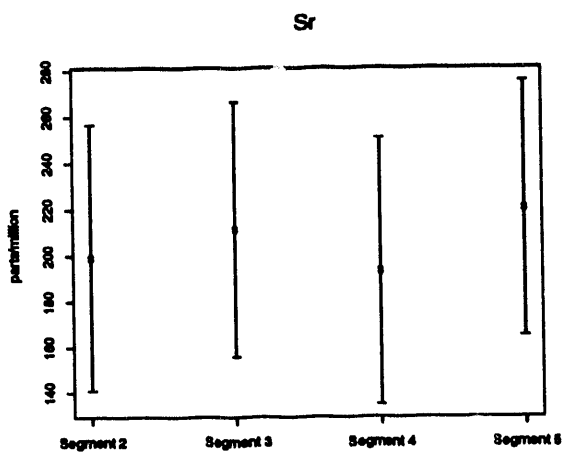
Sr
parts/million
140
160
180
200
220
240
260
280
Segment 2
Segment 3
Segment 4
Segment 5

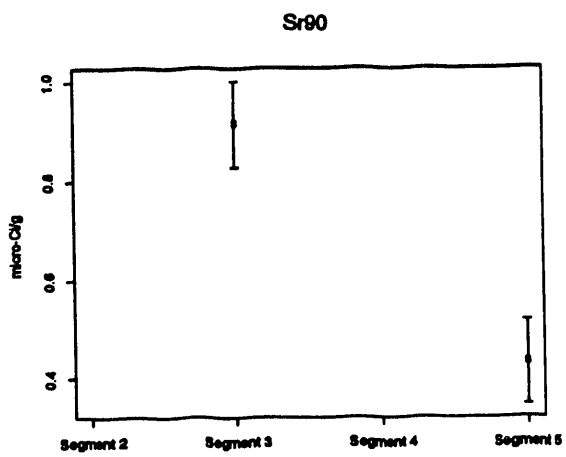
Sr90
micro-Ci/g
0.4
0.6
0.8
1.0
Segment 2
Segment 3
Segment 4
Segment 5

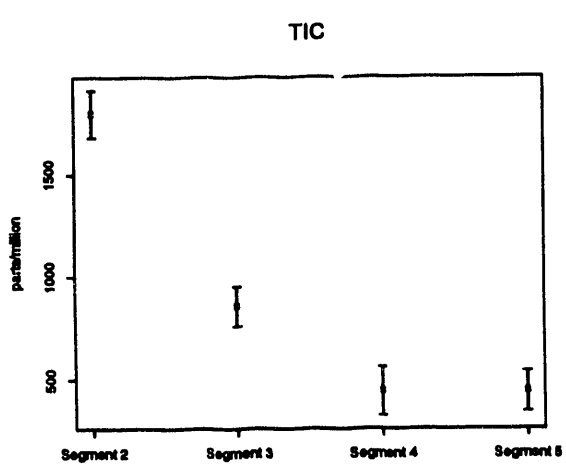
TIC
parts/million
500
1000
1500
Segment 2
Segment 3
Segment 4
Segment 5

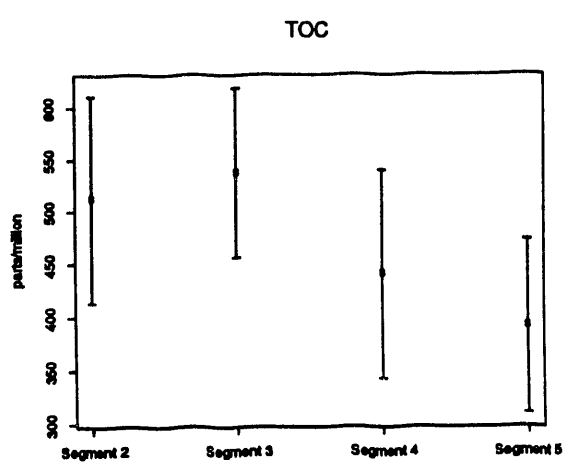
TOC
parts/million
300
350
400
450
500
550
600
Segment 2
Segment 3
Segment 4
Segment 5

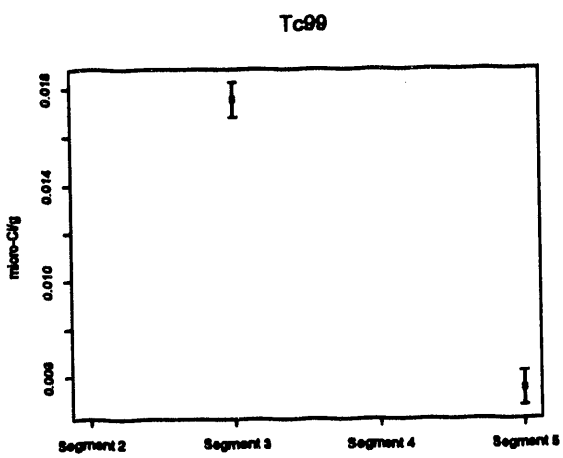
Tc99
micro-Ci/g
0.006
0.010
0.014
0.018
Segment 2
Segment 3
Segment 4
Segment 5

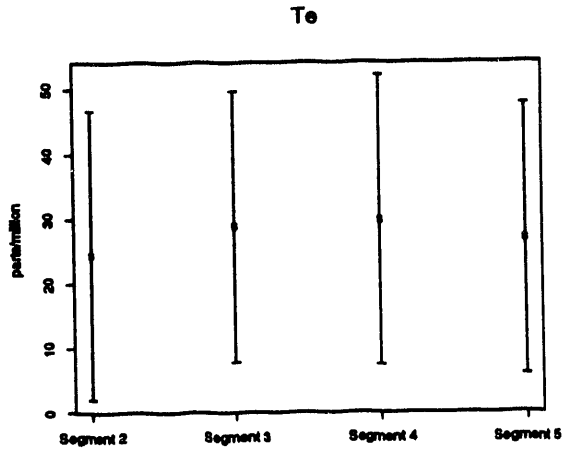
Te
parts/million
0
10
20
30
40
50
Segment 2
Segment 3
Segment 4
Segment 5

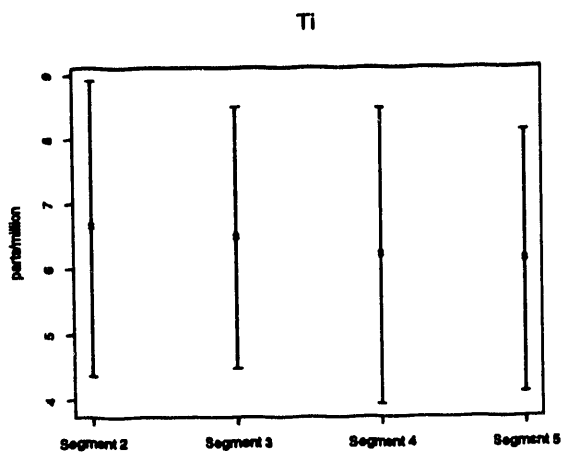
Ti
parts/million
4
5
6
7
8
9
Segment 2
Segment 3
Segment 4
Segment 5

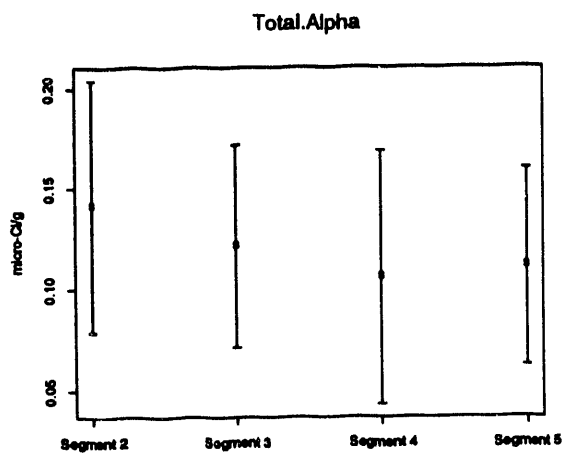
Total.Alpha
micro-Ci/g
0.05
0.10
0.15
0.20
Segment 2
Segment 3
Segment 4
Segment 5

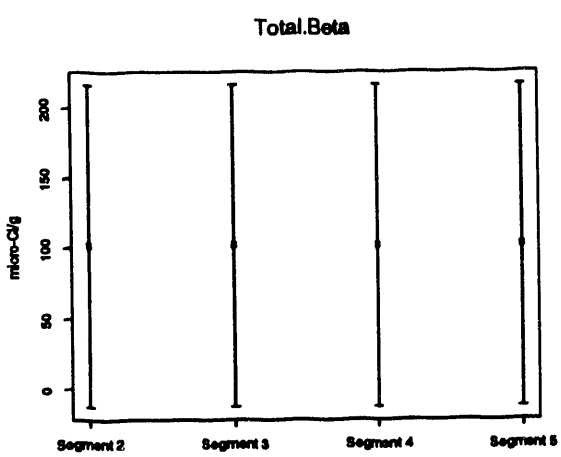
Total.Beta
micro-Ci/g
0
50
100
150
200
Segment 2
Segment 3
Segment 4
Segment 5

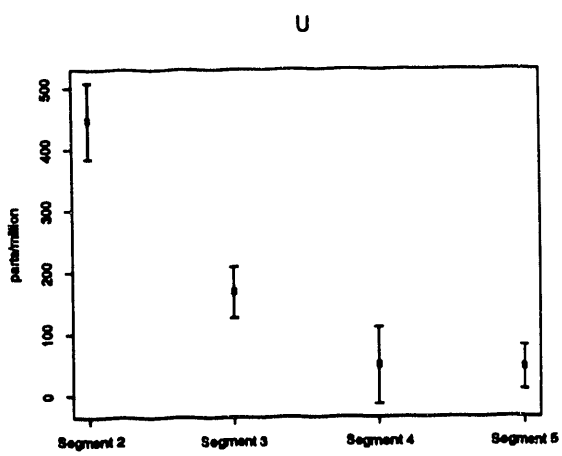
U
parts/million
0
100
200
300
400
500
Segment 2
Segment 3
Segment 4
Segment 5

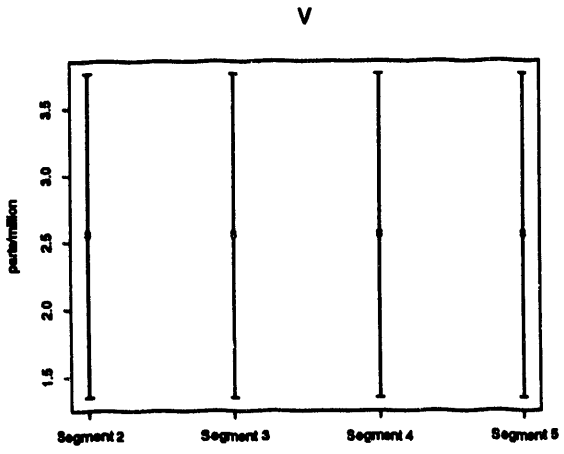
V
parts/million
1.5
2.0
2.5
3.0
3.5
Segment 2
Segment 3
Segment 4
Segment 5

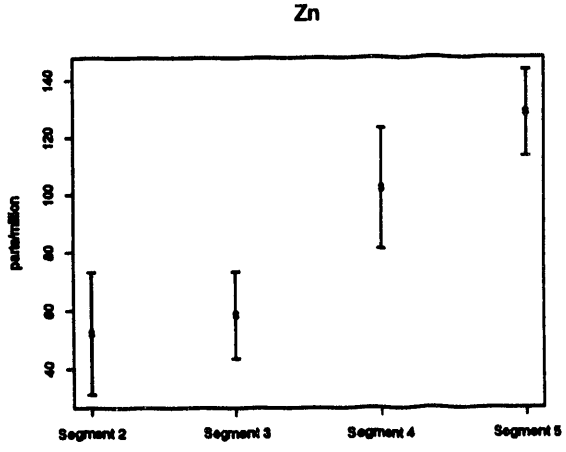
Zn
parts/million
40
60
80
100
120
140
Segment 2
Segment 3
Segment 4
Segment 5

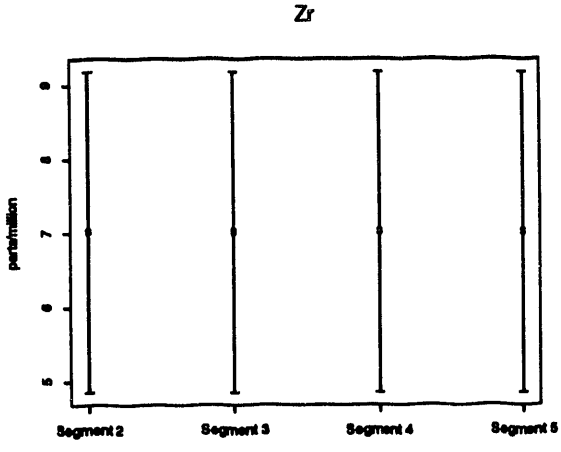
Zr
parts/million
5
6
7
8
9
Segment 2
Segment 3
Segment 4
Segment 5

APPENDIX E

COMPARISON OF SEGMENT AND COMPOSITE MEASUREMENTS

Appendix E - Comparison of Segment and Composite Measurements

This appendix contains riser concentration plots. Each plot displays the terms $\mu + Riser_i$ for each constituent, surrounded by 95% confidence bounds. Since riser concentration can be computed from both composite and segment-level data sets, two estimates are plotted for each riser. The segment-level estimates are marked with an "s" and the composite with a "c".

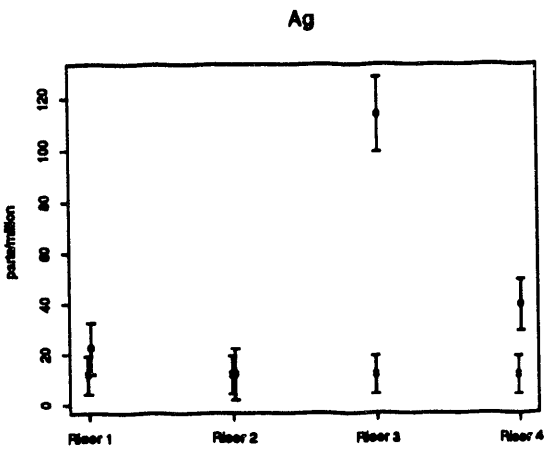
Ag
parts/million
0
20
40
60
80
100
120
Riser 1
Riser 2
Riser 3
Riser 4

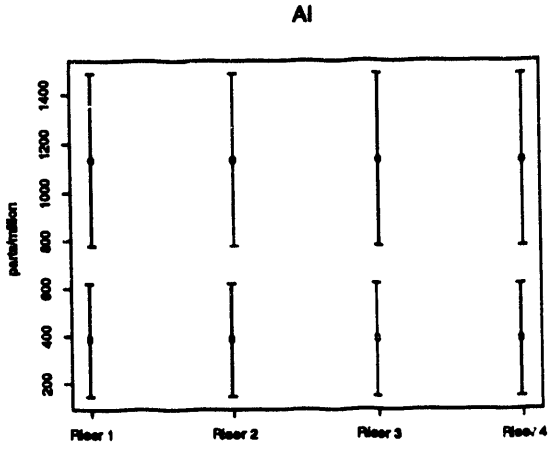
Al
parts/million
200
400
600
800
1000
1200
1400
Riser 1
Riser 2
Riser 3
Riser 4

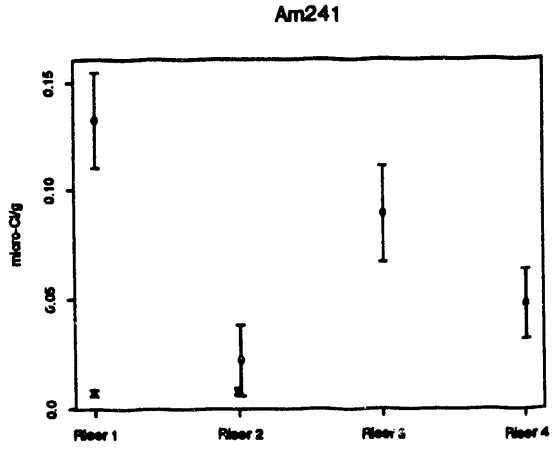
Am241
micro-Ci/g
0.0
0.05
0.10
0.15
Riser 1
Riser 2
Riser 3
Riser 4

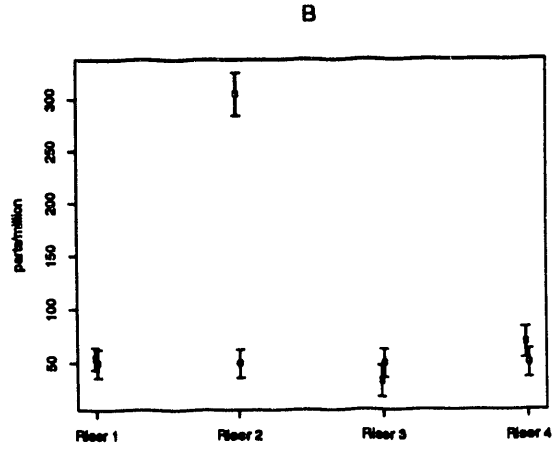
B
parts/million
50
100
150
200
250
300
Riser 1
Riser 2
Riser 3
Riser 4

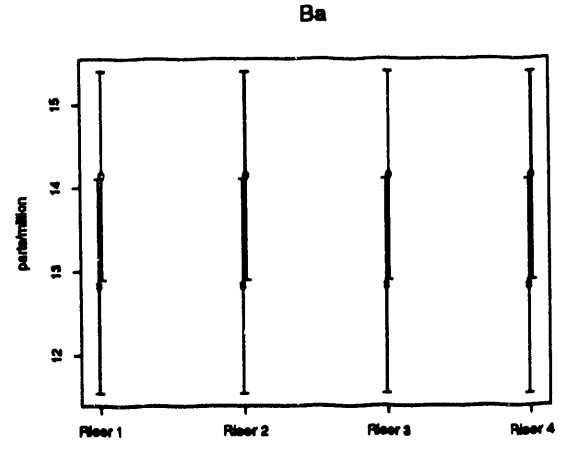
Ba
parts/million
12
13
14
15
Riser 1
Riser 2
Riser 3
Riser 4

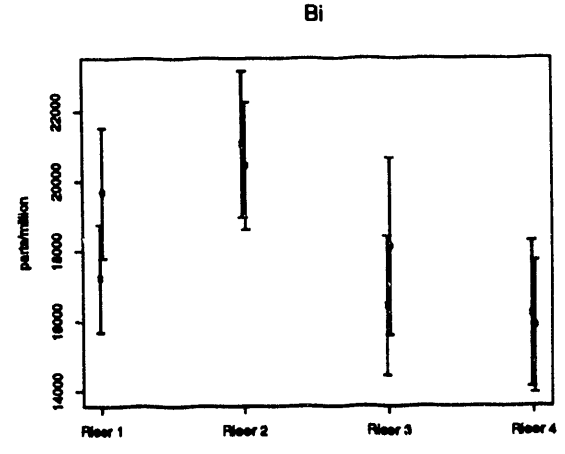
Bi
parts/million
14000
16000
18000
20000
22000
Riser 1
Riser 2
Riser 3
Riser 4

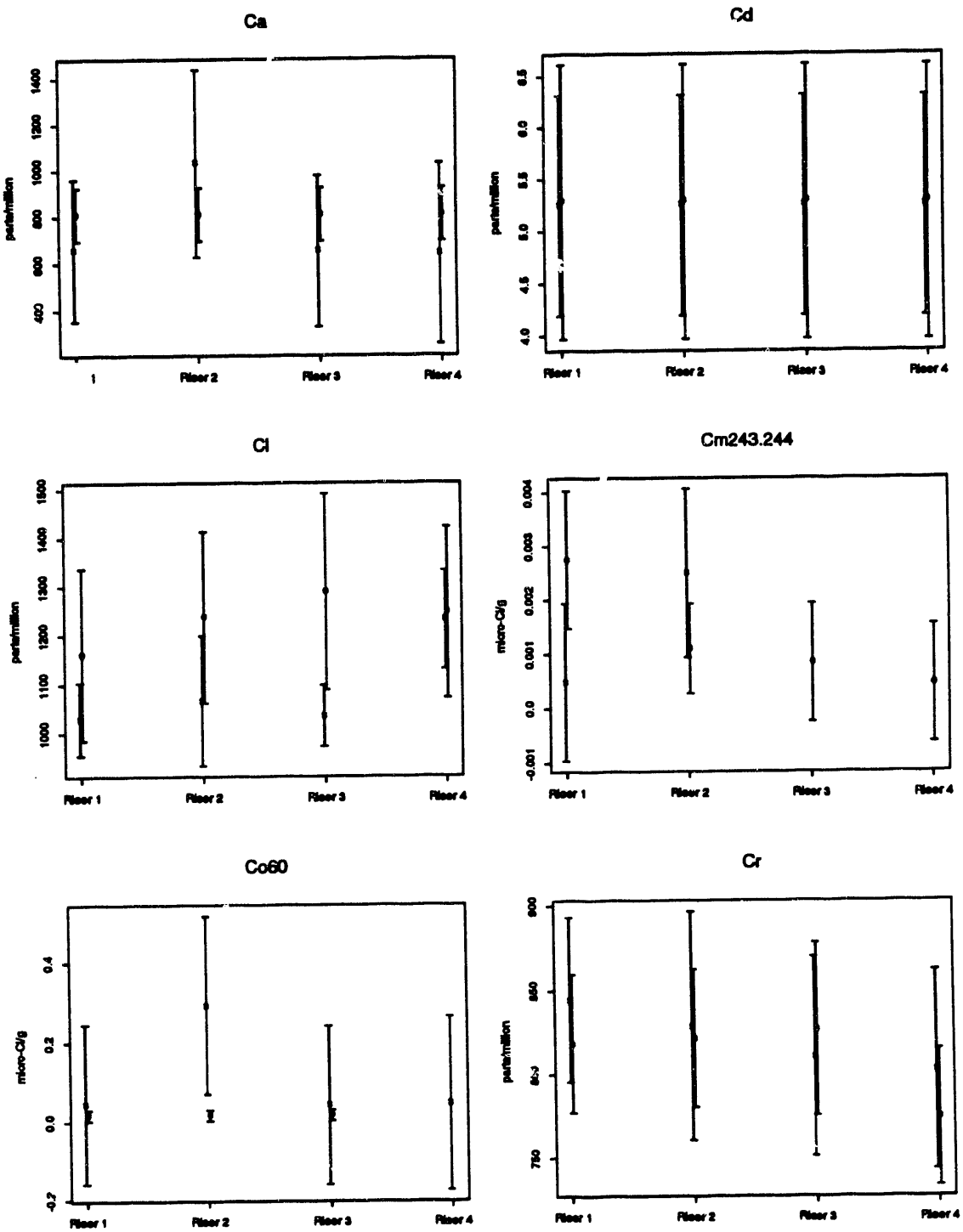
Ca
parts/million
400
600
800
1000
1200
1400
1
Riser 2
Riser 3
Riser 4
Cd
parts/million
4.0
4.5
5.0
5.5
6.0
6.5
Riser 1
Riser 2
Riser 3
Riser 4
Cl
parts/million
1000
1100
1200
1300
1400
1500
Riser 1
Riser 2
Riser 3
Riser 4
Cm243.244
micro-Ci/g
-0.001
0.0
0.001
0.002
0.003
0.004
Riser 1
Riser 2
Riser 3
Riser 4
Co60
micro-Ci/g
-0.2
0.0
0.2
0.4
Riser 1
Riser 2
Riser 3
Riser 4
Cr
parts/million
750
850
900
Riser 1
Riser 2
Riser 3
Riser 4

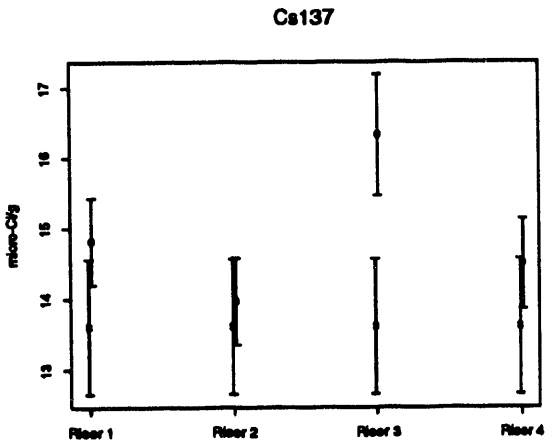
Cs137
micro-Ci/g
13
14
15
16
17
Riser 1
Riser 2
Riser 3
Riser 4

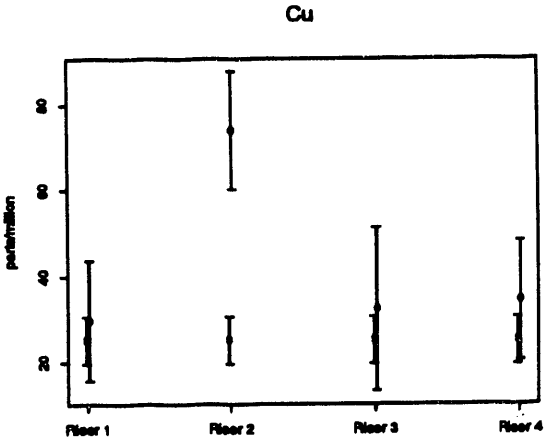
Cu
parts/million
20
40
60
80
Riser 1
Riser 2
Riser 3
Riser 4

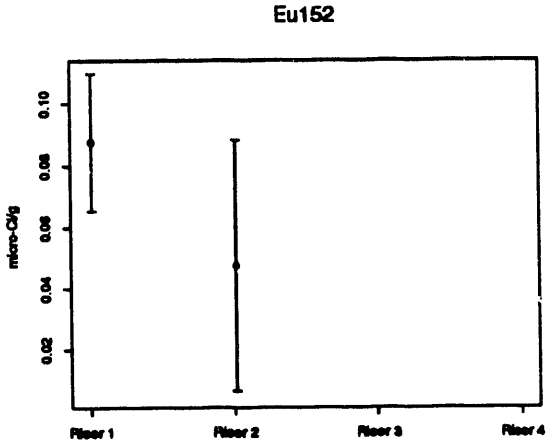
Eu152
micro-Ci/g
0.02
0.04
0.06
0.08
0.10
Riser 1
Riser 2
Riser 3
Riser 4

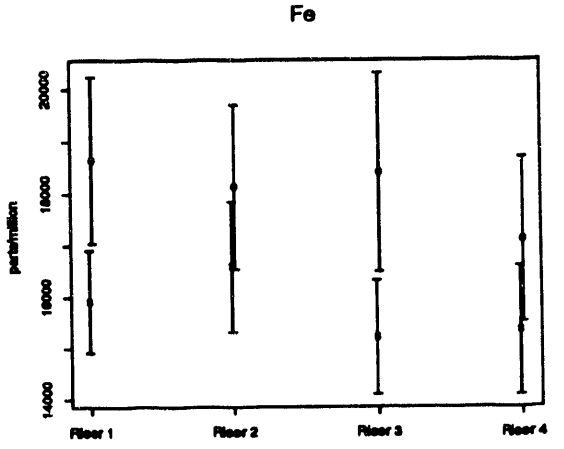
Fe
parts/million
14000
16000
18000
20000
Riser 1
Riser 2
Riser 3
Riser 4

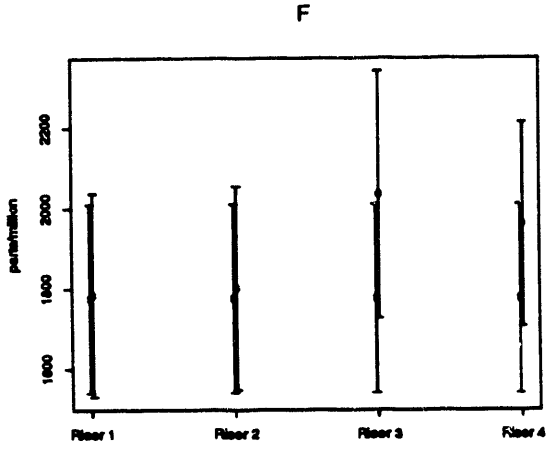
F
parts/million
1600
1800
2000
2200
Riser 1
Riser 2
Riser 3
Riser 4

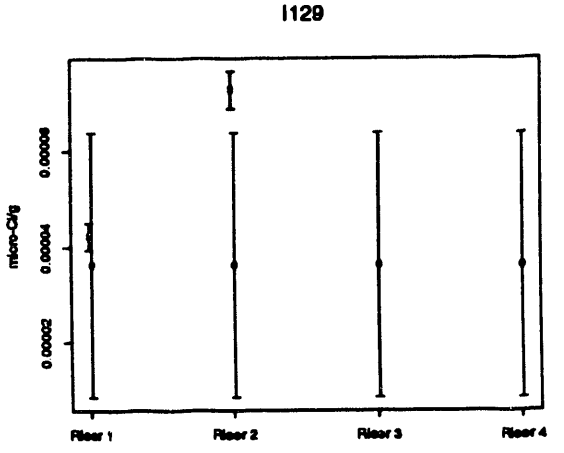
I129
micro-Ci/g
0.00002
0.00004
0.00006
Riser 1
Riser 2
Riser 3
Riser 4

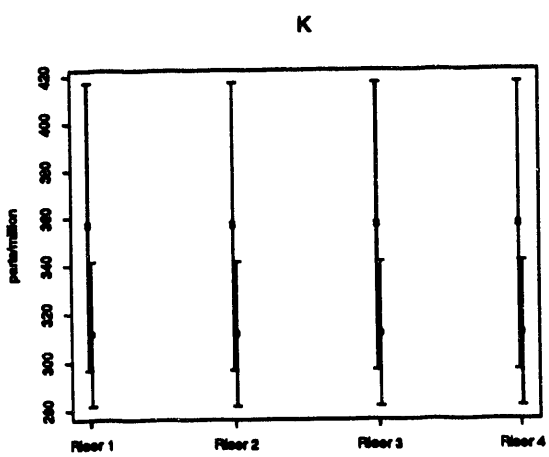
K
parts/million
Riser 1
Riser 2
Riser 3
Riser 4

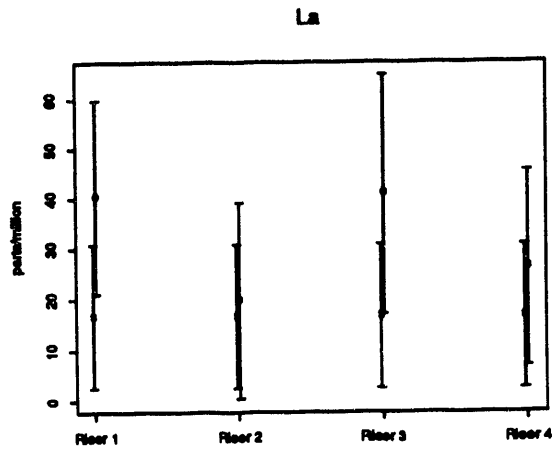
La
parts/million
Riser 1
Riser 2
Riser 3
Riser 4

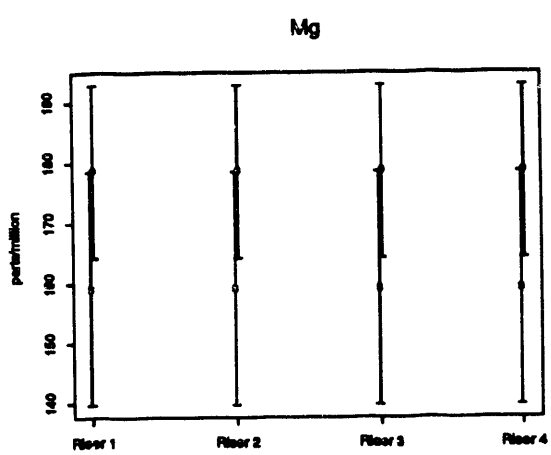
Mg
parts/million
Riser 1
Riser 2
Riser 3
Riser 4

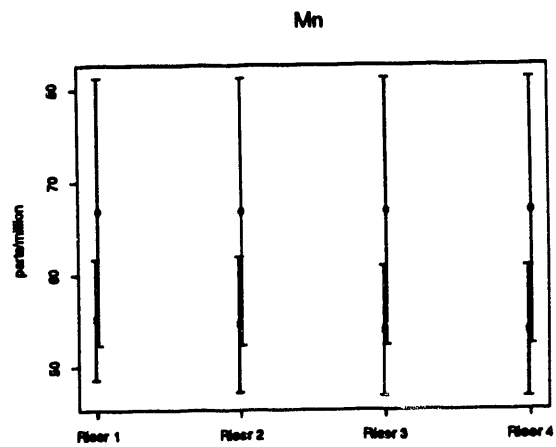
Mn
parts/million
Riser 1
Riser 2
Riser 3
Riser 4

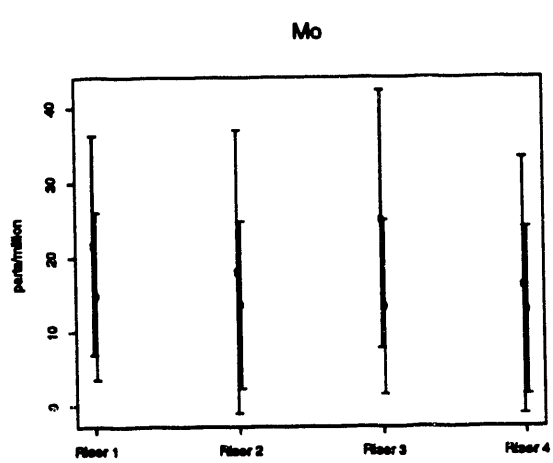
Mo
parts/million
Riser 1
Riser 2
Riser 3
Riser 4

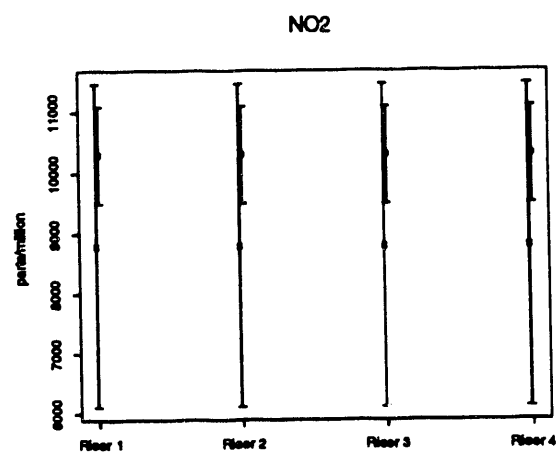
NO2
parts/million
Riser 1
Riser 2
Riser 3
Riser 4

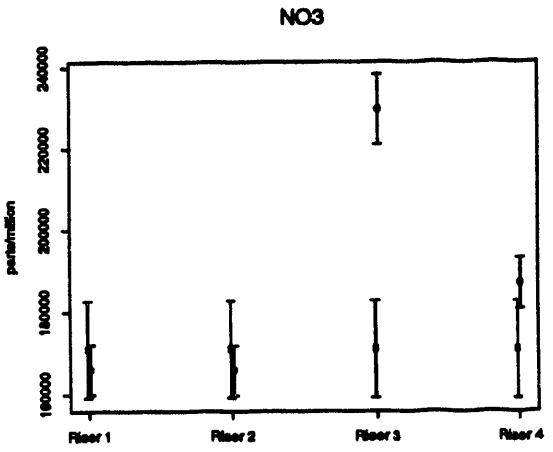
NO3
parts/million
160000
180000
200000
220000
240000
Riser 1
Riser 2
Riser 3
Riser 4

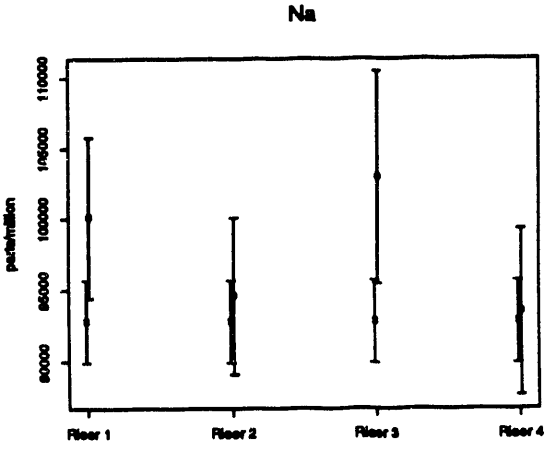
Na
parts/million
80000
85000
90000
95000
100000
105000
110000
Riser 1
Riser 2
Riser 3
Riser 4

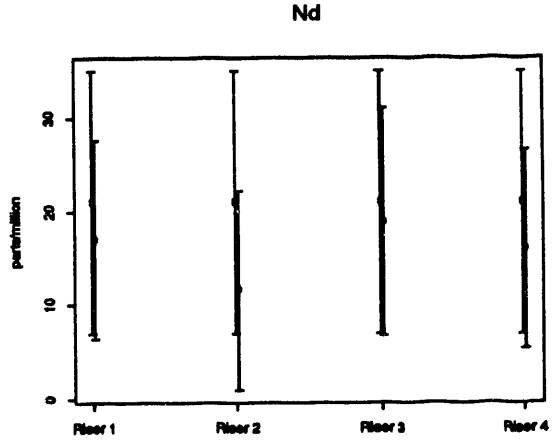
Nd
parts/million
0
10
20
30
Riser 1
Riser 2
Riser 3
Riser 4

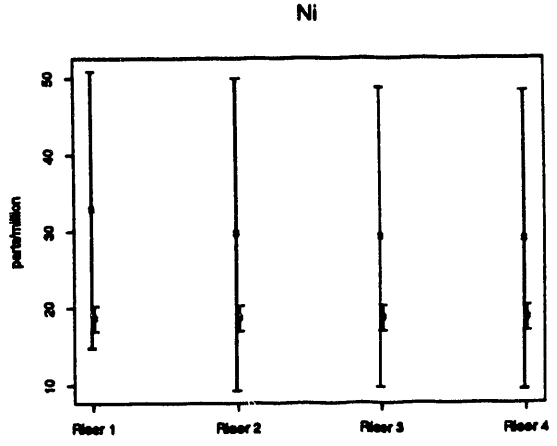
Ni
parts/million
10
20
30
40
50
Riser 1
Riser 2
Riser 3
Riser 4

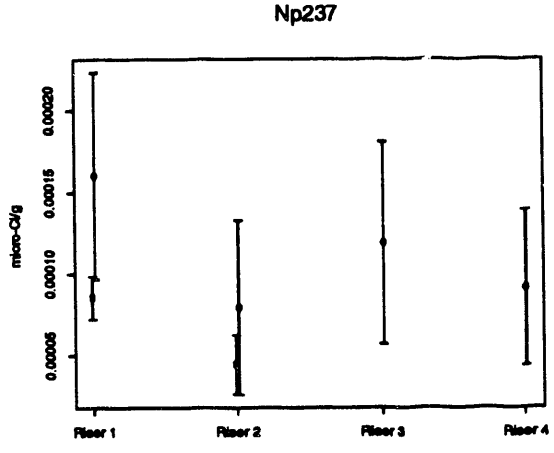
Np237
micro-Ci/g
0.00005
0.00010
0.00015
0.00020
Riser 1
Riser 2
Riser 3
Riser 4

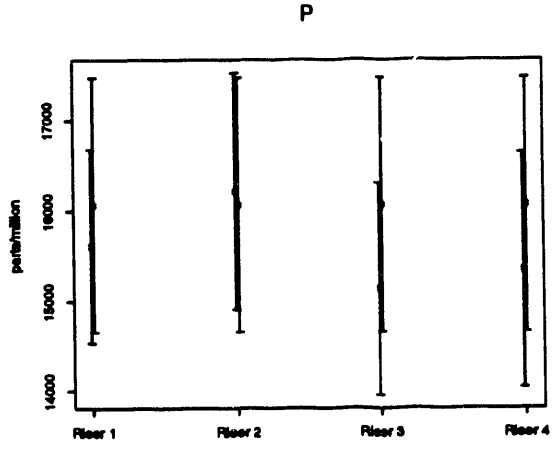
P
parts/million
14000
15000
16000
17000
Riser 1
Riser 2
Riser 3
Riser 4

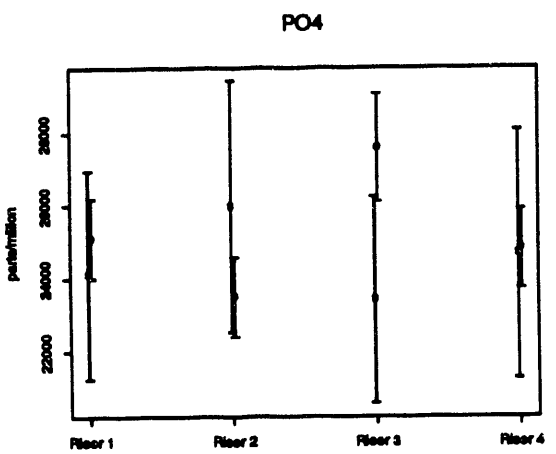
PO4
parts/million
22000
24000
26000
28000
Riser 1
Riser 2
Riser 3
Riser 4

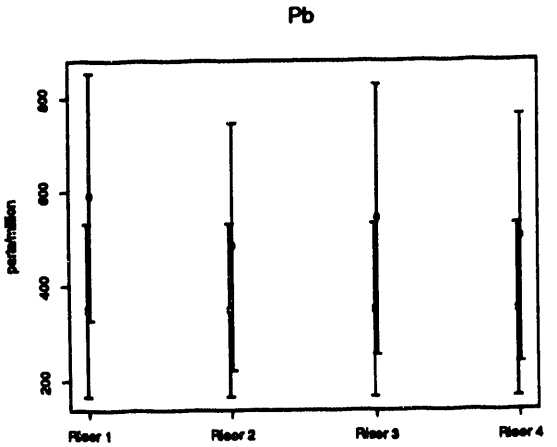
Pb
parts/million
200
400
600
800
Riser 1
Riser 2
Riser 3
Riser 4

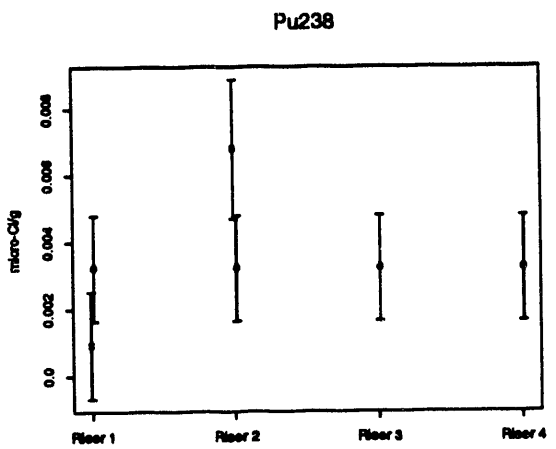
Pu238
micro-Ci/g
0.0
0.002
0.004
0.006
0.008
Riser 1
Riser 2
Riser 3
Riser 4

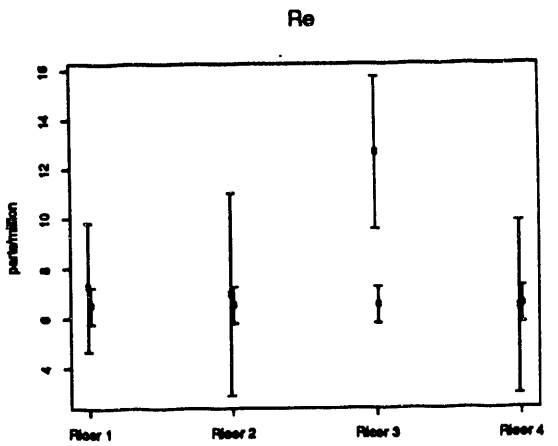
Re
parts/million
4
6
8
10
12
14
16
Riser 1
Riser 2
Riser 3
Riser 4

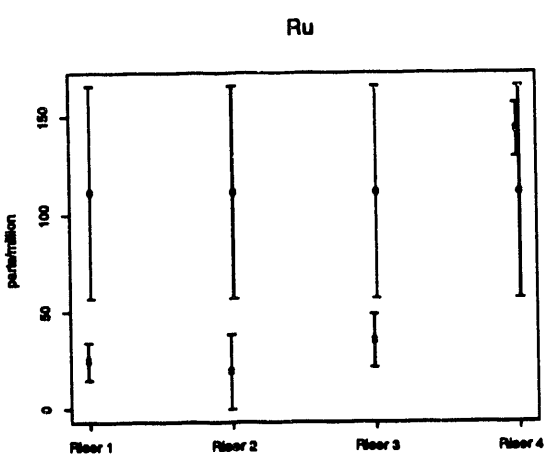
Ru
parts/million
0
50
100
150
Riser 1
Riser 2
Riser 3
Riser 4

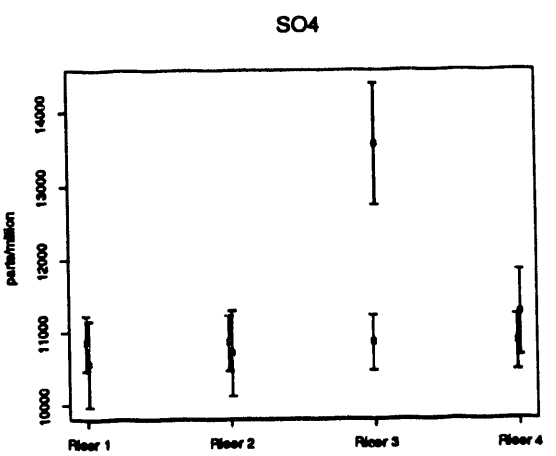
SO4
parts/million
10000
11000
12000
13000
14000
Riser 1
Riser 2
Riser 3
Riser 4

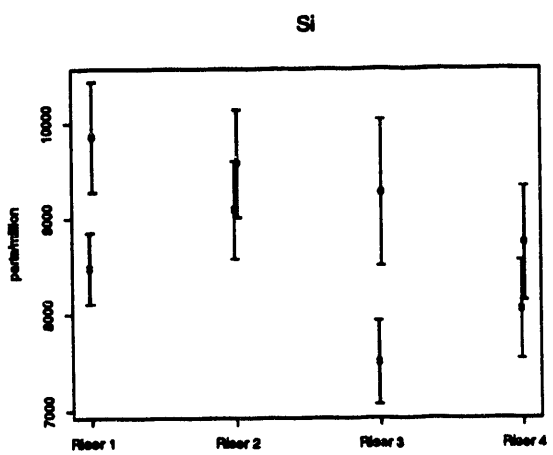
Si
parts/million
7000
8000
9000
10000
Riser 1
Riser 2
Riser 3
Riser 4

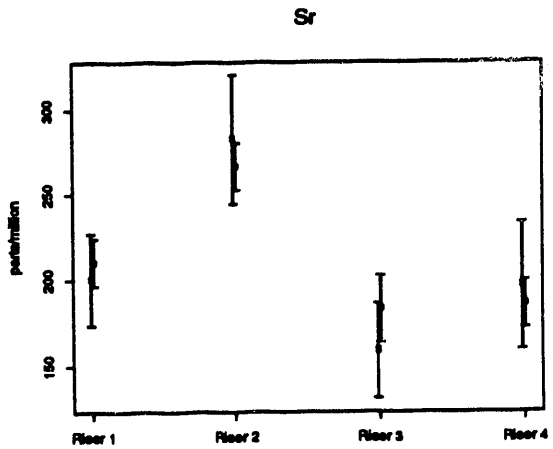
Sr
parts/million
150
200
250
300
Riser 1
Riser 2
Riser 3
Riser 4

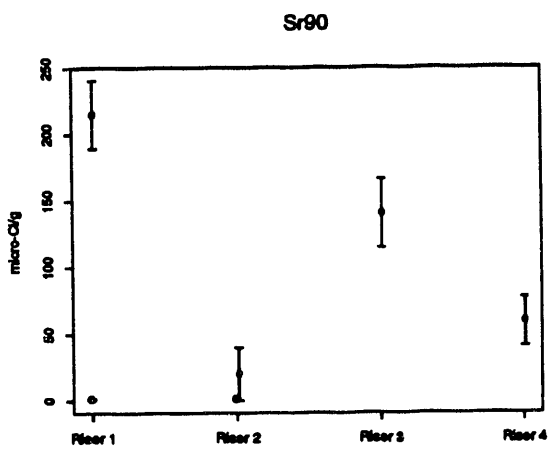
Sr90
micro-Ci/g
0
50
100
150
200
250
Riser 1
Riser 2
Riser 3
Riser 4

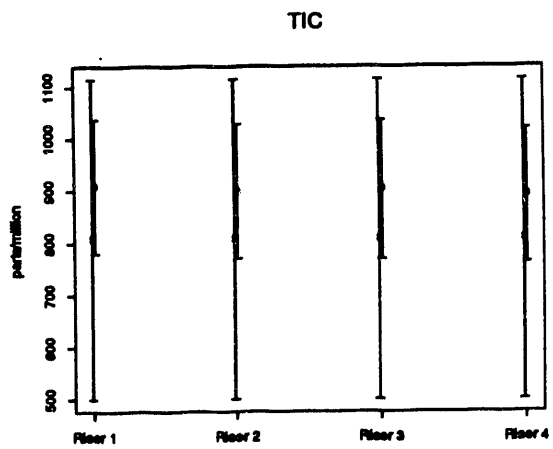
TIC
parts/million
500
600
700
800
900
1000
1100
Riser 1
Riser 2
Riser 3
Riser 4

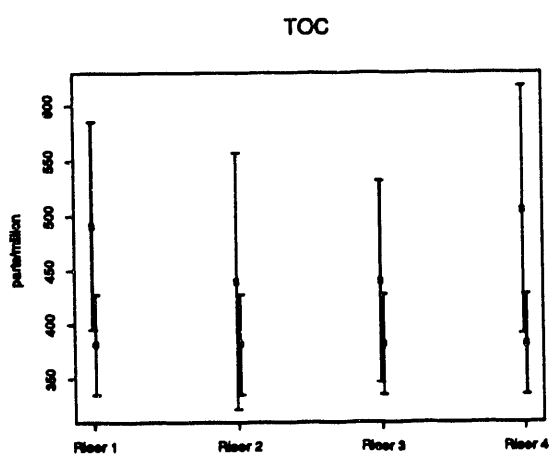
TOC
parts/million
350
400
450
500
550
600
Riser 1
Riser 2
Riser 3
Riser 4

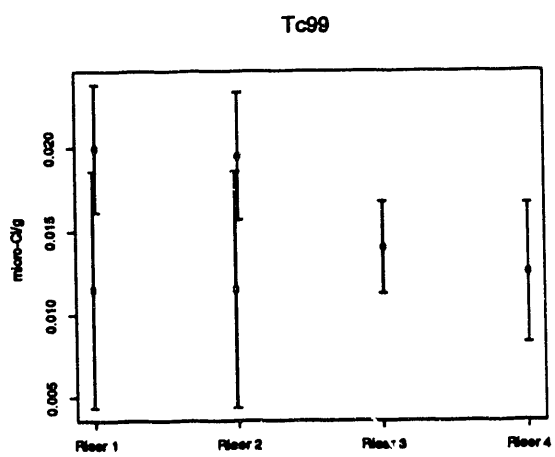
Tc99
micro-Ci/g
0.005
0.010
0.015
0.020
Riser 1
Riser 2
Riser 3
Riser 4

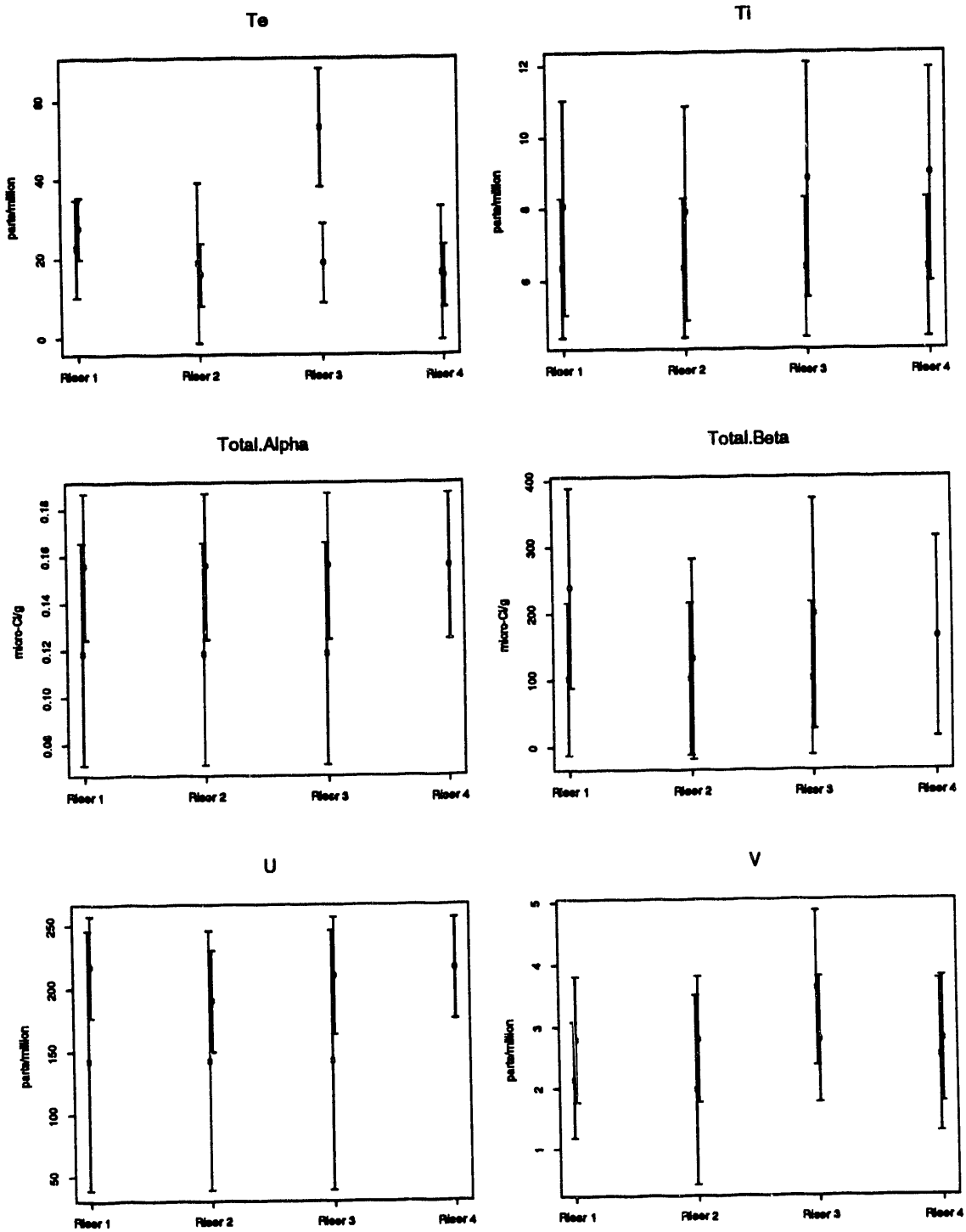
Te
parts/million
0
20
40
60
Riser 1
Riser 2
Riser 3
Riser 4
Ti
parts/million
6
8
10
12
Riser 1
Riser 2
Riser 3
Riser 4
Total.Alpha
micro-Ci/g
0.08
0.10
0.12
0.14
0.16
0.18
Riser 1
Riser 2
Riser 3
Riser 4
Total.Beta
micro-Ci/g
0
100
200
300
400
Riser 1
Riser 2
Riser 3
Riser 4
U
parts/million
50
100
150
200
250
Riser 1
Riser 2
Riser 3
Riser 4
V
parts/million
1
2
3
4
5
Riser 1
Riser 2
Riser 3
Riser 4

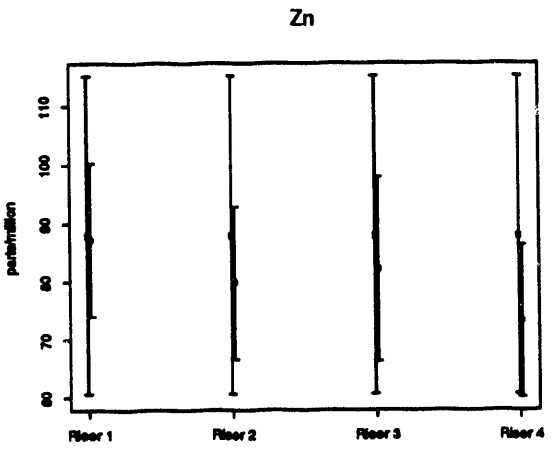
Zn
parts/million
110
100
90
80
70
60
Riser 1
Riser 2
Riser 3
Riser 4

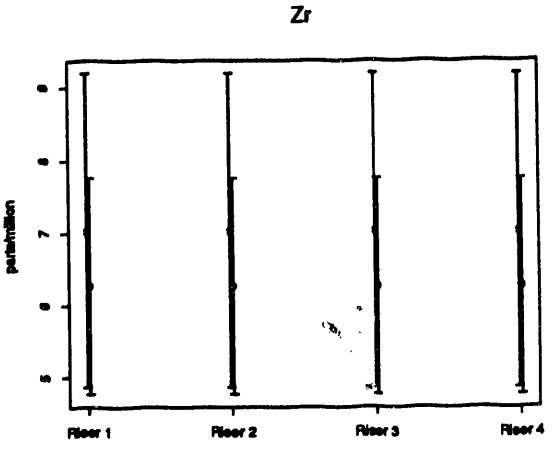
Zr
parts/million
9
8
7
6
5
Riser 1
Riser 2
Riser 3
Riser 4

DISTRIBUTION

No. of
Copies

OFFSITE

2 DOE/Office of Scientific and Technical Information

K.T. Lang
U.S. Department of Energy, Headquarters
EM-36/329 Trev
1990 Germantown Road
Trevion Building
Germantown, MD 20874-1290

S.F. Agnew
Los Alamos National Laboratories
C-345
Los Alamos, NM 87545

K.W. Thomas
Los Alamos National Laboratories
J-514
Los Alamos, NM 87545

H. Sullivan
Los Alamos National Laboratories
K-556
Los Alamos, NM 87545

S.M. Blacker
Vice President, Environment
MACTechnical Services Co.
8310 Center Brook Place
Alexandria, VA 22308

M.H. Campbell
MACTechnical Services Co.
8310 Center Brook Place, B1-42
Alexandria, VA 22308

W.W. Schultz
7200 Montgomery Blvd. N.E.
Albuquerque, NM 87109

No. of
Copies

ONSITE

DOE Richland Operations Office

J.M. Clark, A4-02
T. Noble-Dial, A4-02

22 Westinghouse Hanford Company

J.N. Apple, S4-58
H. Babad, R2-78
M.L. Bell, T6-16
T.M. Brown, R2-12
D.A. Dodd, T6-50
D.L. Herting, T6-09
J.G. Hill, R2-12
J.C. Fulton, R2-31
L. Jensen, T6-07
E.J. Kosiancic, T6-16
A.F. Noonan, R2-12
J.G. Propson, R2-18
K.M. Remund, T6-07
D.A. Reynolds, R2-11
L.M. Sasaki, R2-12
E.J. Shen, S4-58
J.P. Sloughter, T6-07
R.L. Weiss, H4-23
J.A. Voogd, R4-03
T.L. Welsh, T6-07
E.T. Wever, G6-08
W.I. Winters, T6-50

28 Pacific Northwest Laboratory

C.M. Anderson, K7-34
D.B. Baird, K7-34
J.W. Buck, K6-96
P.G. Heasler, K7-34 (10)
T.E. Jones, K1-30
A.M. Liebetrau, K7-34
M.S. Peffers, K7-94
B.A. Pulsipher, K7-34

No. of
Copies

J.L. Scott, P7-34
R.J. Serne, K6-81
D.M. Strachan, K2-38
P.D. Whitney, K7-34
T.M. Wood, K6-47
Publishing Coordination
Technical Files (5)

DATE
FILMED
10/13/93

END